NMR AND KINETIC STUDIES OF ACTINOMYCIN D BINDING TO DNA AND MODEL OLIGONUCLEOTIDE SYSTEMS

by

Stephen Colby Brown

A. B., Oberlin College, 1972

DISSERTATION

Submitted in partial satisfaction of the requirements for the degree of

DOCTOR OF PHILOSOPHY

in

PHARMACEUTICAL CHEMISTRY

in the

GRADUATE DIVISION

of the

UNIVERSITY OF CALIFORNIA

San Francisco

Date **University Librarian**

Degree Conferred: . . . . . .

NMR and Kinetic Studies of Actinomycin D Binding to DNA and Model Oligonucleotide Systems.

Stephen C. Brown

Department of Pharmaceutical Chemistry
University of California
San Francisco, Ca. 94143

ABSTRACT

The actinomycins are a class of antibiotics which inhibit DNA-directed RNA synthesis in both eucaryotic and procaryotic cells by binding to the DNA template. Actinomycin D was shown to be one of the most effective of the natural analogues, which share the same chromophore structure but differ by amino acid subtitutions in the pentapeptide lactone moieties. The biological activity of the actinomycins has been shown to correlate not with binding constants but to the rates of association/dissociation from DNA, which are quite low ($5x10^{-3}$ s^{-1}) compared to other typical DNA binding drugs such as ethidium and daunomycin ($10\text{-}10^{3}$ s^{-1}).

The molecular structural elements responsible for the slow kinetics of actinomycin binding to DNA have been in dispute for some time. The energy barrier ($\Delta G^{\ddagger}_{\simeq}$ 20 kcals/mole) has been postulated to arise from either solvation effects or major structural changes in the polynucleotide , drug, or both. A structural study of free actinomycin D and its complex with DNA was therefore undertaken to ascertain which hypothesis was correct. The heterogeneity of binding sites in DNA presents a problem when detailed structural data are required. A search for an appropriate

model compound for the DNA binding site was therefor initiated. Stopped-flow kinetic experiments were used to determine whether actinomycin D bound in a kinetically similar manner to small oligonucleotides as to DNA. Actinomycin D labelled by ^{15}N was used in ^{15}N-NMR experiments that established whether the bound structures of actinomycin D to the model oligonucleotide dATGCAT or to DNA were similar. Association kinetics, circular dichroism, and ^{15}N-NMR results indicated that the hexanucleoside pentaphosphate duplex dATGCAT was an appropriate model for a DNA binding site of actinomycin D. A combination of one-dimensional and two-dimensional 1H-NMR experiments using the model complex actinomycin D/dATGCAT(1:2) provided structural data in sufficient detail to establish that the drug bound by intercalation between the GC base pairs and that no major structural changes in the polynucleotide or pentapeptide lactones occurred upon binding of the drug. It thus appears that solvation factors are the important determinant of the slow binding kinetics of this class of compounds.

August 25, 1984

ACKNOWLEDGEMENTS

The contributions and assistance of many people are behind the completion of this dissertation. First, I would like to thank Professor Richard Shafer, who was very generous with his time and resources, especially for the NMR time at U. C. Davis. Professors Peter Kollman and Tack Kuntz, who taught me that sometimes theory was more reliable than experiment, will be missed very much as well. Professor Tom James was very helpful on NMR theory and taught me that protons were more than gyroscopes. Professor Martin Shetlar's advice on the fine points of chromatography saved me a lot of frustrating time, and unfortunately went away on sabbatical before I could get my act all wrapped up. Vladimir Basus and Joe Murphy were greatly appreciated for keeping the machines working under the continual assault of graduate students. Vladimir Basus in particular is appreciated for taking the time to think over some of my more puzzling results. The comments and comaraderie of Bob Tilton, Nancy Shine, Peter Mirau, Dan Cashman, Alain Delbarre, Tom Keller, Tom Marschner, Stewart Oatley, Janine Rose, Michelle Broido, Sal Profeta, Andrew Dearing, Elisha Berman, Scott Weiner, Kelley Horn, and, last but not least, Michael Mosely made it all seem worthwhile during several dark moments. I would especially like to thank Laurie Jarvis and Pat of the Computer Graphics Lab for helping me become a more friendly user of computers. I particularly want to thank Professor A. L. Burlingame for his generous help during my first year and for bringing this department to my attention when I had decided to pursue a post- graduate degree. On the home front, I would like to thank Ruth Slavin for keeping me sane before my oral prequalifying exams, and ever since.

TABLE OF CONTENTS

1. Introduction

The actinomycins are a class of antibiotics first isolated from laboratory cultures of actinomycetes, a common soil bacterium, by Waksman & Woodruff in 1940. It was not realized until the late 1950's, after an extensive series of experiments by groups led by Brockman in Germany and Bullock & Johnson in England, that "actinomycin" was in fact composed of a variety of similar compounds, each sharing the same chromophoric structure but differing in the types of attached amino acids. Chemical degradation experiments finally established the basic structure of the actinomycins several years later(Figure 1). The chromophoric structure, 2-amino-4,5-dimethyl-3-phenoxazone-1,8-dicarboxylic acid, is known as actinocin, and has two pentapeptide lactones attached to the carboxyl groups via an amide linkage to the 1' amino acid which is always threonine. The threonine provides the alcoholic functional group that forms a lactone with the 5' amino acid carboxyl group. Actinomycins where the pentapeptide lactones are identical are termed isoactinomycins and those with different pentapeptides are called anisoactinomycins. A number of isomers has been isolated and characterized from various strains of actinomycetes and others have been synthesized by modified biosynthesis or chemical modification of naturally occuring isomers (Meienhofer & Atherton, 1973). Modified biosynthesis has been possible since incorporation of amino acids in the actinomycins can be altered by the addition of various amino acids to the growth medium. (For reviews of actinomycin, see: Meienhofer & Atherton, 1973; Remers, 1979).

The actinomycins were the first antibiotics recognized to have antitumor activity. They are effective against Gram(+) bacteria, but significant mam-

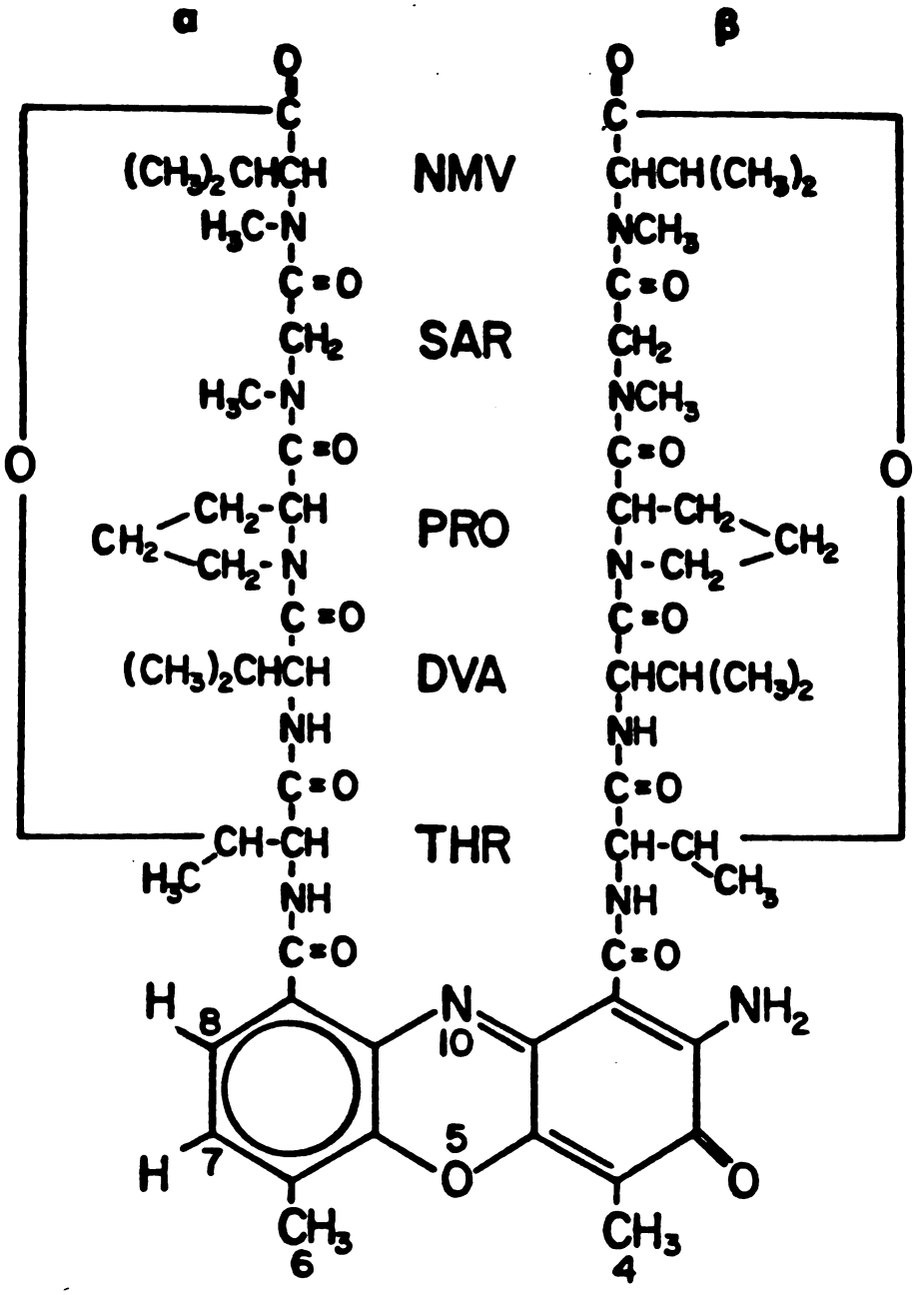

FIGURE 1

Structure of Actinomycin D. Pentapeptide lactones are labeled α(connected to the chromophore at C9) and β(at C1). A pseudo-twofold axis passes through atoms N10 and O5 of the chromophore in the three-dimensional structure.

malian toxicity was found also, precluding their clinical use as bacteriostatic agents. However, it was soon discovered that actinomycin was effective in the treatment of Hodgkin's disease and other human neoplasias including Wilms' tumor, lymphomas, rhabdomyosarcoma, gestational choriocarcinoma, and Kaposi's sarcoma. The actinomycins are ineffective against the major human cancers, and a large number of structure-activity studies have ensued with the hope of discovering an analogue possessing a broader spectrum of activities and a better therapeutic index. So far, these studies have not produced substantial improvement and actinomycin D (Figure 1) is still considered the most effective antitumor actinomycin.

The predominant biological effect of the actinomycins is inhibition of DNA-directed RNA synthesis. *In vitro* assays with RNA polymerase determined that actinomycin retarded the elongation step but not initiation of RNA synthesis. It was also determined that the drug bound to the DNA template and not the polymerase. Subsequent experiments using a suite of actinomycins showed that RNA synthesis inhibition correlated not with binding constants of the analogues to the DNA template, but to dissociation constants (Muller & Crothers, 1968). Apparently the actinomycins inhibit progression of RNA polymerase along the DNA template and their activity is proportional to the slow rates of dissociation from DNA, which are of the order 10^{-3} sec^{-1}.

In order to rationally design a more effective actinomycin, it was necessary to ascertain those parts of the actinomycin structure which determine the slow dissociation rates. Actinomine (Figure 2) has a DNA binding constant similar to that of actinomycin D, but fast dissociation rates from DNA. Actinocin (Figure 2) does not bind to DNA and neither do actinomycins where one or both of the peptide lactones has been opened by hydrolysis. It is

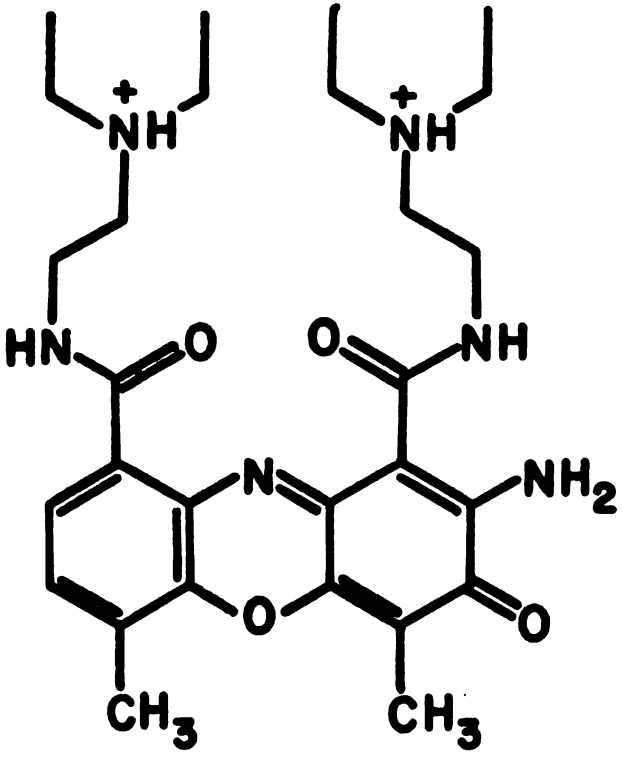

ACTINOMINE

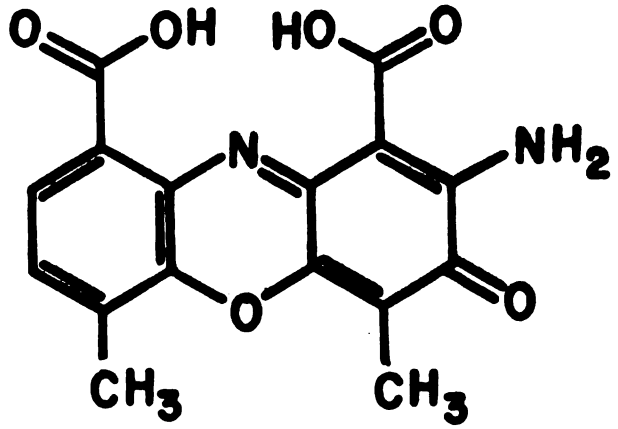

ACTINOCIN

FIGURE 2

Structures of actinomine and actinocin.

apparent that intact pentapeptide lactones are required for the slow dissociation kinetics and biological activity of the actinomycins. Correlations of biological activity with pentapeptide lactone structure were inconclusive in regard to identification of molecular determinants responsible for the slow kinetics of the actinomycin-DNA complex. However, the following generalizations could be gleaned from the data: 1) configurational integrity, i.e. L,D,L isomers in positions 1',2',5' of the peptides is required; 2) N-Methyl amino acids are required in positions 4' and 5'; 3) bulky and β-branched side chains at the 2' position enhance activity; 4) Proline or other imino acids are required at the 3' position, but relatively minor substitutions can have large effects(i.e. 4-oxo proline > proline > 4-OH proline). Hydrophobicity and rigidity of the pentapeptide lactones seems to optimize activity. Thermodynamic parameters of actinomycin C binding to DNA indicated a large hydrophobic effect was involved (Gellert et.al., 1965), while thermodynamic parameters calculated from the temperature dependence of the actinomycin D -DNA association rates indicated a highly restricted transition state (Bittman & Blau, 1975)[see Table III].

An actinomycin D/deoxyguanosine(1:2) crystal was analyzed by X-ray diffraction and provided the first experimental structure (Figure 3) for the pentapeptide lactone configurations(Jain & Sobell, 1972). A model of the actinomycin D/dATGCAT(1:2) complex was built from this X-ray structure (Sobell & Jain, 1972) but was modified later due to unfavorable steric contacts and a new structure was proposed(Sobell, 1977). The new model contained coordinates for a dGCGCGC hexanucleotide instead of the criginal dATGCAT sequence, but otherwise the general structural features of the two models are the same. The Actd chromophore is intercalated between the central GC base pairs, with the pentapeptide lactone moieties nestled in the

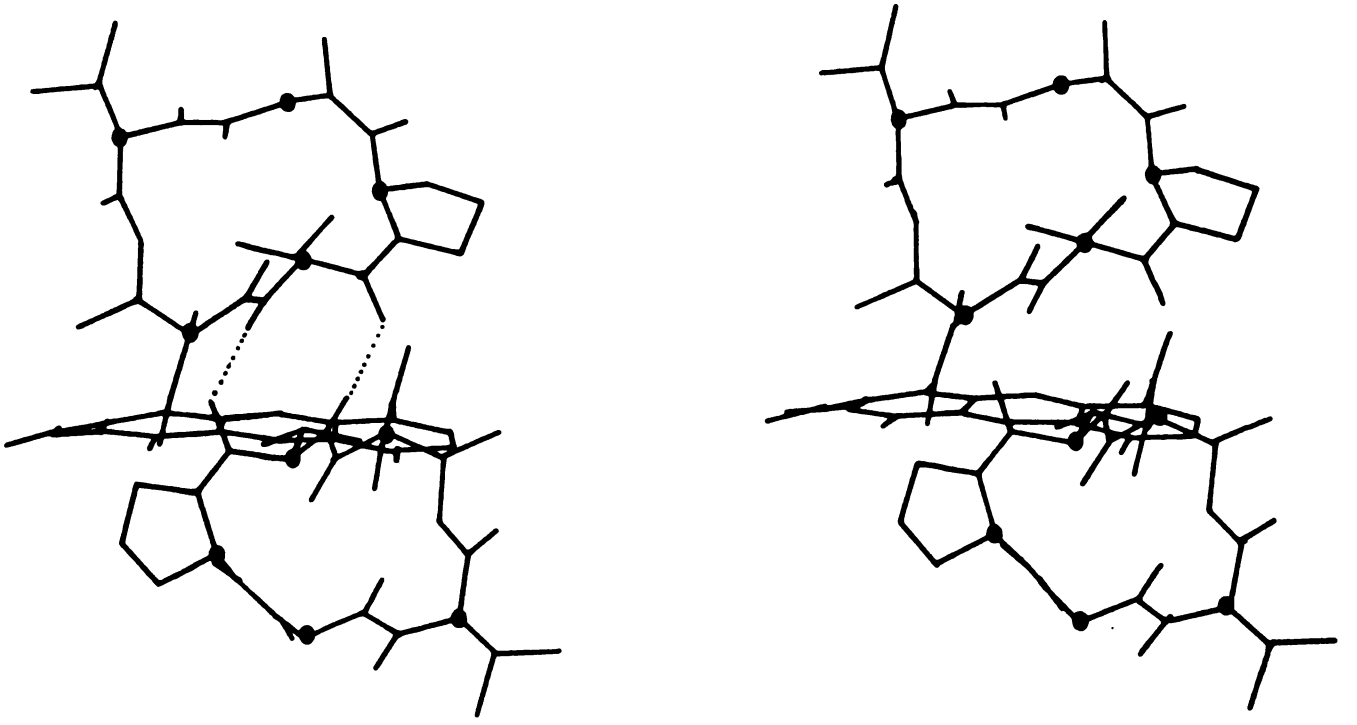

FIGURE 3

Stereo projections of the Actinomycin D crystal structure determined by Jain & Sobell, (1972). Amino acid C_α atoms are marked by the black circles. Inter-pentapeptide lactone hydrogen bonds are indicated by the dashed lines. View approximately along the pseudo-twofold axis.

minor groove of the double helix, which remains intact but distorted by a kink and a slight shift in the helix axis at the intercalation site. The general features of the pentapeptide lactone configurations are: 1) peptide bond configurations thr-Dva-pro-sar-nmv *(trans-cis-cis-trans);* 2)intercycle hydrogen bonds from α-Dva NH---β-DVA C=O and α-Dva C=O---β-Dva N-H ; 3) a pseudo-twofold symmetry axis for the molecule passing through the phenoxazone N10 and O5 atoms.

Theoretical studies had predicted this configuration by a semi-empirical approach incorporating IR, NMR, and x-ray experimental data available at that time with molecular mechanics calculations (De Santis et al., 1972). These calculations predicted an energy minimim with intercycle hydrogen bonds between the Dva residues and peptide bond configurations of either *trans-cis-cis-trans* (found later in the crystal structure) or *trans-cis-trans-trans*. The all *trans* configuration featuring an intracycle hydrogen bond between sar C=O---Dva N-H was calculated to have an energy 3 kcals/mole greater than the minimum energy conformations. This conformation was later observed by NMR in chloroform when the pentapeptide lactone was freed of the chromophore, changing the intercycle Dva hydrogen bonds from intramolecular to intermolecular in character *(vide infra)*.

Hypotheses advanced to explain the known thermodynamic binding properties and multistep kinetics of the actinomycin-DNA interaction have invoked either 1) structural rearrangements in the pentapeptide lactones (Muller & Crothers, 1968); 2) structural rearrangements of the polynucleotide (Sobell, 1974) or 3) structural rearrangements of the solvating water shell around the interacting molecules (Sobell & Jain, 1977). Conformational studies by ^{13}C- and ^{1}H-NMR of actinomycin D pentapeptide lactones freed of

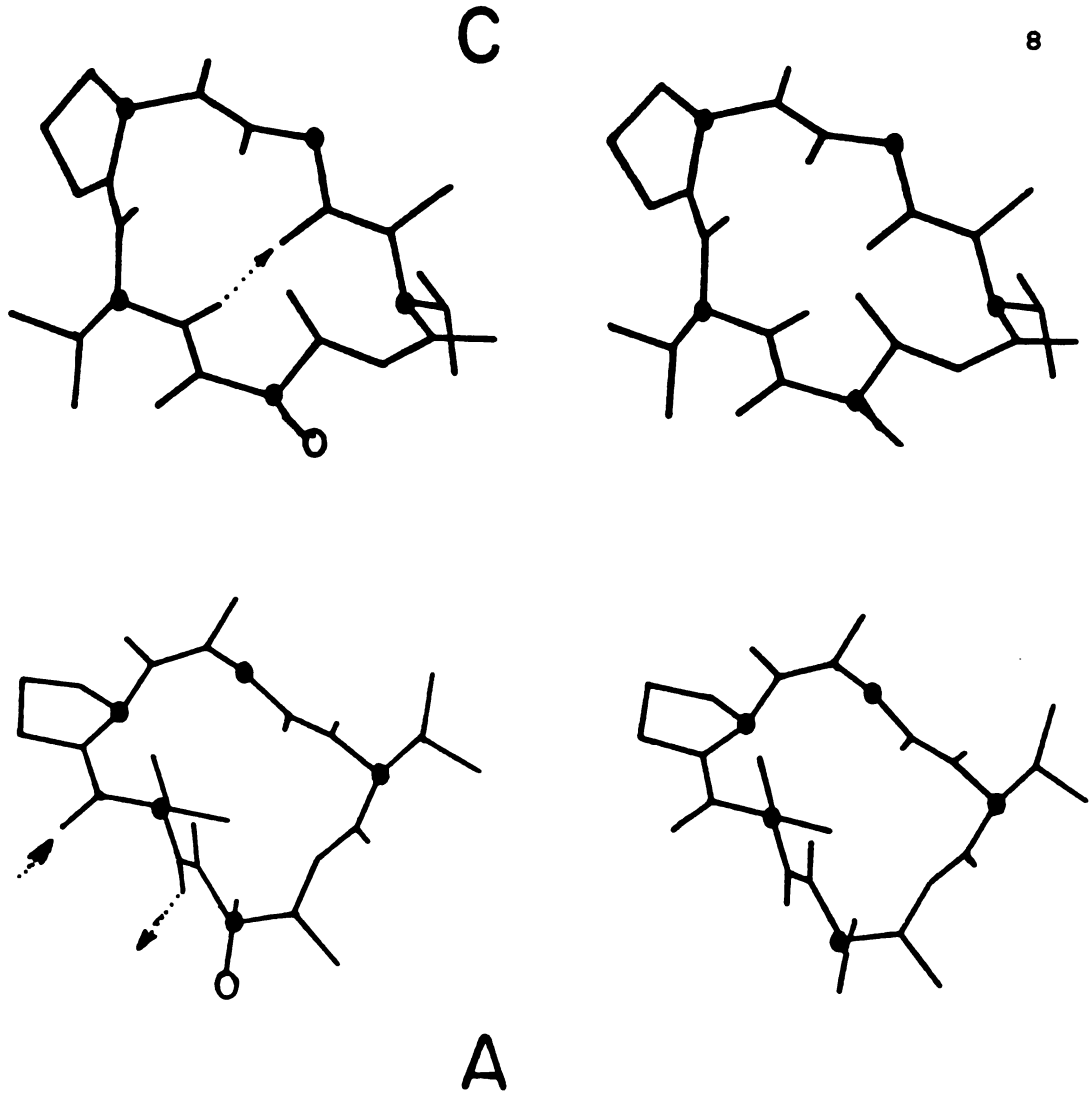

FIGURE 4

Stereo projections of the 'C' (top) and 'A' (bottom) conformations determined by Lackner(1975) for the actinomycin D pentapeptide lactones in solution under various conditions. Open circles mark the threonine N atom, black circles mark the amino acid C_α atoms. Dashed lines represent hydrogen bonds with the arrow pointing toward the oxygen atom. The 'C' conformation exibits an internal hydrogen bond from Dval NH--O=C sar, while the 'A' conformation hydrogen bonds to solvent molecules.

attachment to the phenoxazone chromophore indicated two possible conformations (Lackner, 1975) that were observed in different solvents (Figure 4). The structure of the 'A' conformer, found in acetone and other hydrogen bond accepting solvents, was similar to the structure found in the crystal of the actinomycin D:deoxyguanosine(1:2) complex (Jain & Sobell, 1972). The 'C' conformer was found in chloroform and was found to be significantly different. An internal hydrogen bond between the D-valine N-H and sarcosine C=O was found as well as a different peptide bond configuration. Each peptide bond in the 'C' conformer was *trans* in configuration but the D-valine-proline and proline-sarcosine peptide bonds in the 'A' configuration were found to be *cis*.

Subsequent studies on the dissociation kinetics of actinomycin D homologues where the proline residue was replaced by 2-carboxyazetidine and pipecolic acid showed a striking correlation of DNA dissociation rates and size of the 3' residue (Shafer et al., 1980; Mirau & Shafer, 1982a). Proton NMR studies in benzene also suggested that a larger degree of conformational freedom existed at the H-alpha protons of the 3' residue than at other locations in the molecule (Mirau & Shafer, 1982b). The known thermodynamic barrier of ≃20 kcals/mole involved in the slow dissociation process was similar to that of proline-X cis/trans isomerizations found in other peptides and proteins. It was therefore proposed that a configurational isomerization accompanied actinomycin binding to DNA, and that the Dva-pro and/or pro-sar peptide bonds were involved. An attempt to determine the configuration of the pentapeptide lactones of actinomycin D, both when free in aqueous solution and when bound to DNA or an appropriate model oligonucleotide was then begun.

2. Kinetic Studies of Actinomycin D Binding to Poly-, Oligo-, and Mononucleotides

High resolution structural data on the actinomycin D(ActD)-DNA complex in solution could best be obtained by NMR techniques. Due to the large size and binding site heterogeneity of DNA, however, NMR techniques could not be expected to yield much information. A model oligonucleotide of DNA would greatly facilitate the acquisition of NMR data by: 1) eliminating the effects of site heterogeneity around the strong dGC binding site; 2) reducing τ_c and therefore signal linewidths; 3) reducing the number of resonances. It was important to choose an oligonucleotide that was long enough to mimic the DNA binding site and minimize end effects but short enough to optimize the NMR data. It was therefore necessary to determine the minimum oligomer length required to mimic the binding of ActD to DNA. Most importantly, it was necessary that the oligomer mimic the slow dissociation kinetics of the ActD/DNA complex.

Previous studies had established that the dissociation or association of actinomycins with DNA was slow relative to most other DNA binding drugs and demonstrated three unimolecular steps ($\tau_{ass.}$= 1.8, 20, 285 sec, $\tau_{diss.}$= 12, 44, 570 sec.) as well as at least two bimolecular steps (Muller & Crothers, 1968). Later studies using the heterocopolymers poly-dGC and poly-d(DAP-T) showed multiple unimolecular processes with similar pseudo-first order rate constants (Bittman & Blau, 1975). In contrast, studies with dinucleotides or mononucleotides reported fast bimolecular or termolecular kinetics (Reinhardt & Krugh, 1972; Davanloo & Crothers, 1976; Krugh & Chen, 1975). ^{31}P- and ^{1}H-NMR or optical temperature jump experiments were used to

study the kinetics of mono- or dinucleotides whereas kinetic measurements with polynucleotides were obtained using optical techniques in a stopped-flow apparatus. Dissociation times are the most relevent physico-chemical measurement correlating to biological activity of the actinomycins (Muller & Crothers, 1968), but can be measured only by dilution of pre-equilibrated complexes or the addition of Sodium Dodecylsulphate (SDS) to sequester the free drug. It was found that the measured rate constants were independent of SDS concentration, so that the presence of SDS had not truly perturbed the dissociation reaction. However, dilution of ActD-oligonucleotide complexes does not compare the same states as dilution of ActD-DNA complexes since the end state of DNA is double stranded whereas dilute oligonucleotide concentrations at reasonable salt levels have a substantial population of single strands. SDS dissociation of ActD-oligomer complexes produces curves that demonstrate slow kinetic components, but these curves cannot be fit accurately to several exponentials and also demonstrate marked dependence on SDS concentrations. Fortunately, association kinetics monitor the sum of the forward and backward rate constants as well and avoid the problems inherent to measurement of the dissociation rates.

Materials and Methods

Actinomycin D was obtained from Sigma or Merck. Purity was checked by TLC (Silica Gel G F-254, Ethyl Acetate(100%)). Nucleotides were obtained from Collaborative Research or Sigma except for dATGCAT which was a gift from Drs. Kary Mullis and Corey Levinson of the Cetus Corporation, Emeryville, Ca. Actinomycin concentrations were determined optically at 440 nm

($\varepsilon^{20^{\bullet}}$ = 24,450) and nucleotide concentrations at 260 nm using molar extinction coefficients supplied by the manufacturers. All solutions were made up in BPES buffer (0.100 M. Phosphate, 0.180 M. NaCl, 0.010 M. EDTA, pH=7.0) and degassed by stirring under vacuum for at least 30 minutes prior to use. All solutions were filtered through .22μm. filters (Millipore GS-22) prior to use.

Association kinetics were followed in a temperature controlled Durrum D-110 Stopped-Flow Spectrometer using a 2 centimeter pathlength cell. Data was acquired, stored, and analyzed on a Northstar microcomputer supplied by On-Line Instrument Systems, Route 2, Jefferson, Ga. 30549, using the model 3820 software supplied by same. Instrument dead time was 4 milliseconds and stability was +/-.002 OD over 2000 seconds. Some data was also obtained by hand mixing into a 1 cm. cuvette in either a Beckman Acta C-III or Gilford 2600 spectrophotometer, but sample volumes were much larger and stability was less favorable. The stopped-flow instrument was used primarily for its stability and economy. Generally, 256 data points were acquired over 500 seconds and the baseline optical density was measured at 1000 seconds after mixing equal volumns of an ActD solution and nucleotide solution. Kinetic curves were fit by a Marquardt-Levenberg non-linear least squares regression program written by Professor Richard Shafer of UCSF. R^2 values were better than .990 and the residuals were examined to evaluate the goodness of fit. The first seven points (t=0,14 seconds) were dropped and curves were fit to two exponentials and baseline. To increase signal to noise in most cases, 3 or 4 successive identical runs were averaged before being fit by the program. Standard deviations of fitted values were taken from the results of the fit. Total OD changes at 425 nm were measured by comparing the optical density difference between the ActD/nucleotide solution at

equilibrium and an ActD/buffer solution. Final ActD concentrations ranged from 1.5-4.0 x 10^{-5} M. with final nucleotide concentrations given by either P/D(Phosphate to Drug) or DS/D(Double Strands to Drug).

Dissociation reactions were monitered by mixing an ActD/nucleotide complex (ActD concentrations=4 x 10^{-5} M. with stated P/D) with an equal volumn of a 4% Sodium Dodecyl Sulphate(SDS) solution in the same buffer. The SDS solution was diluted to determine whether its concentration had any effect on the measured dissociation rates. Crystals were observed to form in more concentrated solutions of SDS after several days. Dissociation curves were monitored for 5000 seconds with the reference taken at 10,000 seconds after mixing.

Circular dichroism(CD) spectra were measured on a Jasco J-500A spectrometer at Professor J. T. Yang's laboratory at UCSF. Actinomycin concentrations were 1.84x10^{-5} M. for all samples(in BPES buffer) and the amount of nucleotide added is found in Figure 8. Sample temperatures were 20 °C. in all spectra, which were taken in a 1 cm. pathlength cell. The baseline was checked for the cell while it contained the identical buffer alone and was found to be 0.0 ±.2 Δ in the wavelength range monitered.

Results and Discussion

Typical visible spectra of ActD free and bound are shown in Figure 5. The maximum OD change upon binding to all guanine containing nucleotides is found at 425 nm. This wavelength was chosen to maximize sensitivity of the kinetic measurements. Kinetic studies by circular dichroism showed that at least three optical transitions exist within the ActD absorption

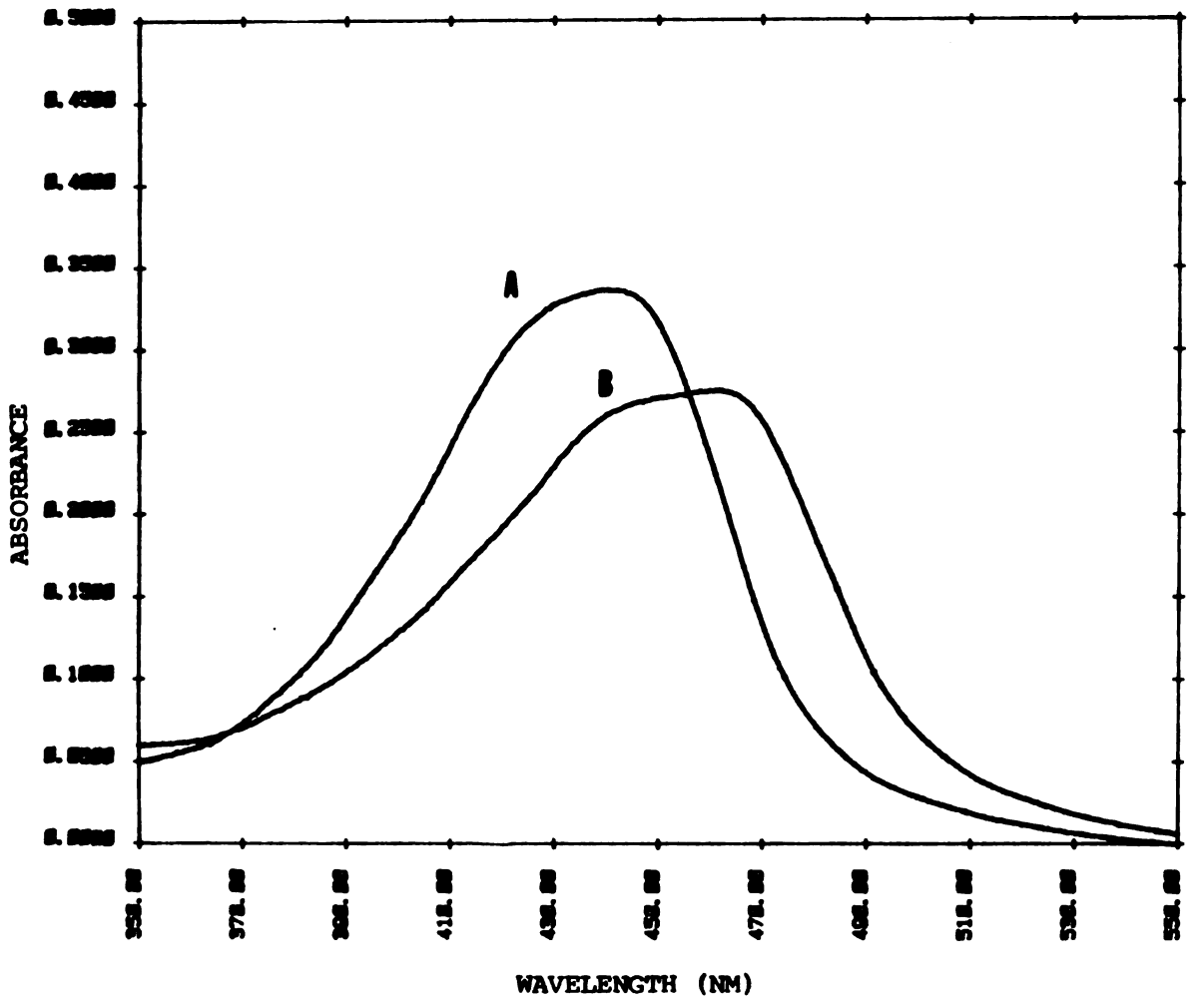

FIGURE 5

Spectra of actinomycin D in BPES buffer(A) and bound to the tetranucleotide double helix; dCGCG(B) in the identical buffer. The maximum OD change upon binding is found

envelope (Auer et al.,1978; Auer & Thompson, 1978). The transition at 370 nm moniters preponderantly effects at the benzenoid portion, that at 490 nm the quinoid portion, and that at 420-440 nm the entire phenoxazone chromophore.

Association kinetics of ActD to calf thymus DNA were first investigated to confirm the published data. As expected, three slow, unimolecular processes and at least two fast, bimolecular processes were found with similar pseudo-first order rate constants to those reported (Table I). Initial control experiments done to moniter instrument stability over the long observation periods required showed that the noise level was +/-.002 OD units and no drifting was observed as long as the solutions were thoroughly degassed immediately prior to use. These controls included mixing ActD with buffer, proflavin with DNA, proflavin with 5'-dGMP, ActD with 5'-dCMP and 5'-TMP, and monitoring ActD/DNA solutions after equilibration in the stopped-flow cell. Representative kinetic traces with fitted curves may be found in Figure 6.

TABLE I

ActD/DNA Association Rate Dependence on P/D[a]

[DNA(P)]/[ActD]	$k_1(x10^3)\ s^{-1}$	$\%\Delta OD_{tot}$	$k_2(x10^2)\ s^{-1}$	$\%\Delta OD_{tot}$
18	5.0(±.9)	4	4.2(±.4)	9
27	4.5(±.2)	6	4.2(±.2)	9
34	3.7(±.3)	6	4.4(±.2)	7
46	5.0(±.6)	8	3.9(±.3)	9
65	4.7(±.3)	6	3.8(±.7)	9

k_3≃0.50(±.5) 10%, k_4,k_5 are bimolecular ~10-100 s^{-1}

[a][ActD]$_f$= $2.1x10^{-5}$ M., T=23.0°C.

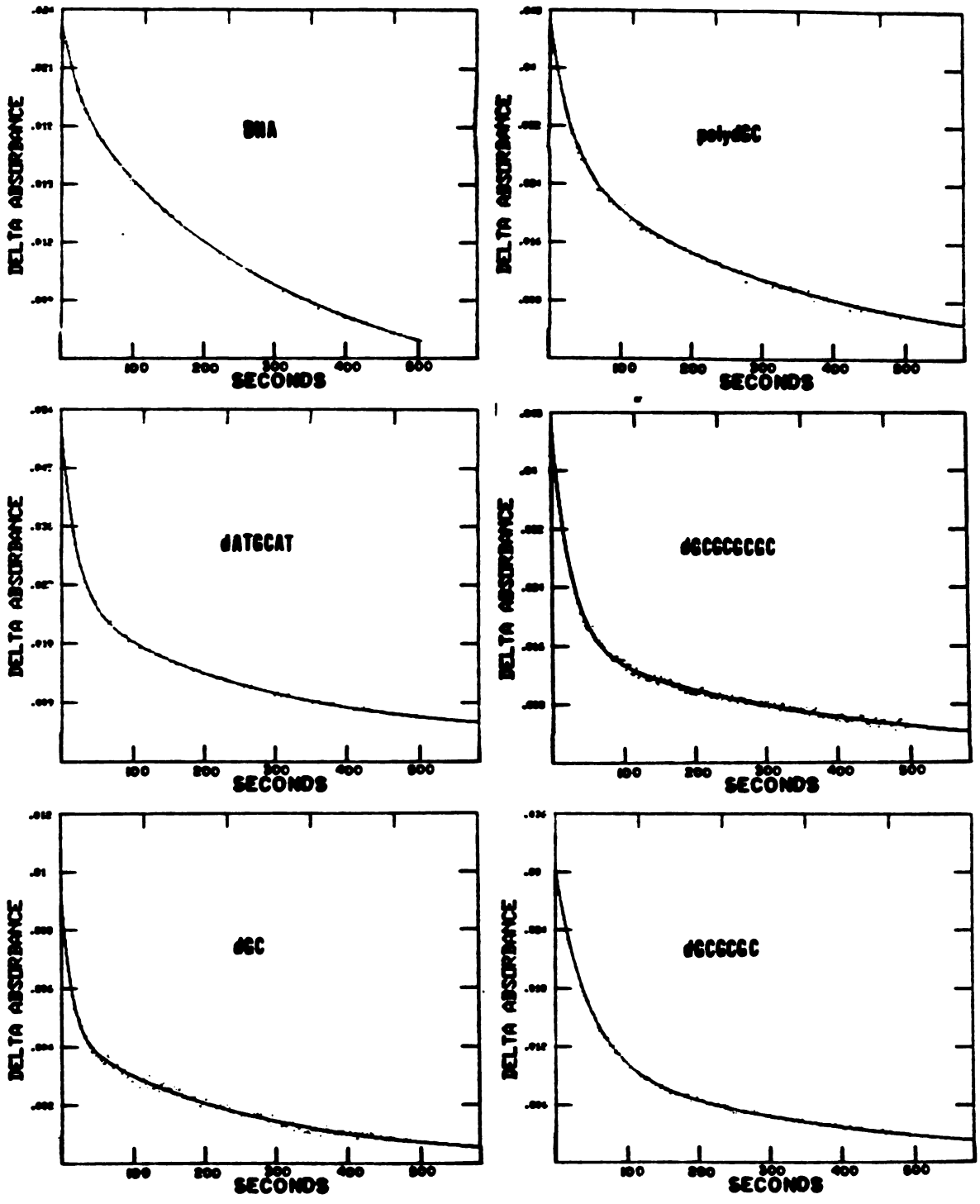

FIGURE 6

Representative kinetic traces of ActD binding to poly- and oligonucleotides indicated, monitered at 425 nm. Data displayed as digitally acquired dots, solid curves are double exponentials fitted to the data by a nonlinear Marquardt-Levenberg algorithm. Only the two slowest kinetic processes, k_1 and k_2, are observed at this time scale.

Association of ActD and 5'-dGMP was also done as a control, since this interaction was thought to occur only as a fast bimolecular process (Krugh & Chen, 1975). However, two slow unimolecular processes were observed in the association of ActD to 5'-dGMP, dG, 5'-GMP, and 5'-dAMP (Figure 7). These slow processes (Table II) have rate constants and $\%\Delta OD_{tot}$ values comparable to those found in the association of ActD with polymers and oligonucleotides and demonstrate a clearly unimolecular rate dependence (i.e., independent of initial concentrations). Only two slow processes are observed for mononucleotides, since the bimolecular association occurs on a time scale too fast to be observed by stopped-flow techniques at the initial concentrations required given the smaller equilibrium association constants of ActD to mononucleotides. The slow association to 5'-dAMP is not observed until concentrations far in excess of those required to observe slow association to guanine containing nucleotides are used. This is due to a sensitivity problem because the K_a of 5'-dAMP to ActD is roughly an order of magnitude smaller than that of 5'-dGMP. Moreover, the slowest phase of 5'-dAMP binding to ActD consists of only 2% of the total OD change versus a 4% change for 5'-dGMP. The thres-

TABLE II

Slow Unimolecular Kinetic Parameters for the Association of ActD with Mononucleotides

Species	K_a*	[N]/[ActD]	$k_1(x10^3)\ s^{-1}$	$\%\Delta OD_{tot}$	$k_2(x10^2)\ s^{-1}$	$\%\Delta OD_{tot}$
5'-dGMP	$7x10^3$	25-1000	3.8(±.8)	4	3.7(±1.0)	6
dG	$2x10^3$	100-207	2.7(±2.)	4	2.1(±1.7)	4
5'-GMP	$9x10^2$	250-500	3.1(±.7)	3	4.6(±.1)	4
5'-dAMP	$7x10^2$	227	4.4(±.6)	2	4.5(±.7)	4

*From Auer et al., 1978

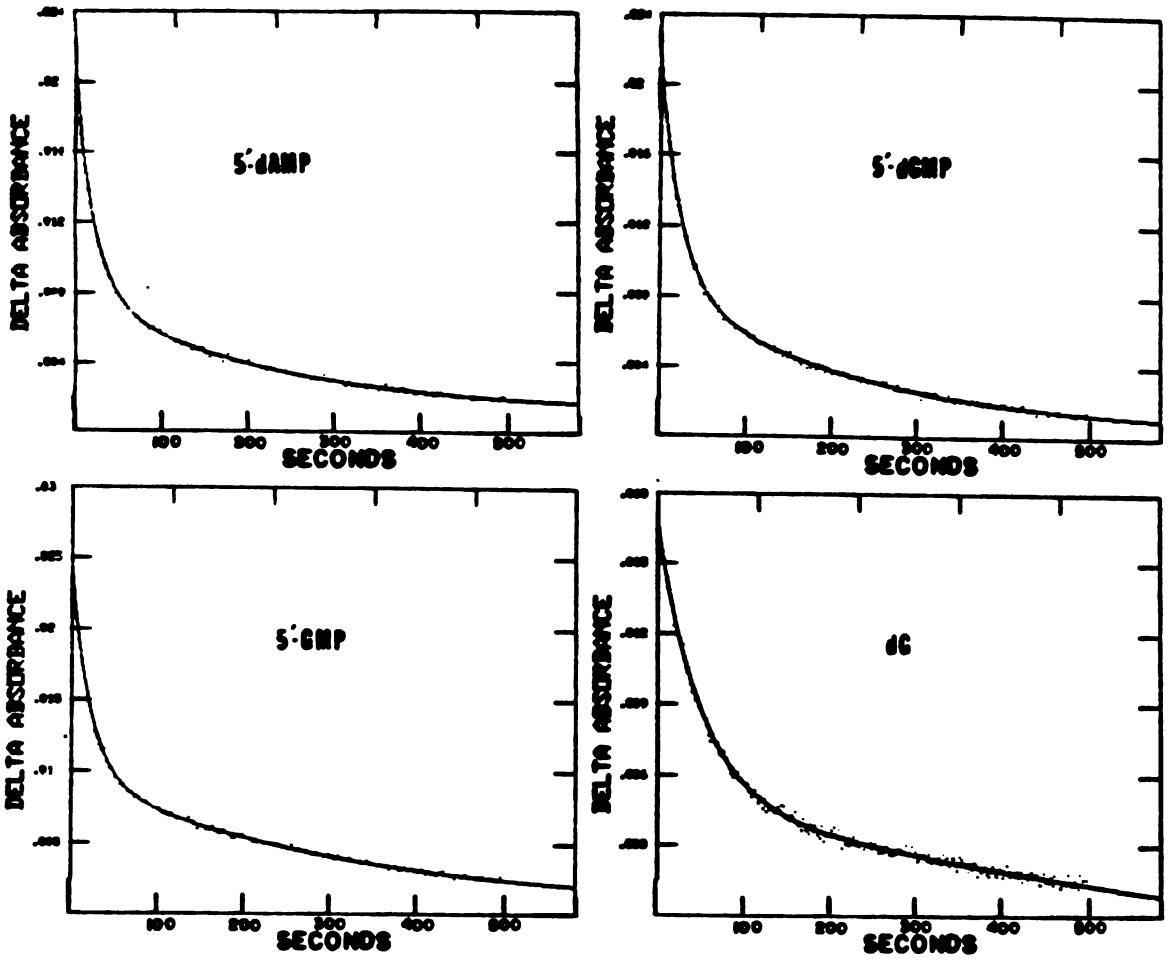

FIGURE 7

Representative kinetic traces of ActD binding to the mononucleotides indicated, monitored at 425 nm. Semilogarithmic plots of the same data show two exponential behavior. Data displayed as digitally acquired dots, solid curves are double exponentials fitted to the data by a nonlinear Marquardt-Levenberg algorithm. Only two kinetic processes, k_1 and k_2, are observed at this time scale given the concentrations of reacting species. The time constants of k_1 and k_2 are independant of nucleotide concentration.

hold concentration of mononucleotide required to observe the slow unimolecular binding processes corresponds to the rank of equilibrium dissociation constants(K_d): 5'-dAMP > 5'-GMP > 5'-dGMP. Equilibrium binding studies (Davanloo & Crothers, 1976) have shown that 5'-dGMP, 5'-dAMP, and dGpC have different binding modes to actinomycin C_3 and that the specificity of ActD for guanine is much less pronounced at the mononucleotide level than at the polymer level. Equilibrium CD titrations of ActD with these monomers allowed only rough calculations of their equilibrium association constants (Auer et al., 1978) due to evidence of multiple equilibria which are neither chemically independent nor spectroscopically non-interacting. It must also be noted that extensive self-association of purine nucleotides at millimolar concentrations in aqueous solutions has been detected (For discussion, see "Basic Principles in Nucleic Acid Chemistry", (ed. P. O. Ts'o), Vol I, pp. 537).

The observation of slow unimolecular association of ActD with mononucleotides was completely unexpected and confounding. Given that the slow processes represent $\Delta G^{\ddagger}$ of 19-21 kcals/mole and are unimolecular, it is difficult to envision a driving force for an intracomplex rearrangement given the model of mononucleotide stacking on the ActD chromophore. The temperature dependence of the two unimolecular processes of ActD/5'-dGMP association were measured in the stopped-flow apparatus and Arrhenius plots were constructed from this data covering a temperature range of 10°-°50 C. Convex curved Arrhenius plots resulted for this data as well as for data derived from ActD/DNA associations over this temperature range. It became necessary to check the temperature regulation of the instrument more carefully. A test was derived by mixing a solution of the dye m-cresol purple (m-cresol sulfonphthalein) in a 0.010 M. Tris-HCl buffer at pH=8.2 with equal volumes of the same buffer. The temperature dependence of the Tris-HCl

buffer is very large and the dye has a pKa close to the pKa of this buffer (8.08), so that a substantial change in optical density at 577 nm. occurs with temperature (-.015 OD/°C). Experimental runs on the stopped-flow instrument revealed a temperature difference of several degrees between the loading syringes and the observation chamber when both were held to a temperature more than five degrees different from ambient. Therefore, Arrhenius plots were constructed using data from the relatively narrow temperature range of 15-25°C., and so the resulting thermodynamic parameters have a rather high level of uncertainty. Thermodynamic parameters for the two slowest, unimolecular processes of ActD association to DNA were calculated using Arrhenius plots of log k vs. 1/T and were found to agree within experimental error to the published values (Table III). Comparison of the data from ActD associations to DNA and 5'-dGMP reveals that the transition states are both characterized by large negative $\Delta S^{\ddagger}$ and positive $\Delta H^{\ddagger}$ values(Table III), implying but by no means proving that similar net forces are responsible for the two slowest processes of association between ActD and either DNA or 5'-dGMP. Solvation of the interacting species may be involved. In the case of mononucleotides, perhaps more than two nucleotides interact with ActD and the slow process represents a pre-formed stacked complex of mononucleotides on the ActD chromophore that gradually 'squeezes out' solvent water between the stack and the pentapeptide lactones. It was subsequently discovered that the slow processes of mononucleotide association to ActD had been observed before, but were not investigated in any detail (T. R. Krugh, personal communication). The CD spectrum of the ActD/5'-dGMP complex (P/D= 380) is very different from that of the DNA, dATGCAT, and poly-dGC complexes (Figure 8), so the structure of this complex must be very different from that of the oligomer and polynucleotide complexes. It is

TABLE III

Thermodynamic Activation Parameters for ActD Associations				
Nucleotide	Process	$\Delta G^{\ddagger}$(kcals/mole(ActD)	$\Delta H^{\ddagger}$(kcal/mole)	$\Delta S^{\ddagger}$(e. u.)
DNA[a]	k_1	21.0	13.4(±1.3)	-26.0
	k_2	19.4	14.2(±0.9)	-17.7
5'-dGMP P/D= 370	k_1	20.3	9.5(±2.6)	-37.0
	k_2	19.0	16.4(±2.4)	-9.0
5'-dGMP P/D= 186	k_1	20.3	7.9(±3.2)	-42.3
	k_2	18.6	16.8(±2.9)	-6.1

[a]From Bittman & Blau, 1977)

therefore even more surprising that slow kinetics are observed in the association of ActD to mononucleotides. The possible implications of this observation will be developed in the conclusion of this section.

Association kinetic data of ActD to oligonucleotides is summarized in Table IV. Two slow unimolecular processes are observed for each oligomer and no variation between oligomer lengths and rate constants is found within experimental error. The kinetics of dATGCAT association to ActD was investigated in more detail since the presence of a single binding site is expected to simplify the kinetic behavior. Three unimolecular steps and at least two bimolecular steps are observed to this oligomer (Table V). Apparent second order rate constants ($\simeq 1 \times 10^6$) are intermediate to those found for association to DNA($\simeq 4 \times 10^4$) and actinomine to DNA(4×10^6). Uncertainties in fits of experimental curves, especially for k_3-k_5 obviate more quantitative treatment of this data. Enough data to test against kinetic models will not be available until dissociation kinetics for ActD/oligonucleotide systems can be appropriately measured. The presence of three slow unimolecular processes

TABLE IV

Slow Unimolecular Kinetic Parameters for the Association of ActD with Oligonucleotides

Species	DS/D[a]	$k_1(x10^3)$ s^{-1}	$\%\Delta OD_{tot}$	$k_2(x10^2)$ s^{-1}	$\%\Delta OD_{tot}$
dCGCGCGCG	0.3-1.2	4.0(±.5)	5	5.5(±.7)	8
dGCGCGC	1.0-4.6	3.0(±.2)	6	3.4(±.6)	9
dATGCAT	1.5-4.0	2.55(±.2)	2.4	3.8(±.7)	8
dCGCG	1.7-4.6	3.6(±.5)	4	4.2(±.4)	9
dGC	20-27	3.1(±.8)	3	5.8(±1.2)	4

[a]Concentration ratios as double strand of oligonucleotide to drug

TABLE V

Comparison of ActD Association Kinetics to DNA and dATGCAT[a]

Process[b]	DNA(P/D=20)	dATGCAT(DS/D=1.5)	dATGCAT(DS/D=4)
k_1	$3.5x10^{-3}$(5)	$2.7x10^{-3}$(2.4)	$2.7x10^{-3}$(5)
k_2	$5.0x10^{-2}$(10)	$4.6x10^{-2}$(6)	$4.0x10^{-2}$(8)
k_3	.55(20)	1.0(6)	0.8(2.5)
		2.9(18)	2.1(3.5)
k_4	5.0(35)	11.(45)	39.(40)
k_5	54.(20)	52.(18)	85.(35)

[a]in BPES buffer, T=20°C.

[b]entries are rate constants(s^{-1}) and $\%\Delta OD_{tot}$(in parantheses)

of similar rate constants to those found for DNA implies that the mode of binding to dATGCAT is similar to that of DNA. The structure of this complex should be similar to that of ActD bound to a isolated ATGCAT site in the DNA double helix. Additionally, the CD spectrum of this complex is identical to that of the DNA complex (Figure 8).

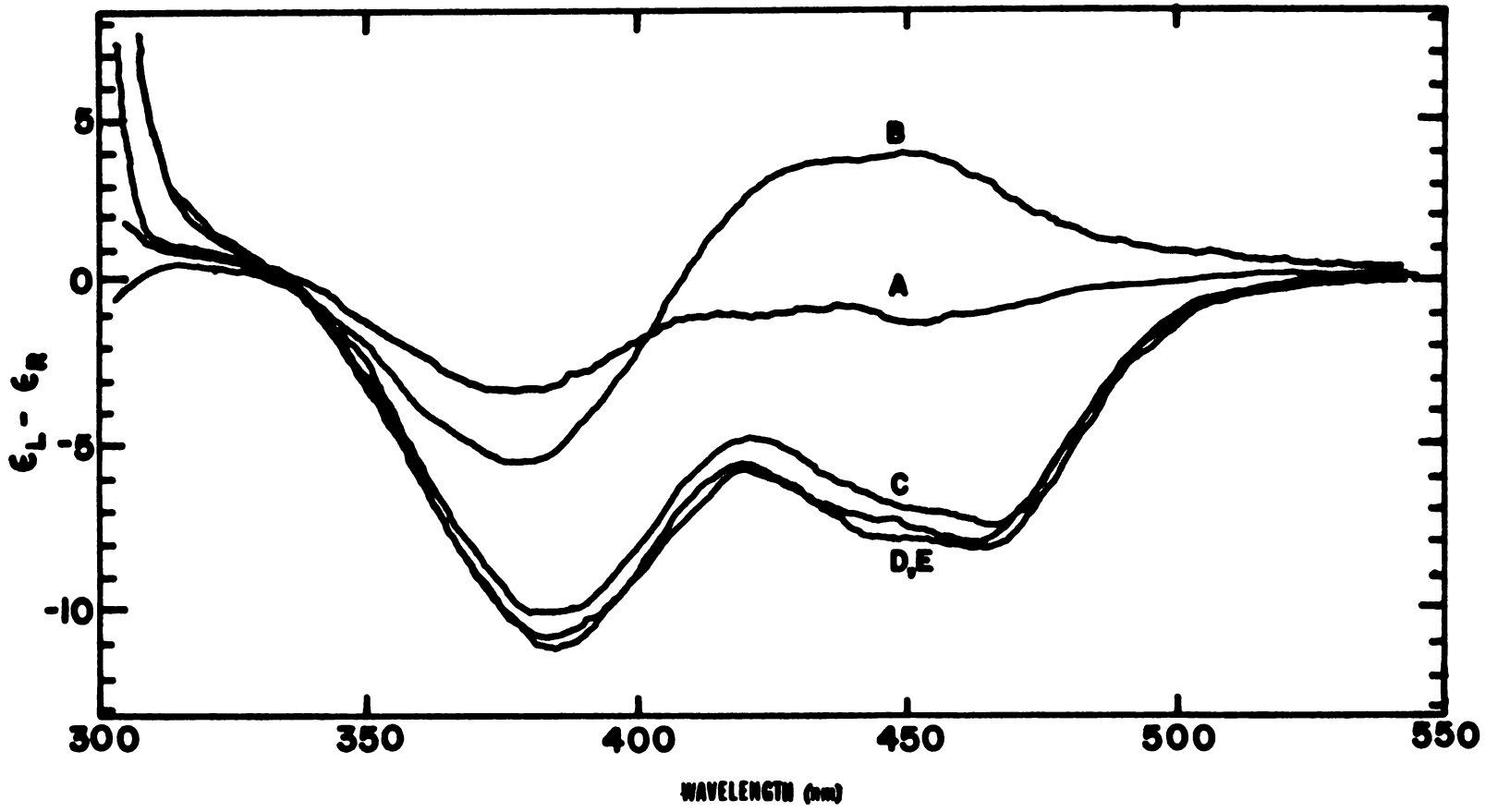

Figure 8

CD spectra of ActD and ActD bound to various nucleotides; A) Free ActD; B) bound to 5'-dGMP(P/D=380); C) ActD bound to poly dGC(P/D=28); D)ActD bound to DNA(P/D=80); E) ActD bound to dATGCAT(DS/D=10). [ActD] = 1.84×10^{-5} M., T= 20 °C.

Association/Dissociation Kinetics of Actinomycin D and Poly dGpC

The association and SDS-dissociation of ActD to poly-dGpC was investigated since published reports of the kinetic behavior of this system were anomalous to results from other polynucleotides, where multiple unimolecular processes of association and dissociation are found. One group reported a single dissociation process involving the total OD change of dissociation (Krugh et al., 1980). Another group (Bittman & Blau, 1977) reported the observation of multiple processes during association reactions. Results of experiments with ActD and poly dGpC are found in Table VI. Multiple association processes comparable to those found for DNA were observed, but dissociations using SDS confirmed the results of Krugh et al., the entire OD change during dissociation fit to a single exponential (Figure 9) whose time constant was dependent on the initial proportion of ActD:poly-dGpC. Thus, the behavior of poly-dGpC is unique compared to that of DNA, oligomers, and

TABLE VI

Actinomycin D/Poly-dGC Kinetics		
Associations[a]		
k_1 s^{-1}	k_2 s^{-1}	k_3 s^{-1}
$3.8(\pm.5)\times10^{-3}$(7%)	$4.6(\pm.7)\times10^{-2}$(14%)	.525(40%)
Dissociations[b]		
Initial P/D	rate constant(s^{-1})	$\%\Delta OD_{tot}$
13	5.4×10^{-4}	(100%±2)
32	8.5×10^{-4}	(97%±5)

[a] P/D range= 5.5-41.0, T=20.0°C.
[b] SDS(4%) driven, T=20.0°C.

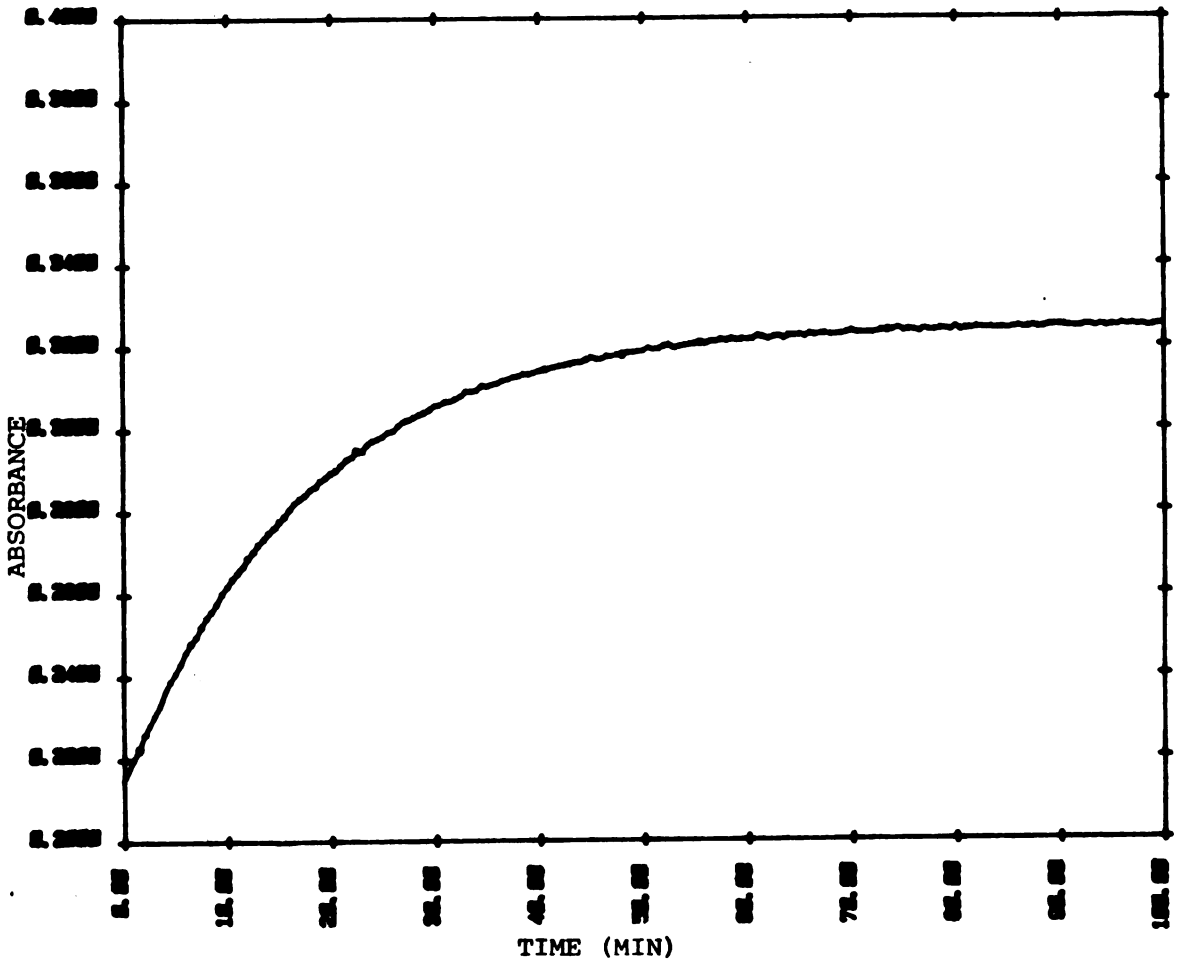

FIGURE 9

Representative kinetic trace of ActD dissociation from poly-dGC driven by mixing with a 4% SDS solution, monitored at 425 nm. Semilogarithm plot of this data reveals a single straight line. The entire OD change during dissociation from poly-dGC occurs in this single kinetic process.

mononucleotides.

This finding of a single dissociation process that is P/D dependent (Figure 10) was interpreted (by Krugh et al.) as meaning: 1) Multiple slow dissociation/association processes derive from binding site heterogeneity and 2) the dissociating complex's behavior is dependent on its history. With regard to the first interpretation, multiple processes are still observed upon association of ActD and poly-dGpC that compare well to the kinetic behavior with DNA, oligomers, and even mononucleotides. Moreover, similar multiple kinetic processes are observed in the association to dATGCAT, which contains a single strong binding site. The second interpretation implies a memory effect of the bound actinomycin on the polynucleotide lattice. The published data does not strongly support this conclusion. Inspection of the dissociation data (Figure 6 in Krugh et al., 1980) reveals a curvature in the semilogarithm plots of $\ln(\Delta OD_{(t)}/\Delta OD_{(tot)})$ vs. time at intermediate P/D(17.7) that is not present at high(P/D=7.1) or low(P/D=73.4) drug binding levels. Thus, it is likely that the P/D dependence reflects two exponential processes, whose rate constants vary by a factor of two or so, and whose relative contributions to $\Delta OD_{(t)}$ vary with initial P/D.

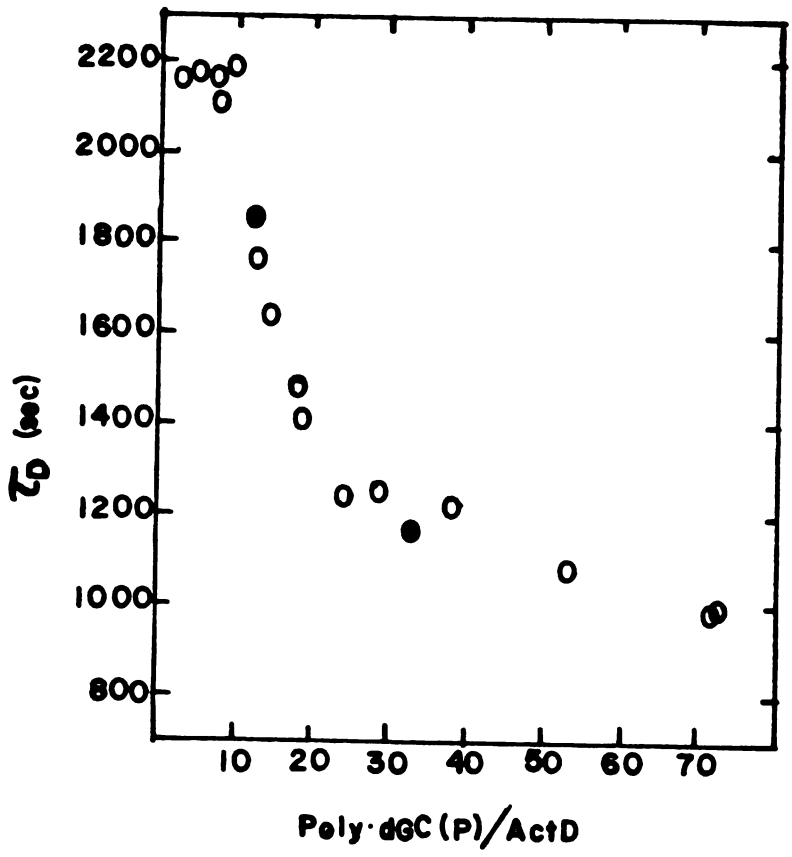

FIGURE 10

Dependance of the ActD dissociation lifetime from poly-dGC on the saturation level of the double helix. Open circles are taken from Krugh et al., 1981; closed circles are data from the present study.

Conclusions

It is difficult to envision, let alone prove what structural changes are occuring at the molecular level which lead to slow kinetics of ActD association to mononucleotides. However, given that these changes occur whenever ActD bind to guanine (or at higher concentrations, adenine) containing monomers and that the rate constants of the two slowest unimolecular processes are independent of nucleotide length, the appearance of slow kinetics reflects a property of the drug alone, when stacking to purine bases containing exo-amino groups. For NMR structural investigations of the ActD/DNA complex, it would be advantageous to use an oligonucleotide that most closely resembles the kinetic behavior of the ActD/DNA system and that contains a single strong binding site. The oligonucleotide dATGCAT posesses these qualities. The hexanucleoside pentaphosphate is also of sufficient length to interact with the pentapeptide lactone moieties. The binding constant is of the same order of magnitude as that to DNA, and the CD spectra of the two complexes are identical as well (Figure 8). This oligonucleotide was therefore chosen as a model compound of DNA for the NMR investagations.

The peculiar kinetic behavior of ActD dissociation from poly-dGpC could be due to several reasons, but this behavior is unique among all the nucleotide systems investigated and is not representative of the ActD/DNA interaction. It was suggested that the observation of a single process of dissociation from poly-dGpC implied that multiple processes observed during dissociation from DNA were due to heterogeneity of binding sites-each site possessing a single dissociation process (Krugh et al., 1980). However, it is clear that mul-

tiple processes are still observed during association of ActD to poly-dGpC and that these processes have similar rate constants and $\%\Delta OD_{tot}$ to those observed in the association of ActD to DNA, dATGCAT, and other oligo- and mononucleotides. Further studies of ActD dissociation from poly-dGpC may reveal that there are indeed at least two slow processes, but that they have more similar rates (x2) than those found for other systems (x10).

^{15}N-NMR Studies of Biosynthetically Labeled [^{15}N]Actinomycin D

Introduction

In order to obtain information concerning the conformation and dynamics of the actinomycin D pentapeptide lactones when bound to DNA, it was necessary to label the molecule with an NMR probe. Otherwise, the large number of unresolved resonances in DNA would severely limit the acquisition of interpretable data. It was known that exogenously supplied amino acid precursors could be biosynthetically incorporated into the actinomycin pentapeptide lactones under certain conditions (Meienhofer & Atherton, 1972). The 3' amino acid (proline in ActD) was considered to be the optimum position to place a label which could probe the conformation and dynamics about the 2'-3'-4' portion of the cyclic ring shown by Lackner (1975) to be capable of adopting different conformations in solution. Substitutions at the 3' amino acid also produced dramatic changes in the dissociation kinetics of actinomycin cogeners from DNA (Shafer et al., 1980; Mirau et al.,1982a).

Fluorine-19, carbon-13, nitrogen-15, and deuterium were considered as candidates for substitution into the proline residue of actinomycin D. These nuclei would minimally perturb the structure of the molecule and provide suitable NMR probes for solution studies. It was of particular interest to moniter the peptide bonds and hydrogen bonding properties of ActD. Whereas ^{13}C, ^{19}F, or ^{2}H probes would be relatively distant from the atoms of interest, ^{15}N probes would be optimally situated to provide the desired information. Isotopic enrichment was necessary, since the natural abundance of ^{15}N is only 0.37% and the relative sensitivity to protons is only 1.04×10^{-3} due

to the low gyromagnetic ratio of this nucleus. Fortuitously, the bacterial strain *actinomycetes parvulus* utilizes glutamate as its sole nitrogen source and produces only actinomycin D as a major product (>90% of total actinomycins produced). Thus, it appeared feasable to efficiently label all 12 nitrogens on ActD to a high degree (>90%) by utilizing ^{15}N-glutamate and this bacterial strain.

Investigations of various peptide systems by ^{15}N-NMR had demonstrated the utility of this technique in monitoring solvent accessibility, hydrogen bonding, and *cis/trans* peptide bond equilibria. For a review of the NMR properties and applications of ^{15}N, see "Nitrogen-15 Nuclear Magnetic Resonance Spectroscopy", (ed. G. C. Levy and R. L. Lichter), Wiley, New York, 1979. Studies on the cyclic decapeptide gramicidin S (Hawkes et al., 1975; Khaled et al., 1978; Hawkes et al., 1980) showed that the solvent dependence of the ^{15}N chemical shift in amide bonds reflects exposure of the carbonyl group to solvent. Transfer from non-hydrogen bond donating solvents (e.g., DMSO) to hydrogen bond donating solvents (e.g., methanol, 2,2,2-trifluoroethanol) causes large downfield shifts (5.0-7.5 ppm) of ^{15}N resonances in amide bonds where the carbonyl group is exposed to solvent and the amide proton either does not exist (e.g., proline) or is buried in an intramolecular hydrogen bond. Smaller upfield shifts occur for amide bonds when the carbonyl is buried and the proton is exposed to solvent. A study of the cyclic peptide hormone oxytocin and a related peptide by ^{15}N-NMR showed that the ^{15}N chemical shifts in water correlated to the relative shifts of the correspoding N'-acetyl amino acids in DMSO. Deviations from this correlation could be related to conformational restrictions or lack of exposure to solvent (Live et al., 1979). Another method for probing hydrogen bonding by ^{15}N-NMR is observation of the ^{15}N-H scalar coupling collapse due

to rapid proton exchange upon the addition of base (Hawkes et al., 1978). Amide protons involved in hydrogen bonds, or buried from solvent, will not exchange as rapidly as amide protons exposed to solvent under basic conditions. This technique could not be applied to actinomycin due to the base sensitivity of the lactone functional group and the chromophore.

Several studies of peptides by ^{15}N-NMR have shown the utility of this method for the detection of *cis/trans* isomerism of amide bonds involving proline. An investigation of the cyclic peptide:

[gly(1)--pro--gly(2)--D-ala--pro--]

demonstrated an equilibrium (~1:4) between *cis* and *trans* configurations of the gly(1)-pro peptide bond that led to ^{15}N chemical shift differences of 2.4 ppm in the gly(1) resonance and a 0.5 ppm difference in the gly(2) resonance (Williamson et al., 1979). Another demonstration of *cis/trans* proline configurational equilibria in peptides revealed ^{15}N chemical shift differences of 0.3-5.0 ppm at the proline and neighboring residues (Hull & Kricheldorf, 1980). Thus, ^{15}N-NMR can be a highly useful technique in probing conformations of peptides similar to the pentapeptide lactone moieties found in the actinomycins.

Materials and Methods

Chemicals, Reagents, and Isotopes. Solvents are from Aldrich(Gold Label) while deuterated solvents are from Stohler Isotopes. Dimethyl Sulfoxide(DMSO), chloroform, and methanol were dried over 3 Å molecular sieves for NMR experiments. The protocol for production and purification of [^{15}N]ActD is presented in Appendix I.

Mass Spectrometry. Mass spectra were acquired at the NIH Regional Facility at the Space Sciences Laboratory, University of California at Berkeley. Spectra were acquired using a homebuilt cesium SIMS source mounted on a Kratos MS-50. Data was accumulated and stored on the homebuilt LOGOS-II system and plotted out as intensity vs. mass to charge ratio(m/z). Samples (~100-500 μg.) were dissolved in a drop of glycerin and placed on the copper stage of the probe. The SIMS source was turned on after high vacuum was re-established and spectra were acquired by repeated slow scans(8 seconds/decade) from m/z 1500-500. The mass calibration of the instrument was done by running mass standards (either Fomblin or KI) immediately before and after the experimental runs. Constant B/E scans were done to probe for fragmentation of the molecular ion, but no significant fragmentation was observed. Only positively charged ions were measured. SIMS ionization usually produces even electron pseudo-molecular ions at an m/z of $[M+H]^+$.

NMR. Proton spectra at 100 MHz and ^{15}N spectra at 10.14 MHz were obtained on a Varian XL-100 in the FT mode equipped with a Nicolet 1080 data system. Spectra were also obtained on the homebuilt widebore system (5.64T) using the Nicolet 1180 data system and a 293B pulse programmer at the UCSF magnetic resonance laboratory. ^{15}N-NMR spectra of [^{15}N]ActD in chloroform were also obtained at 20.5 MHz on the UCB-200 spectrometer at the University of California, Berkeley Chemistry Dept. NMR facility. ^{15}N spectra at 50 MHz of [^{15}N]ActD bound to digested DNA fragments were obtained at the Southern California Regional High Field NMR Facility at the California Institute of Technology. ^{15}N spin-lattice relaxation times were measured by fast inversion recovery(delay>$3T_1$) at ten τ values and fitted to a two parameter equation (Hanssum et al., 1978) using a non-linear least squares

Marquardt-Levenberg fitting routine.

^{13}C carbonyl assignments at 60.5 MHz of [^{15}N]ActD in chlorcform were done by triple irradiation and run unlocked. Spectra were accumulated over 5 hrs. each, the stability of the superconducting magnet and electronics being better than 3 Hz over this time period. Protons were continuously decoupled using the decoupling coil while ^{15}N resonances were selectively irradiated using the retuned lock coil. All other spectra were obtained with either an external or internal deuterium lock as indicated. Proton and carbon spectra were referenced to internal Tetramethylsilane(TMS), while ^{15}N spectra were referenced to external neat formamide.

DNA digestion. One gram of calf-thymus DNA(Sigma) was digested enzymatically by DNAse II and S1 nuclease (Early & Kearns, 1979). The reaction was quenched after ~90% completion as determined by the observed optical density increase at 260 nm. The DNA was phenol extracted twice, washed with ether(x3) and ethanol precipitated(x2). The DNA was then taken up in BPES buffer and dialyzed extensively. A sample was loaded onto a polyacrylamide gel(5%, 40:1, 2mm) and electrophoresed at 150 Volts, constant voltage in standard TBE buffer(Tris-Borate-EDTA, pH=8.0). Neighboring lanes contained $d(pGpC)_4$, $d(pGpC)_3$, and a HAE III digest of Φx-174RF(Bethesda Research Labs) containing fragments at 1353, 1078, 872, 603, 310, 281, 234, 194, 118, and 72 base pairs as standards. The gel was stained with ethidium bromide and photographed with Polaroid film. Resolution of the standards was excellent and the digested DNA was calculated to have an average length of 40 base pairs with a distribution of ±30 base pairs(2σ). The digested DNA had an OD260/OD280 ratio of 1.86, a melting point at 36°C. in BPES buffer and bound ActD(P/D=18) shifted the melting

point to 58°C. in the identical buffer.

Results and Discussion

Characterization of [^{15}N]Actinomycin D. The optical spectrum of [^{15}N]ActD in ethanol(95%) and in BPES buffer was identical to that of unlabeled ActD. The extinction coefficients at various wavelengths in BPES were determined to be identical to those of the unlabeled standard as well. The labeled compound bound to DNA, showing the same characteristic changes in the visible spectrum as authentic ActD. Thin layer Chromatography (Silica Gel 60, F-254) in three solvent systems [100% ethyl acetate, 100% methanol, (n-butanol, acetic acid, water(6:2:2))] revealed a single yellow spot with R_f values identical to standard ActD. No other spots could be visualized by UV absorption or H_2SO_4 charring.

Partial proton NMR spectra at 240 MHz of [^{15}N]ActD and ActD in chloroform are shown in Figure 11. This region contains the valine and threonine amide protons, each appearing as a doublet due to scalar coupling to the corresponding H^{α} proton. Assignment of peaks to the α- or β- peptides was achieved by Lackner (1971) using selective deuteration. The spectra are identical except for the characteristic one bond ^{15}N-^{1}H scalar coupling constants of 92.5(±0.3) Hz found for the amide protons of the labeled compound. The measured $^{1}J_{^{15}N\text{-}^{1}H}$ values for these amide protons are within the range determined for amide bonds in the *trans* configuration(92.1-94.5 Hz) rather than that for amide bonds in the *cis* configuration(89.3-91.1 Hz), consistent with the crystal structure (Jain & Sobell, 1972) and previous ^{13}C and ^{1}H NMR studies (Lackner, 1975). Longer range coupling constants are not readily

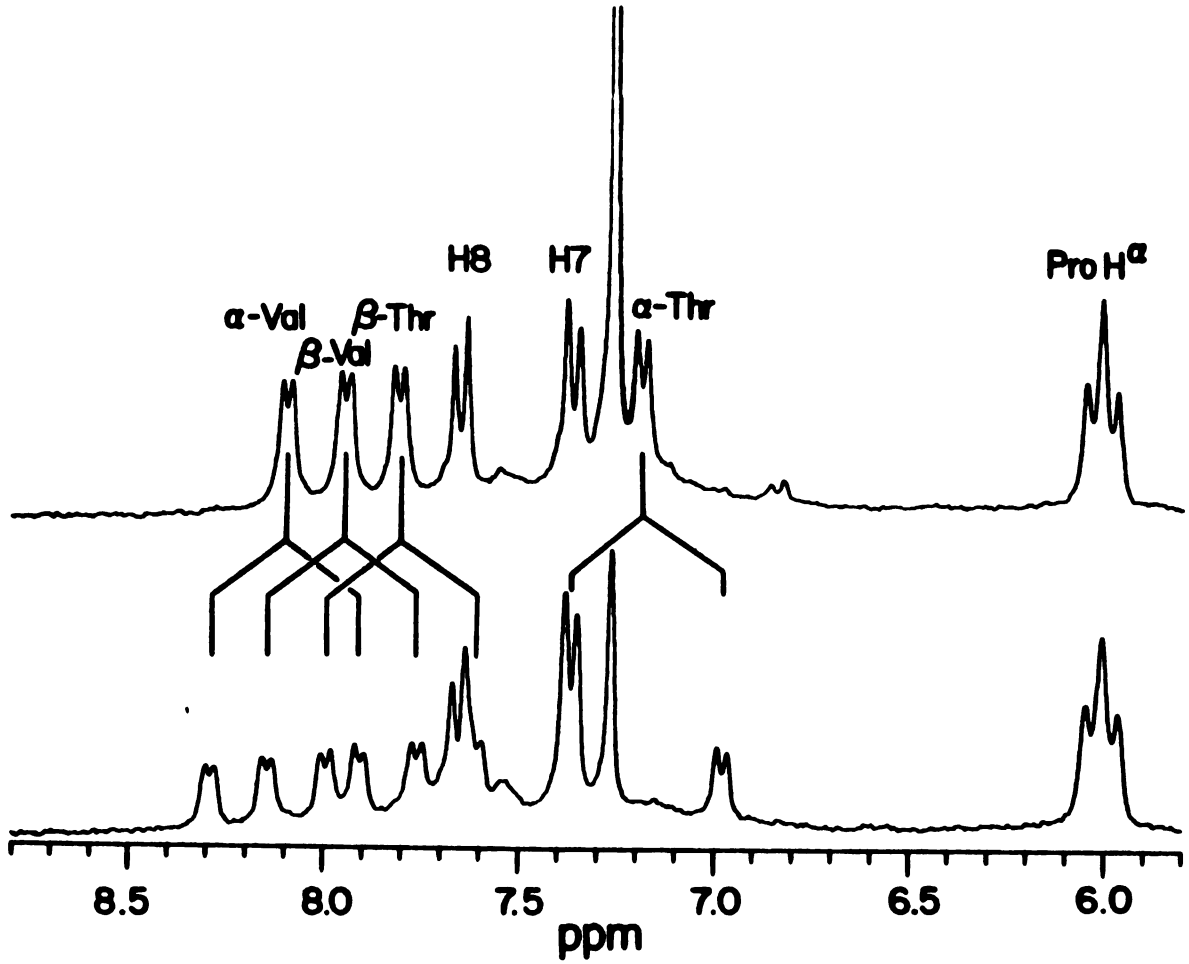

FIGURE 11

Low field portion of the ^{1}H-NMR spectra at 240 MHz. of Actinomycin D(Top) and (^{15}N)Actinomycin D(Bottom) in $CDCl_3$(10 mM.). T= 20 C., 600 transients each. Assignments by selective deuteration (Lackner, 1971).

apparant in the higher field portion of the [^{15}N]ActD proton spectrum, but they are expected to be very small, on the order of 0-3 Hz. The absence of any significant intensity at frequencies expected for unlabeled ActD in the labeled spectrum attests to the high level of labeling achieved at the valine and threonine nitrogens.

Mass spectra of [^{15}N]ActD and ActD are presented in Figure 12. The pseudo-molecular ion of [^{15}N]ActD is found 12 mass units higher (1269.5) than that of ActD(1257.4). Constant B/E scans were done to measure fragmentation of the pseudo-molecular ion, but very little was observed due to the stability of this species. However, the pseudo-molecular ions are both found 2 mass units higher than expected with this technique. Usually, SIMS ionization from the glycerin matrix yields $[M+H]^+$ even electron ions, which in the case of ActD(M.W.=1254.6) would be found at m/z= 1255.6 amu. The mass calibration of the spectrometer was checked by two different standards (Fomblin and KI) and found to be accurate before and after the mass measurement of the actinomycins was done. It was thought that a two electron reduction of the ActD chromophore had possibly occured with the addition of two protons in the glycerin matrix during ionization and transfer to the gas phase. Daunomycin, another DNA intercalating drug that contains an easily reduced quinone function, was tested in the mass spectrometer and found also to yield a pseudo-molecular ion 2 mass units higher than expected. This unusual behavior was not investigated further, but the fact that the pseudo-molecular ion of [^{15}N]ActD is found 12 mass units heavier than that of ActD indicates a 90-95% level of labeling at all 12 nitrogens in the molecule.

^{15}N-NMR. The ^{15}N-NMR spectrum of [^{15}N]ActD at 20.5 MHz in $CDCl_3$ is shown in Figure 13. The spectrum obtained with the ^{15}N-^{1}H nuclear

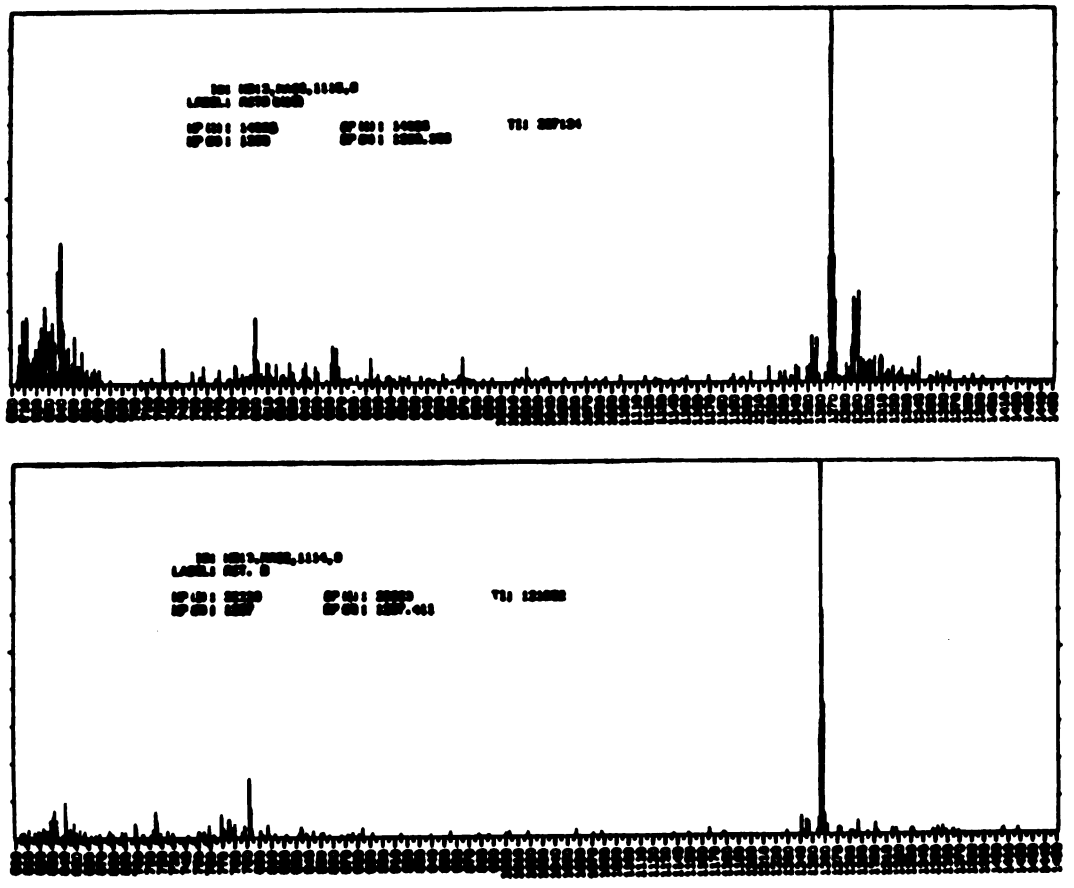

FIGURE 12

Mass spectra of Actinomycin D(Bottom) and (^{15}N)Actinomycin D(Top), using SIMS soft ionization, under identical conditions. The pseudo-molecular ion of the ^{15}N labeled compound is 12 atomic mass units heavier than that of the unlabeled compound. See text for experimental details.

Overhauser effect (NOE) shows six resonances while the spectrum obtained without NOE displays all seven resonances. The farthest downfield peak in the latter spectrum is due to the phenoxazone nitrogen and was always nulled under NOE conditions. This is due to the absence of nearby protons for this atom, so the proportion of relaxation contributed by dipolar coupling compared to CSA or other mechanisms is less for this nitrogen than for others in the molecule. The NOEF for this atom is therefore 1 rather than -4 to -5 at the overall correlation time for this molecule. All other peaks were inverted when spectra were obtained with NOE due to the negative gyromagnetic ratio of the ^{15}N nucleus. Figure 14 presents ^{15}N-NMR spectra at 24.1 MHz with and without proton decoupling, but both with NOE. As can be seen in both Figures 13 and 14, all resonances (especially proline, D-valine and threonine) appear split due to the magnetic nonequivalence of the α- and β-pentapeptide rings. The proton NMR spectrum of ActD shows the most magnetic nonequivalence in the same three residues.

Assignment of the ^{15}N resonances was accomplished by analogy with model compounds, proton decoupling, and selective $^{15}N\{^{1}H\}$ NOE experiments. The data in Figure 14 reveal that the only resonance appearing as a triplet in the proton coupled spectrum is the one at -30.4 ppm, which must be the 2-amino nitrogen on the chromophore. This chemical shift is typical of aromatic amines(Levy & Lichter, 1979). The phenoxazone ring nitrogen (N10) was assigned to the farthest downfield resonance at 172.4 ppm in the bottom spectrum of Figure 13, based on the large deshielding typical of pyridine-like nitrogens and the nulling of the resonance when the ^{1}H-^{15}N NOE is applied.

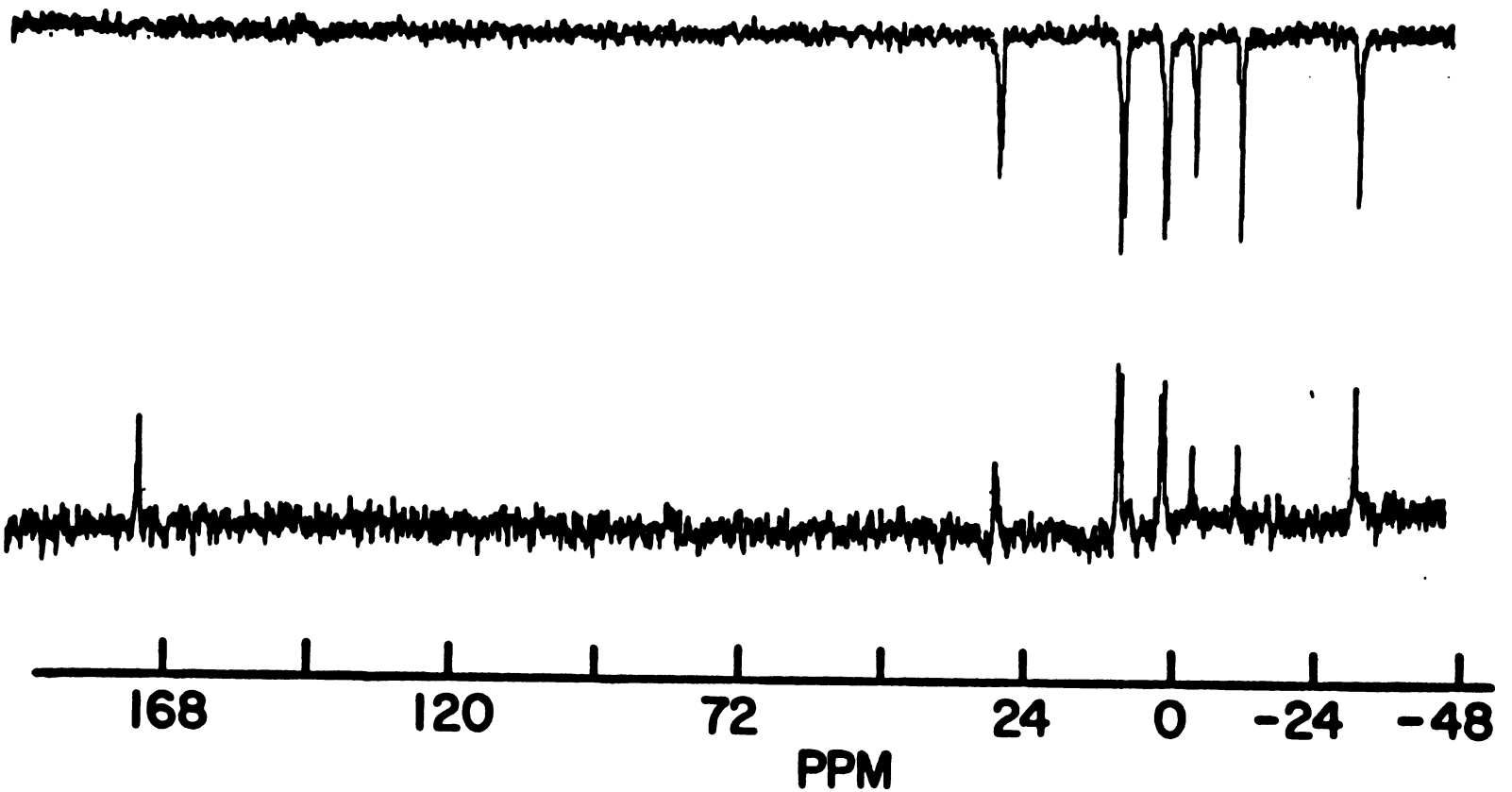

FIGURE 13

^{15}N-NMR spectra at 20.5 MHz. of (^{15}N)Actinomycin D, 17 mM. in $CDCl_3$ at 22 C: with broad band proton decoupling and NOE, 332 transients (top); with gated decoupling to suppress the NOE, 1000 transients (bottom). Spectra were obtained with a 45 degree pulse, a 1.2 second acquisition time, and a 5 second delay, referenced to external neat formamide.

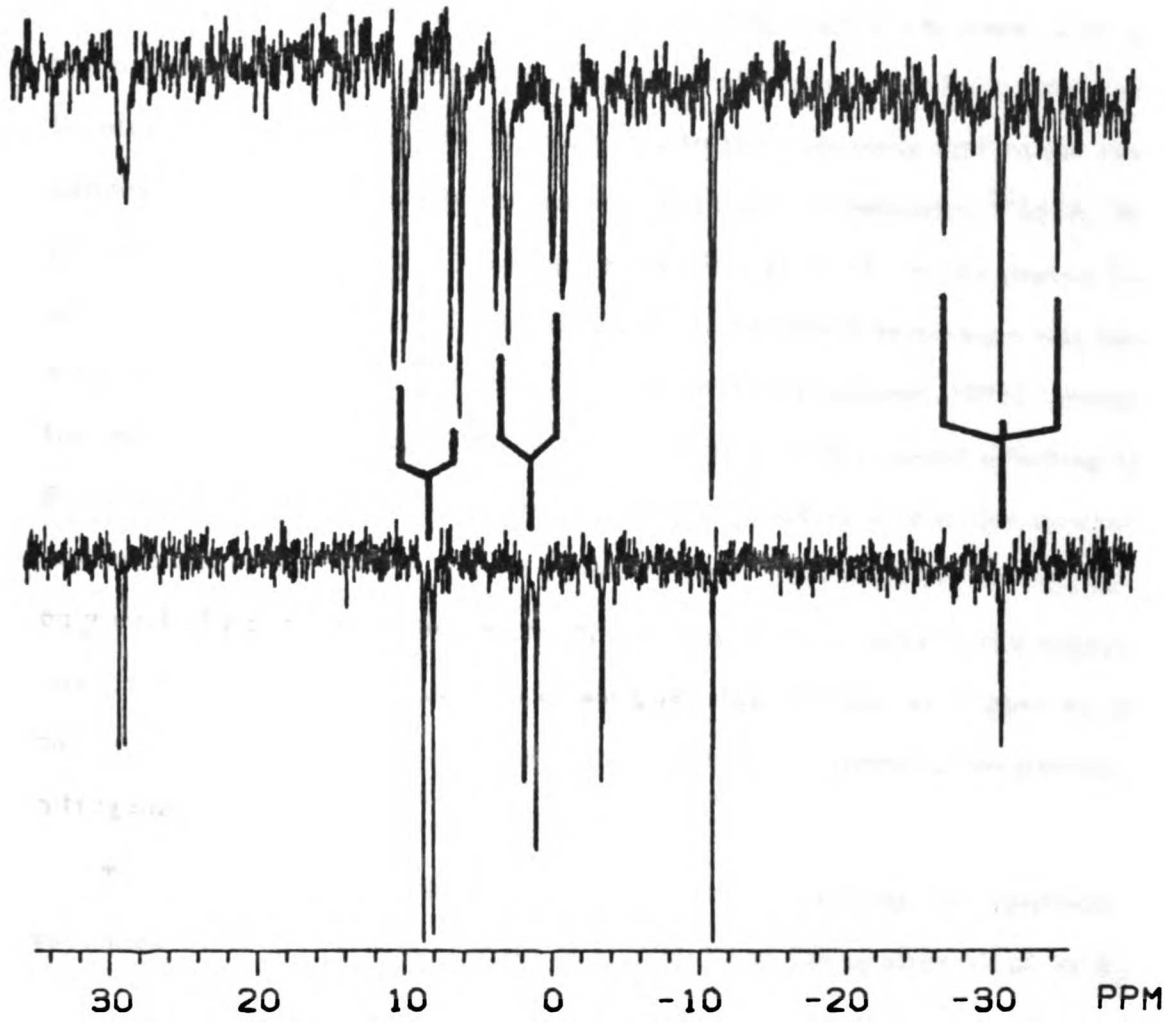

FIGURE 14

^{15}N-NMR spectra at 24 MHz. of (^{15}N)Actinomycin D(12 mM.) in $CDCl_3$ at 15 C. with broad-band proton decoupling and NOE (bottom) and with gated decoupling to retain the NOE and ^{1}H coupling (top). Spectra were obtained in 600 transients with a 45 degree pulse, a 1.5 second acquisition time, and a 0.5 second delay.

The spectrum obtained by gated decoupling (Figure 14) shows that the two doublets at 8.4 and 7.8 ppm and at 1.6 and 0.9 ppm arise from singly protonated nitrogens which must correspond to the threonine and valine resonances. Assignment of these resonances was made by selective $^{15}N\{^{1}H\}$ NOE experiments, the results of which are shown in Figure 15. In the proton NMR spectrum of ActD in chloroform, the farthest downfield resonance has been assigned to the α-valine (Figure 11) amide proton (Lackner, 1971). Irradiation was carried out downfield from the α-valine proton to avoid affecting the β-threonine amide proton. As seen in Figure 15(middle), a selective inversion of the nitrogen resonance near 8 ppm resulted. This negative resonance is only partially decoupled due to the off-resonance conditions of the continuous proton irradiation. This firmly assigned the doublet at 8 ppm to the valine nitrogens and, consequently, the doublet near 1 ppm to the threonine nitrogens.

The β-threonine nitrogen was assigned by monitering the kinetics of exchange by both ^{15}N and ^{1}H-NMR of [^{15}N]ActD in $CDCl_3$ after 10 μl. of D_2O was added to the dry chloroform. The *thr* nitrogen at lower field(1.6 ppm) disappeared over several hours in concert with the amide proton assigned to β-threonine, thus assigning this resonance to the β-threonine nitrogen. The other threonine nitrogen resonance disappeared more slowly, while the two valine resonances were not exchanged until several days had passed. The disappearance of the proton resonances is directly due to their exchange with deuterium, while the disappearance of the ^{15}N resonances is due partly to the quadrapolar relaxation and partly to the one bond coupling of the deuterium nucleus.

Assignment of the sarcosine and methylvaline resonances was done in a similar fashion. Selective continuous irradiation of one of the sarcosine H^{α} protons produced the spectrum shown in Figure 15(bottom). While no inversion of any resonances occurred, the peak at -10.9 ppm showed a substantial loss of intensity. Thus, this resonance is assigned to sarcosine. As this nitrogen is not directly bonded to a proton, it is likely that both the methylene and N-methyl protons contribute to its relaxation. Consequently, it is expected that irradiation of only the former would give rise to only a partial NOE, as observed.

Finally, selective irradiation of the proline H^{α} protons also resulted in the doublet at 29.4 and 28.9 ppm in Figure 15 losing intensity to the level of noise(data not shown), assigning it to the proline nitrogens. This is consistent with the general observation that proline resonances are found substantially downfield from all other peptide ^{15}N resonances. This then leaves the peak at -3.4 ppm in Figure 15 assigned to methylvaline, thereby completing the assignments. Assignments in other solvents were done by progressively changing the solvent composition in binary mixtures, from $CHCl_3$ to DMSO or methanol and finally to water. These solvent titrations were done using external neat D_2O in a coaxial tube.

Solvent Exposure Studies. As explained in the introduction to this section, ^{15}N-NMR studies have demonstrated the utility of this technique for probing the hydrogen bonding and solvent exposure properties of peptide nitrogens and carbonyls. A similar approach was used in an effort to characterize the conformation of the ActD pentapeptide lactones in various solvents, particularly water, and when the drug was bound to DNA and other nucleotides.

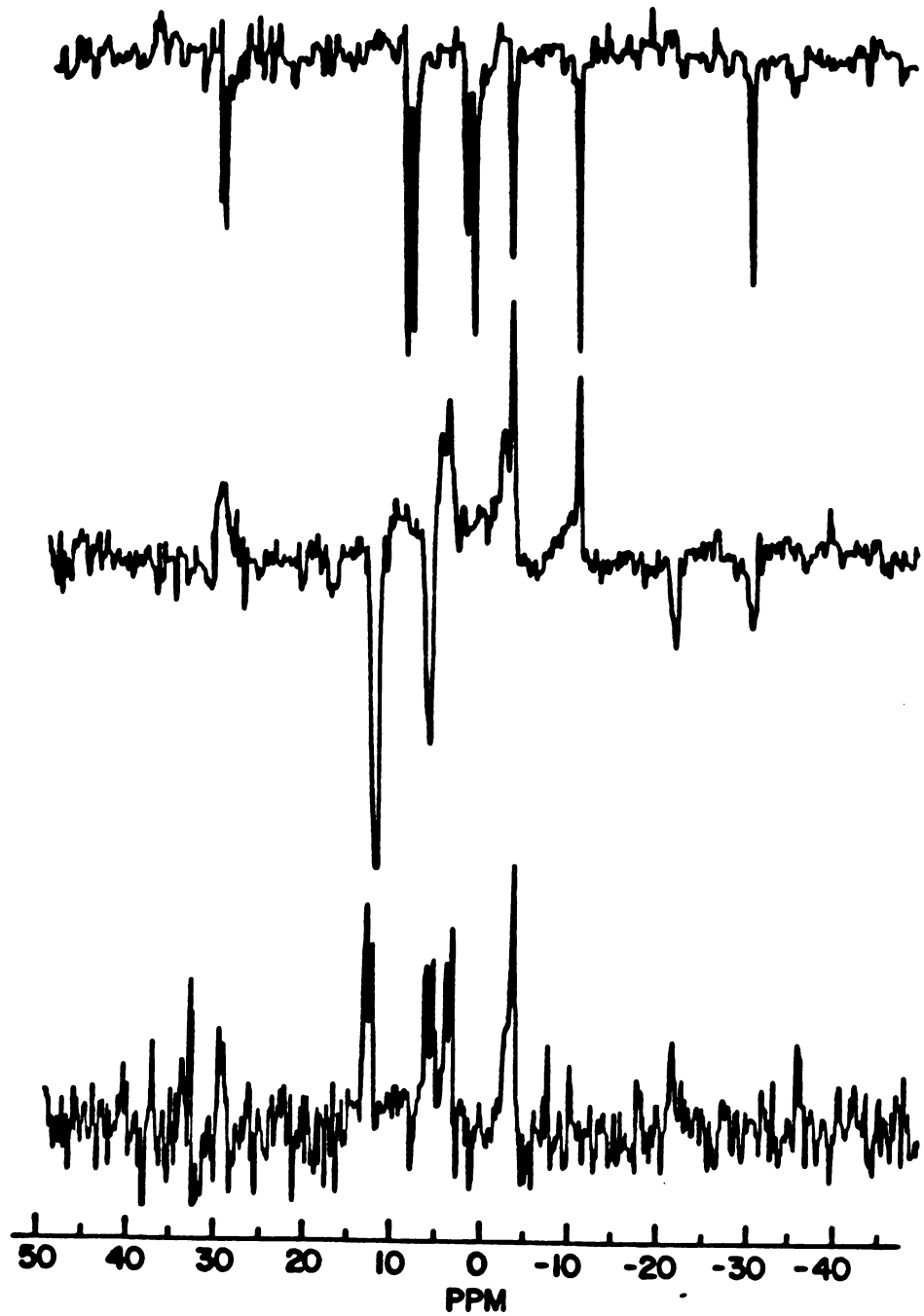

FIGURE 15

Selective NOE spectra of (^{15}N)Actinomycin D (10 mM.) in $CDCl_3$ at 10.14 MHz: with broadband ^{1}H decoupling and NOE, 600 transients (top); with selective irradiation downfield from the Dva amide protons (middle); and with selective irradiation of the low field sar H^{α} resonance (bottom). Selective NOE spectra were obtained in 15,000 transients.

Lackner (1975) had summarized the currently available data pertaining to the conformation of ActD in various solvents. The molecule appears to have a rigid structure whose conformation is essentially the same in organic solvents and water. This apparent conformational rigidity allows a more confident interpretation of chemical shift changes as arising from solvation effects rather than conformational changes. Interpretation of the spectrum in water is somewhat complicated by the existence of a monomer/dimer equilibrium which, at the aqueous concentrations required for these ^{15}N-NMR studies, leads to relative populations of roughly 40% monomer and 60% dimer in fast exchange on the NMR time scale. Interpretation of the spectrum in water is aided by the ActD dimer model proposed by Angerman et al.(1972) based on proton chemical shifts as a function of concentration. The model consists of two ActD molecules with their chromophores stacked, the quinoid ring of one over the benzenoid part of the other, and vice versa. Proton chemical shifts on the peptide groups show little or no dependence on ActD concentration, and thus the peptide rings are assumed not to interact so that a conformational change occurs upon ActD dimer formation. Later experiments involving transient proton-proton NOE observations of ActD in water confirm this model of the aqueous dimer structure *(vide infra)*. Binary solvent mixtures of differing methanol:water ratios showed no significant change in ^{15}N chemical shifts until the concentration of water exceeded 93 mol%. Thus, the spectrum in methanol may closely approximate that of the ActD monomer in water.

Spectra of [^{15}N]ActD in various solvents are shown in Figure 16 and the chemical shifts are listed in Table VII. All the peptide resonances are shifted downfield when the solvent is changed from a hydrogen bonding acceptor (DMSO) to a hydrogen bond donator/acceptor (water). The downfield shifts

can be explained in terms of solvent effects at the amide hydrogen and carbonyl groups. Solvent interactions resulting in electron delocalization lead to downfield shifts (Llinas et al., 1976; Khaled et al., 1978). Usually, donation of an amide proton to an acceptor solvent produces a small upfield shift while donation of a solvent proton to an amide carbonyl (Hawkes et al., 1980) leads to a larger downfield shift. Interpretation of the N-substituted amino acid chemical shift changes is facilitated by the absence of an amide proton, so solvent perturbations of the ^{15}N chemical shift are due to interactions at the carbonyl group of the previous residue in the peptide chain. Thus, the downfield shift of ~7 ppm for the sarcosine(sar) resonance upon transfer from DMSO to water reflects the hydrogen bonding donation of H_2O to the proline(pro) carbonyl, which must be exposed to solvent. This shift is somewhat larger than that seen by Kricheldorf et al. (1977) for polysarcosine undergoing the same change in solvent (~5 ppm), but is approximately the same magnitude and direction. The N-methylvaline (nmv) and *pro* resonances shift downfield by 5-6 ppm when the solvent is changed from DMSO to water, which suggests that the *sar* and *Dva* carbonyls are also exposed to solvent. Alternatively, these downfield shifts could indicate the presence of intramolecular hydrogen bonding patterns in the water dimer that are not present in DMSO. These shifts are similar to those observed in gramicidin S for the valine nitrogen, whose amide proton participates in an intramolecular hydrogen bond, and for the proline nitrogen upon transfer from DMSO to trifluoroethanol(Khaled et al., 1978; Hawkes et al., 1980).

Solvent effects at the *Dva* and *thr* resonances may involve interactions at both the carbonyl and amide proton positions. The chemical shift changes for these peaks are in general smaller than those found for the N-substituted residues. This may reflect the overall effect of increasing proton-donating

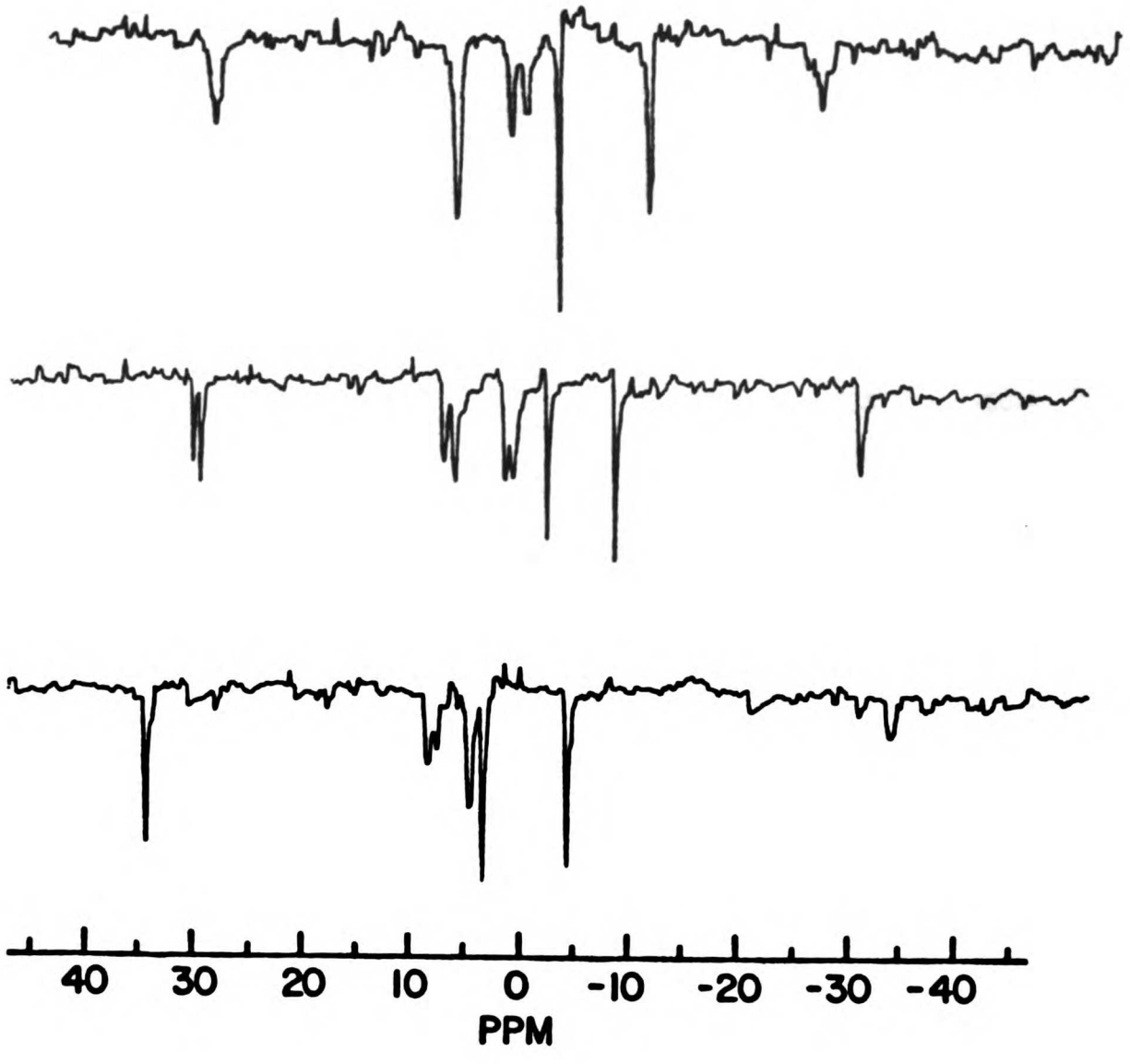

FIGURE 16

^{15}N-NMR spectra of (^{15}N)Actinomycin D at 10.14 MHz. with broadband proton decoupling and NOE, at 15 C.: 12 mM. in 86% DMSO/14% DMSO-d_6, 600 transients (top); 12 mM. in MeOH, 600 transients (middle); 3.7 mM. in 90% H_2O/10% D_2O, BPES buffer, 3600 transients (bottom). All spectra obtained with a 1.46 s. acquisition time and a 3.5 s. delay.

TABLE VII

[^{15}N]ActD ^{15}N Chemical Shifts in Various Solvents						
Solvent	chemical shift (ppm)[a]					
	Dva	thr	pro	sar	nmv	-NH_2
$CDCl_3$	8.4	1.6	29.4	-10.9	-3.4	-30.4
	7.8	0.9	28.9			
DMSO	7.0	1.9	29.1	-10.7	-2.5	-26.4
		1.8		-10.9		
methanol	7.6	1.9	30.4	-8.2	-2.0	-30.5
	6.5	1.2	29.8			
water	8.9	5.0	34.5	-3.9	3.8	-33.2
	8.0	4.8				

[a]at 15°C., referenced to external neat formamide, downfield shifts are positive.

capacity of the solvent to the carbonyl with decreasing proton-accepting capacity of the solvent from the amide proton. Both proton NMR (Victor et al., 1969; Conti & De Santis, 1970) and IR (Von Dreele & Stenhouse, 1974) studies in chloroform indicate that the *Dva* amide proton participates in an intramolecular hydrogen bond. Thus, it is expected that the major effect on the *Dva* resonance is due to solvent interaction with the *thr* carbonyl. Interestingly, this effect appears to be relatively small as the chemical shift changes upon transfer from DMSO to water are smallest for the *Dva* peak(~1-2 ppm). The *Dva* nitrogen also shows small chemical shift differences between DMSO and methanol, appearing as a singlet in the former and a doublet in the latter. Thus, the magnetic nonequivalence of the *Dva* resonances appears to be greatly reduced in DMSO compared to other solvents, but there are no significant average shift differences in the two solvents. This indicates that the *Dva* amide protons are indeed participating in intramolecular hydrogen bonds, and the *thr* carbonyls are moderately buried

from solvent.

The effect of changing the solvent from DMSO to water is seen to be more substantial for the *thr* resonance (-3 ppm), reflecting interactions at the chromophore carbonyl and *thr* amide proton. In organic solvents, the *thr* amide proton NMR resonance shows very little temperature dependance, as does the *Dva* proton (Victor et al., 1969; Mirau & Shafer, 1982b). Also, Conti & De Santis (1970) have shown that in $CDCl_3$ the α-Thr amide proton requires a considerable time for exchange with D_2O, while the β-Thr proton exchanges at a somewhat shorter time. These results indicate that the *thr* amide protons are somewhat shielded from solvent. The small shifts of the *thr* ^{15}N-NMR resonances between DMSO and methanol are consistent with this data and indicate that the chromophore carbonyls are also shielded from solvent. Upon transfer to water, these groups appear to be significantly more exposed to solvent.

Finally, the chromophore amine group shows a considerable downfield shift following transfer from $CHCl_3$ to DMSO due to the increasing hydrogen bond accepting potential of the latter. An upfield shift for this amino resonance is seen following transfer from DMSO to methanol or water due to decreasing hydrogen bond accepting potential of the latter two solvents compared to DMSO. In addition, ring current effects arising from chromophore stacking in the water dimer may contribute to the amino nitrogen chemical shift in this solvent.

In summary, the above analysis provided an indication of the degree of solvent exposure or hydrogen bonding of all peptide carbonyls except the *nmv* carbonyl involved in the lactone functional group. Of these four, substantial downfield shifts are observed for the *pro*, *sar*, and *nmv* nitrogens

upon transfer rom DMSO to water, indicating that the *sar*, *pro*, and *Dva* carbonyls are exposed to solvent. The *Dva* amide protons are involved in intramolecular hydrogen bonds and the *thr* carbonyl and amide protons are buried from organic solvents but are more solvent accessable in water. The currently accepted model for the solution conformation of ActD (Mauger, 1980; Meienhofer & Atherton, 1973; Lackner, 1975), based on the ActD/deoxyguanosine(1:2) crystal complex (Jain & Sobell, 1972), involves intramolecular hydrogen bonds from the *Dva* carbonyls of each lactone ring to the *Dva* amide protons of the other peptide ring. The ^{15}N-NMR solvent titrations are consistent with this model of the ActD pentapeptide conformation but for one exception. The large ^{15}N chemical shifts of the *pro* nitrogen upon transfer from methanol to water indicate a change in hydrogen bonding or solvent accessability of the *Dva* carbonyl upon transfer from organic solvents, where ActD is a monomer, to water, where ActD is in a monomer/dimer equilibrium with relative populations of ~(40:60) at these experimental concentrations.

In the water dimer, formation of the two interpeptide *Dva-Dva* hydrogen bonds would explain the downfield shift of the *pro* nitrogen. These interpeptide hydrogen bonds might keep the peptide groups of the water dimer away from each other when the chromophores stack. The amide protons are certainly hydrogen bonded in organic solvents (Victor et al., 1969; Conti & De Santis, 1970; Von Dreele & Stenhouse, 1974), so the only model consistent with all data would involve a change in the intramolecular hydrogen bond acceptor for the *Dva* amide protons upon transfer from organic solvents to water. The large downfield shifts observed for the *pro*, *sar*, *and nmv* nitrogens suggest that neither the *Dva*, *pro*, *nor sar* carbonyls are intramolecular hydrogen bonding acceptors in organic solvents. The ^{15}N-NMR results

provide no information concerning the *nmv* carbonyl in this possible role, which was proposed by Conti & De Santis(1970) but has been considered unlikely on the basis of the overall rigidity of ActD in all solvents (Victor et al., 1969; Ascoli et al., 1972; and De Santis et al., 1972). A change in intramolecular hydrogen bonding that does not require a major conformational change in the pentapeptide lactones is the most likely explanation for these results.

The possibility of a hydrogen bond from the *Dva* amide proton to the phenoxazone carbonyl groups was also considered by De Santis et al.(1972). This intramolecular hydrogen bonding scheme does not involve a major conformational change in the pentapeptide lactones, only a change in their relative configurations with respect to each other. Thus, a change from the ActD monomer in organic solvents featuring an *intra-pentapeptide* hydrogen bond from the *Dva* amide protons to the corresponding chromophore carbonyls to an *inter-pentapeptide* hydrogen bond from the same *Dva* amide protons to the *Dva* carbonyl of the other pentapeptide in the water dimer would be consistent with the very small changes observed in the *thr* nitrogen chemical shift from DMSO to methanol(Table VII). The downfield shift of 3 ppm in the *thr* resonance upon transfer from methanol to water may seem too large to be consistent with this model, but consideration of the solvent inaccessability of the amide protons in organic solvents suggests that interactions at both the *thr* amide protons and chromophore carbonyls play a role in determining the *thr* ^{15}N chemical shift in water.

The general conclusion from the ^{15}N-NMR data in conjunction with previously published data is that the conformation of the pentapeptide lactones is similar in all the solvents investigated, but that the *Dva* amide proton hydro-

gen bond accepting carbonyl shifts upon dimer formation in aqueous solvents. The *Dva* carbonyls are buried from solvent in organic media, while becoming the *Dva* amide proton hydrogen bond acceptors in the aqueous dimer. The most likely acceptor carbonyl in organic solvents is the chromophore carbonyl group of each peptide.

^{15}N-NMR Study of [^{15}N]ActD Bound to Various Nucleotide Systems The same ^{15}N-NMR techniques were then used to elucidate the ActD pentapeptide lactone conformations when the drug was bound to various nucleotide systems. ^{15}N-NMR spectra of [^{15}N]ActD are found in Figures 17 and 18 while the chemical shifts are summarized in Table VIII. ActD forms a tightly bound complex with d(pGpC), dATGCAT, and DNA. The prefered binding site on DNA is GpC,though this dinucleotide is too short to interact with the *sar* and *nmv* residues of the drug. The hexanucleoside pentaphosphate dATGCAT is long enough to span the pentapeptide lactones and was judged to be a good model system for the prefered DNA binding site by the CD of the complex and the association kinetic behavior. Finally, the presence of an ^{15}N label on the drug could probe the pentapeptide lactone conformation when ActD was bound to DNA itself, allowing a comparison of the bound states to the different nucleotide systems. The dimerization of actinomycin in aqueous solutions at millimolar concentrations is well documented, and a large effect on the ^{15}N chemical shifts was observed upon dimerization. The kinetic and CD data were acquired at much lower concentrations where the population of ActD dimers is less than 2%, which is also more appropriate for *in vivo* conditions. Thus, the spectrum of ActD in 7 mol% methanol will be used to approximate the spectrum of the ActD monomer in aqueous solutions.

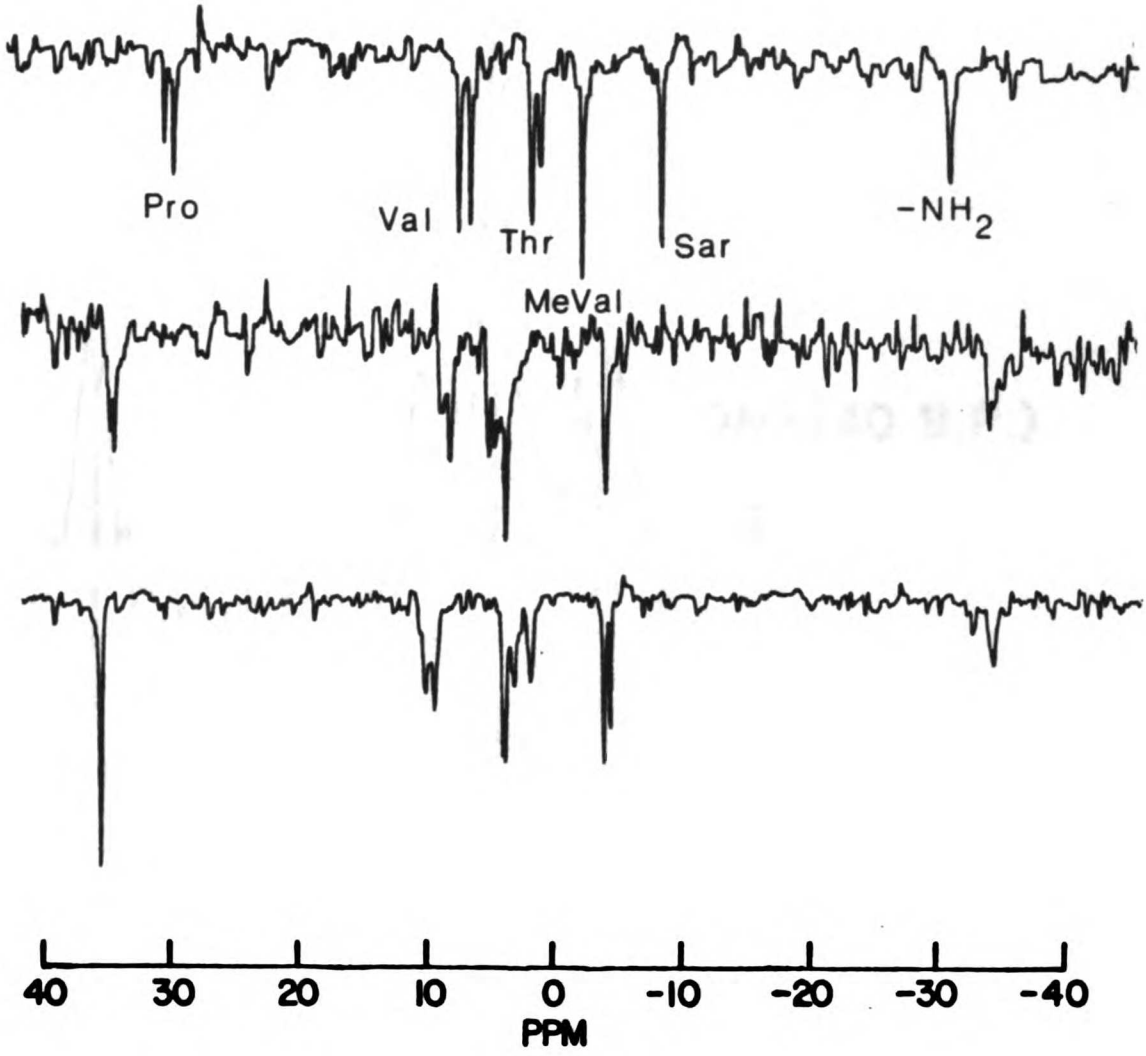

FIGURE 17

^{15}N-NMR spectra of (^{15}N)Actinomycin D at 10.14 MHz., 15 C.: (top) 10 mM. in 93 mol% BPES/7 mol% MeOH, 600 transients; (middle) 1.5 mM in BPES buffer containing 10% D_2O, 16,000 transients; (bottom) 5 mM. in the presence of 20 mM. d(pGpC) in BPES buffer, 15,000 transients. Spectra were obtained with a 40 degree pulse, 1.4 second acquisition time, 2 second cycle time, +/- 1500 Hz. spectral window, internal or external D_2O lock, and continuous broadband ^{1}H decoupling with resultant negative NOE. Assignments are shown for top spectrum.

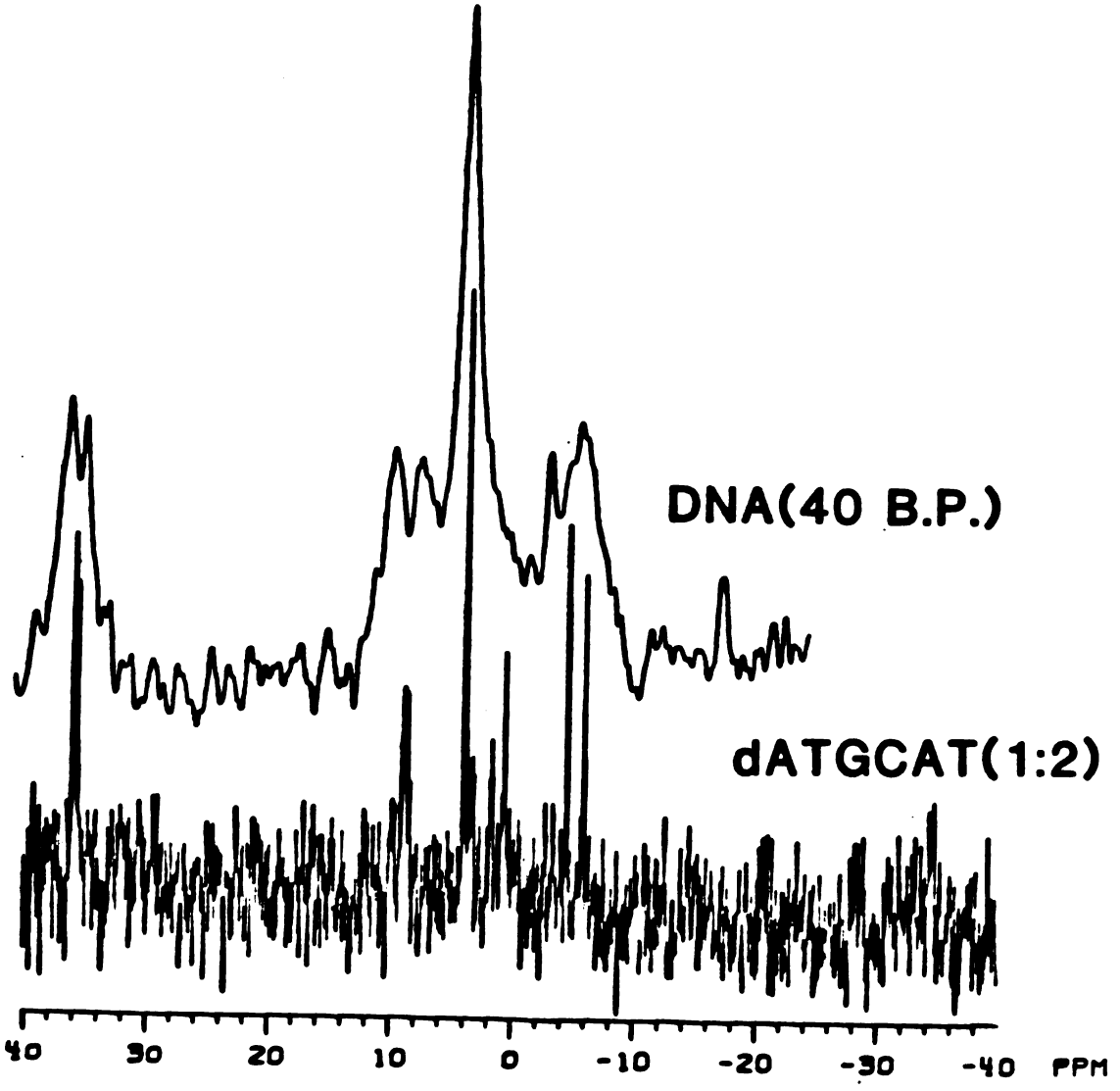

FIGURE 18

^{15}N-NMR spectra of (^{15}N)Actinomycin D bound to: (top), calf thymus DNA (P/D=18) digested to an average length of 40 base pairs, at 50.7 MHz. on a Bruker WM500 without ^{1}H irradiation, 40 degree pulse, .58 s. acquisition time, 2.1 s. cycle time, +/- 7050 Hz. spectral window, 14,000 transients, T= 25 C.; (bottom), dATGCAT (2:1), at 24.4 MHz. on the UCSF WB240 with ^{1}H decoupling, NOE suppressed, 90 degree pulse, 24.5 s. cycle time, +/- 3150 Hz. spectral window, 1500 transients, T= 15 C. Spectra referenced to external neat formamide.

TABLE VIII

^{15}N Chemical Shifts of [^{15}N]Actinomycin D in Aqueous Solutions Free and Bound to Various Duplex Nucleotides[a]

	pro	Dva	thr	nmv	sar	NH_2
monomer[b]	30.4,29.8	7.6,6.5	1.9,1.2	-2.5	-8.2	-30.5
dimer[c]	34.7,34.3	8.9,8.2	5.1,4.5	3.8	-3.8	-33.2
+ d(pGpC)[d]	35.7	10.4,9.8	3.6,2.4	4.5	-3.3,-3.8	-33.3
+ dATGCAT[e]	36.,35.7	8.7	.53,1.55	3.8	-4.6,-6.0	-34.7
+ DNA[f]	36.,34.8	9.6,7.5	-	3.8	-	-

[a]ActD concentration is 3.7mM.,T=15°C.,except DNA spectrum at 25°C., chemical shifts in ppm referenced to neat formamide at 15°C.;downfield shifts are positive. [b]Spectrum of free ActD in 93 mol% BPES/7 mol% methanol. [c]Spectrum in BPES buffer(~60% dimer). [d]Spectrum with d(pGpC) added(4:1). [e]Spectrum with dATGCAT added(2:1), ^1H decoupled, no NOE. [f]Spectrum with digested DNA(avg. BP=40) added(P/D=18), ^1H coupled.

The chemical shifts are sensitive to both solvent and conformation. While the relative importance of these effects has not been completely elucidated for actinomycin, the interpretation of these observed spectral shifts is based on ^{15}N-NMR studies obtained on other peptide systems. The large downfield shifts of the *pro* resonance are consistant with the formation of the *Dva* amide proton interpeptide hydrogen bond to the *Dva* carbonyl in both the aqueous dimer and the complexes. These bonds have been observed in the crystal structure of the ActD/dG (1:2) complex (Jain & Sobell, 1972) and more recently in a crystal structure of the ActD/d(pGpC) (1:2) complex (Takusagawa et al., 1982). The downfield shifts observed for *sar* and *nmv* also reflect interactions at the shared carbonyl of their peptide bond. Overall, the similarities in the spectra of the dimer and the complexes are striking.

The *Dva* and *thr* resonances may be affected by interactions at both the carbonyl and amide protons of the peptide bond. The low field shift of the *Dva* resonance in the dimer and the complexes is expected for the interpeptide

hydrogen bond formation discussed above. These peaks are slightly further downfield in the nucleotide complexes than in the dimer, consistant with the presence of a hydrogen bond from the guanine amino groups to the *thr* carbonyl. This interaction has been found in the crystal structures mentioned above.

The *thr* resonance is shifted upfield from that of the dimer as the drug is bound to d(pGpC) and then dATGCAT. The magnetic nonequivalence of the two /i thr resonances also becomes progressively greater, from 0.6 ppm in the monomer and dimer to ~1.1 ppm in the d(pGpC) and dATGCAT complexes, corroborating the greater degree of asymmetry in the complexes compared to the free drug. The upfield shifts indicate the presence of hydrogen bonds from the *thr* amide protons to the guanine N3 observed in the complexes. These upfield shifts are of a greater magnitude than expected for hydrogen bonding and are probably partly due to the strong ring current effects from the guanine rings that are adjacent to this atom in the intercalated complex. The upfield shift of the chromophore amino group is consistent with ring current effects of the stacked guanines and compares well to ring current effects of the stacked chromophores in the aqueous dimer.

Figure 18 also shows the ^{1}H-coupled ^{15}N-NMR spectrum at 50 MHz of ActD in the presence of excess calf thymus DNA enzymatically digested to an average length of 40 base pairs. The resonances are broad for several reasons: 1) the relatively long correlation time in spite of the short DNA fragments used; 2) binding site heterogeneity; and 3) the ^{1}H coupling. The ^{1}H decoupled ^{15}N-NMR spectrum at 24 MHz of the [^{15}N]ActD/dATGCAT(1:2) complex is also found in Figure 18 and comparison of it with the DNA and d(pGpC) spectra reveals trends in the chemical shift changes as the drug is bound to

longer lengths of duplex nucleotides. Increasing nonequivalence of the α- and β- pentapeptide resonances for the *pro*,sar, and *thr* residues is seen, while the *nmv* and *Dva* residues show the same shifts bound to dATGCAT and DNA upfield from those of the d(pGpC) complex. All resonances shift slightly upfield progressing from d(pGpC) to dATGCAT to DNA.

Comparison of the ActD spectra bound to dATGCAT and DNA reveals a larger asymmetry at the *sar* resonance than found for the free drug. This could be explained either by asymmetry in the complex, as proposed by Sobell (1977), or possibly by a *cis* to *trans* isomerization of the *pro-sar* peptide bond in one of the pentapeptide lactones, as proposed by Mirau et al. (1982a). The *Dva* and *nmv* resonances are at identical chemical shifts in both complexes. The other resonances of the DNA spectrum could not be assigned due to their width and overlap.

In summary, comparison of the ^{15}N-NMR spectra of [^{15}N]ActD bound to dATGCAT and DNA indicates similarity in the bound structure of the drug pentapeptide lactones for these complexes. These data confirm that duplex dATGCAT is an appropriate model for a strong DNA binding site of ActD. The ^{15}N chemical shift changes observed, however, may be interpreted in several ways. These results are consistent with the standard intercalation model, but asymmetry in the α- and β- *sar* resonances upon binding to dATGCAT or DNA may be interpreted as either involving a *cis* to *trans* isomerization about the *pro-sar* peptide bond upon binding of the drug, or as a general asymmetry of the complex which is reflected predominantly at this position.

^{13}C Carbonyl Assignments of Actinomycin D in Chloroform Carbon-13 NMR studies of Actinomycin D, particularly of the carbonyl region in various solvents, could provide complementary information concerning hydrogen

bonding and solvent exposure of the peptide linkages. While the original ^{13}C assignments (Hollstein et al., 1974) have been corrected for the upfield region (Booth et al., 1976), the carbonyl assignments had not been verified. With the correct carbonyl assignments, ^{13}C and ^{15}N-NMR spectra could be compared to obtain a consistent picture of the degree of symmetry along the peptide backbone between the α- and β-pentapeptide lactones.

The ^{15}N-^{13}C one bond coupling constants of ~15 Hz found in amide bonds could be exploited to assign the carbonyl region of ActD once the ^{15}N spectra had been assigned. It was discovered that continuous proton irradiation was required to reduce linewidths in the ^{13}C spectra while the ^{15}N resonances of [^{15}N]ActD were irradiated to observed collapse of the scalar coupling. Triple irradiation experiments were then done, the results of several are shown in Figure 19. Complete carbonyl assignments in chloroform, along with the ^{15}N-^{13}C one bond scalar coupling constants, are given in Table IX. One bond ^{15}N-^{13}C coupling constants to the C^{α} carbons ranged from 8-12 Hz but were not accurately measured due to low signal to noise. As indicated in Table III, the assignments agree with those of Hollstein et al. (1974) for only four of the eleven peaks.

The low field region of the ActD ^{13}C-NMR spectrum shows three residues whose carbonyl resonances are at similar shifts for the two pentapeptide lactones of the drug, those of the *pro*, *nmv*, and *sar* carbonyls, corresponding to the *nmv* and *sar* residue ^{15}N-NMR resonances in chloroform that also show the highest degree of magnetic equivalence in the molecule. These observations are consistent with the proton NMR spectrum and the peptide conformation observed in the crystal structure (Jain & Sobell, 1972) that shows these residues to be furthest from the chromophore which is the major

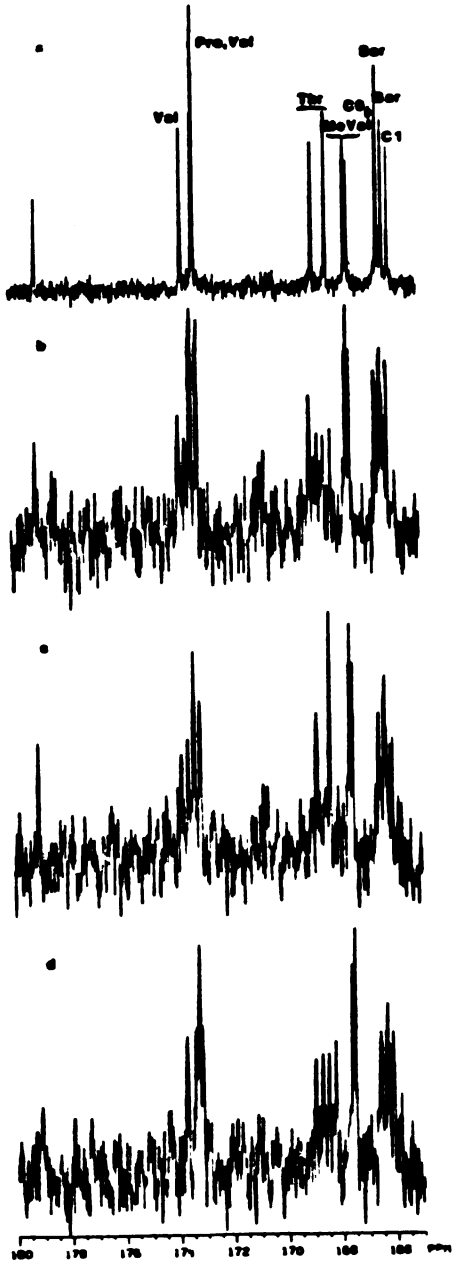

FIGURE 19

^{13}C-NMR spectra of actinomycin D carbonyl region at 60.5 MHz. in $CDCl_3$, with broadband ^{1}H decoupling, 75 degree pulse, 1.5 s. cycle time, referenced downfield from TMS: a) unlabeled drug, 10 mM., 25,000 transients. b) ^{15}N-labeled drug, 7 mM., 12,000 transients. c) same as in b) plus irradiation at the ^{15}N Dva resonance. d) same as in b) plus irradiation at the ^{15}N Pro resonance.

TABLE IX

^{13}C Chemical Shifts and ^{13}C-^{15}N Coupling Constants of Actinomycin D Carbonyls in $CDCl_3$

δ (ppm)[a]	assignment	$^1J_{^{13}C-^{15}N}$ (Hz)
179.11	quinone(C3)	—
173.73	1 valine	14.3
173.30	2 proline	14.4
173.27	1 valine[c]	~14
168.90	1 threonine	16.2
168.41	1 threonine[c]	~15
167.63	N-methylvaline[c]	0
167.54	N-methylvaline[c]	0
166.49	C9[b,c]	~15
166.45	1 sarcosine[b]	~15
166.30	1 sarcosine	~14
166.03	C1[b]	~16

[a]Measured downfield from TMS, in $CDCl_3$; [b]tentative assignments; [c]Assignments differing from those of Hollstein et al., (1974).

source of magnetic asymmetry. It was hoped that these corrected assignments would aid conformational analyses of ActD in aqueous systems, but the limited solubility of the drug in water (~4 mM.) prevented acquisition of good spectra.

Proton NMR Studies of Actinomycin D, $[dATGCAT]_2$, and the ActD/dATGCAT(1:2) Complex

Introduction

The relatively slow rates of Actinomycin D association and dissociation from DNA ($\sim 10^{-3}$ s^{-1}) compared to other typical DNA intercalating drugs such as ethidium bromide and daunomycin ($10\text{-}10^{3}$ s^{-1}) have been attributed to either conformational changes in the pentapeptide lactones of the drug (Muller & Crothers,1968; Shafer et al., 1980; Mirau & Shafer, 1982a) or in the nucleic acid (Sobell, 1974) upon formation of the bound complex.

A crystal structure of actinomycin D (ActD) complexed with deoxyguanosine has been published (Jain & Sobell, 1972) from which a model of ActD bound to the hexanucleoside pentaphosphate duplex dATGCAT was proposed (Sobell & Jain, 1972). NMR data obtained from binding ActD to various dinucleotides (e.g., dCpG, dGpC, etc.), mononucleotides (Reinhardt & Krugh, 1977; Krugh & Chen, 1975; Patel, 1974a) and oligomers (Patel, 1974b; Patel et al.,1981; Reid et al.,1983) have been interpreted to be consistent with the proposed model. However, the mono- and dinucleotide systems investigated show fast kinetics (Davanloo & Crothers, 1976) and may not be truly representative of the slowly dissociating binding mode directly correlated to RNA synthesis inhibition. These previous NMR studies have generally been limited to observations of several resonances in the nucleotide or drug and have not addressed the issue of what structural changes may be responsible for the slow kinetics. Recently, a ^{1}H-NMR investigation of the complex ActD/dAGCT(1:2) demonstrated by NOE effects that the ActD chromophore

was intercalated, but it provided little information concerning the conformation of the ActD pentapeptides or the nucleic acid residues apart from the intercalation site (Reid et al., 1983). A recent crystal structure of an ActD/dGpC(1:2) complex revealed an unusual pseudo-intercalated geometry (Takusagawa et al., 1982) that may exist in solution.

The development of two-dimensional NMR techniques has expanded the possibility of resolving, assigning, and measuring NOE's in crowded spectra (Wuthrich et al., 1982). Several solution structures of relatively large molecules have been elucidated with these techniques (e.g., Braun et al., 1981). These techniques were extended to the determination of structural features in a non-covalently bound complex of ActD and the hexanucleoside pentaphosphate duplex dATGCAT. A recent survey of two dimensional homonuclear NMR techniques can be found in Bax, 1982.

The types of two dimensional spectral acquisition used in this study are the COSY and pure absorption NOESY. The COSY(Correlated Spectroscopy) pulse sequence generates, after appropriate processing, an n by n matrix of data points in two frequency dimensions, ω_1 and ω_2. The size n of this matrix determines the resolution of the spectrum and is essentially limited to 1024 points by currently available NMR data system sizes. Spectral windows of 5000 Hz therefore limit the resolution to about 4-6 Hz/data point. This is generally less than the available resolution from the spectrometer and sample. The most easily interpretable plot of this spectrum is a contour plot, looking down on the plane determined by the two orthonormal frequency axes, where peaks are located by contours drawn about them at regular intervals. Such a contour plot shows the normal spectrum along the diagonal, while off-diagonal peaks (also called cross-peaks) correlate two reso-

nances along the diagonal that are scalar coupled. This experiment thereby locates protons that are scalar coupled, with the intensities of the cross-peaks roughly proportional to the magnitude of the scalar coupling constant. Scalar couplings less than 2 Hz are at the limit of detectability under the experimental conditions employed for this study.

The second type of two dimensional experiment employed herein is the pure absorption NOESY(Nuclear Overhauser Effect Spectroscopy). This pulse sequence generates, after processing, a contour plot where again the normal spectrum is found along the diagonal and cross peaks correlate two diagonal resonances that are cross-relaxed by the NOE effect. The intensities of the individual cross peaks are dependent on the mixing time (τ_m) used in the experiment, the frequency and amplitude of relative motion of the two protons with respect to each other, and most importantly, the distance between the two protons. Observation of a cross peak therefore indicates that two protons are within 5 Å of each other. The calculation of distances from NOE intensities cannot be done accurately unless the relative motions of the protons are known. This will be discussed in the results section. However, the relative intensities of NOE's are roughly proportional to relative distances, with an inverse 1/6 power dependence that can give a fairly accurate proton-proton distance if the motion of the molecule can be fairly accurately modeled, especially within the frequency range

Before proceeding to a two-dimensional NMR conformational study of the ActD/dATGCAT(1:2) complex, it was necessary to assign the resonances of the free drug and the free duplex dATGCAT. It was also of interest to determine as much as possible the conformation of these species in order to ascertain whether major conformational changes had occured upon binding. There-

fore, a two-dimensional ^{1}H-NMR study of these three molecular species was undertaken.

Materials and Methods

Materials. ActD was a generous gift from Merck Sharpe & Dohme, and its purity was checked by TLC and NMR. Buffer reagents were obtained from Sigma. TSP(sodium 3-(trimethylsilyl)-tetradeuteriopropionate) and D_2O were obtained from Wilmad. dATGCAT was synthesized by standard triester techniques (Narang et al., 1980), and its purity was checked by ^{1}H-NMR, ^{31}P-NMR, HPLC, and base composition analysis. This hexanucleoside pentaphosphate was a generous gift of Drs. Kary Mullis and Corey Levinson of Cetus Corporation, Emeryville, Ca. 94608). Solutions for NMR experiments were made up fresh in a BPES buffer (100 mM phosphate, 180 mM NaCl, 0.2 mM EGTA, pH 7.0). EGTA(ethylene glycol bis(β-aminoethyl ether)-N,N,N',N'-tetraacetic acid) was used to sequester any trace paramagnetic ions and did not appear in most proton NMR spectra due to the very low concentrations required. ActD was dissolved to a concentration of 4.0 mM; the solution was lyophilized twice in the 5 mm NMR tube and taken up in an equal volume of D_2O. The complex was formed by the addition of integral stoichiometric ratios of solid dATGCAT (Na^+ salt). Individual samples contained (1) ActD alone, (2) ActD/dATGCAT(1:1), (3) ActD/dATGCAT(1:2), and (4) ActD/dATGCAT(1:4). These were lyophilized in the NMR tube and taken up again into an equal volume of D_2O to which solid TSP was added for an internal chemical shift standard. Samples of duplex dATGCAT were made up at 4.0 mM in strands for the results shown herein. Spectral changes were observed due to increasing aggregation above these concentrations. These changes were particularly

pronounced in the 2',2'' region, with rapidly increasing line widths as the concentration was raised from 4 mM to 12 mM in strands. Thus, even lower concentrations would be advisable but 4 mM was the practical lower concentration limit for data acquisition using the available NMR instrument.

NMR Experimental Parameters. NMR experiments were done either on the WB240 at the UCSF Magnetic Resonance Laboratory, or on the 500 MHz magnet at the U. C. Davis Regional NMR Facility, University of California, Davis, Ca. The UCSF WB240 was homebuilt and features a Nicolet 1180 data system with a 293B pulse programmer. The UCD 500 is a Nicolet commercial system featuring a 1280 data system with a 293C pulse programmer. Temperatures were regulated to ±0.1 °C. for all experiments and D_2O was used as an internal lock. Sample T_1 values ranged from 0.5 to 2.3 s, so the delay time was set to 5 s, unless stated otherwise. The carrier was set to the frequency of the residual solvent peak, which was suppressed by using a phase-cycled soft pulse (t_π = 120 ms) during the acquisition delay for experiments done on the UCD 500, and with the homonuclear decoupler for experiments done on the UCSF 240.

Saturation transfer experiments were done on the UCSF WB240. The homonuclear decoupler was used at the minimum power required to ensure selectivity. Resonances of both the complex and the previously assigned resonances of the duplex dATGCAT were irradiated using the ActD/dATGCAT(1:4) sample. The temperature was controlled at 45 °C., where peaks were observed to be at slow exchange, but saturation transferred with a 0.5 s preirradiation. At this temperature, very small positive NOE's are seen, as the correlation time is close to the NOE null point, so there is no observable interference from NOE effects under these experimental condi-

tions. These experiments were done in the temperature range 10-45 °C. and NOE effects were observed to decrease from ~-50% to zero as the temperature increased, while saturation transfer could not be observed until the temperature reached 40 °C. Spectra were acquired using the interleave mode with appropriate off-resonance controls and the FID's subtracted to obtain difference spectra.

NOE observations in water of the dATGCAT imino proton resonances were done in the identical buffer with 90%H_2O/10%D_2O. The temperature was controlled to 0.0 °C. to minimize exchange with solvent and maximize NOE effects. A jump and return (Plateau & Gueron, 1982) sequence was used to suppress the water resonance, along with a preirradiation of 0.5-1.0 s using the decoupler at frequencies of selected imino proton resonances. The decoupler power was set lower than that required for complete saturation of resonances in order to minimize dispersion by the skirts of the water peak.

Transient NOE (TOE) experiments (Wagner & Wuthrich, 1979) were done using the same pulse sequence used for the saturation transfer experiment, except that NOE's were observed as temperatures were held at 10 or 15 °C. These experiments were done to make several assignments and to check for spin diffusion effects (Kalk & Berendson, 1976; Kumar et al., 1981) so that proper mixing times (τ_m) for the NOESY spectra could be determined. Preirradiation times for selected resonances were from 50 ms to 2 s. Peak intensities were determined by integration of the difference spectra between each preirradiation time and an off-resonance irradiation done as a control.

Two dimensional COSY spectra (Bax et al., 1981) were acquired by using 2K data points in the t_2 dimension (64 transients each) and 200 acquisitions in the t_1 dimension. FID's were apodized in the t_2 dimension by a double

exponential and in the t_1 dimension by a sine bell, yielding after the second transformation a 512 x 512 matrix of real points with a resolution of 9 Hz/DP (ω_1). The sample temperature was regulated at 10 °C. for the free ActD and dATGCAT samples, and 15 °C. for the complex.

Two dimensional NOESY spectra were acquired in the pure absorption mode (States et al., 1982) with 4K data points in the t_2 dimension (64 acquisitions each), stored in alternate blocks, and 200 FID's collected in the t_1 dimension. A mixing time of 200 ms was used on the UCD 500 for the spectrum of the complex, while various other mixing times were used in data acquired on the UCSF WB240 for the ActD and dATGCAT samples. The mixing times for various experiments are specified in the figure legends. No effects attributable to spin diffusion were seen for observation times less than 0.5 seconds in separate TOE experiments. FID's were apodized by Gaussian multiplication in the t_2 dimension and by either a double exponential (DM=3) to enhance resolution, or by gaussian multiplication(GM=20) to check peak intensities in the t_1 dimension, yielding after transformation a 1K x 1K matrix of real points. with a digital resolution of 5.8 Hz/DP. The sample temperatures were regulated to 10 °C for the ActD and dATGCAT samples, and 15 °C for the complex.

Results and Discussion

Actinomycin D Assignments and Structure. Resonances in a previous ^{1}H-NMR study of ActD in D_2O had been assigned by binary solvent mixtures progressing fom the assignments in $CDCl_3$ (Lackner, 1971) through methanol-d_4 to D_2O (Angerman et al.,1972). Large chemical shift differences were observed for many ActD resonances in methanol-d_4 and D_2O, implying

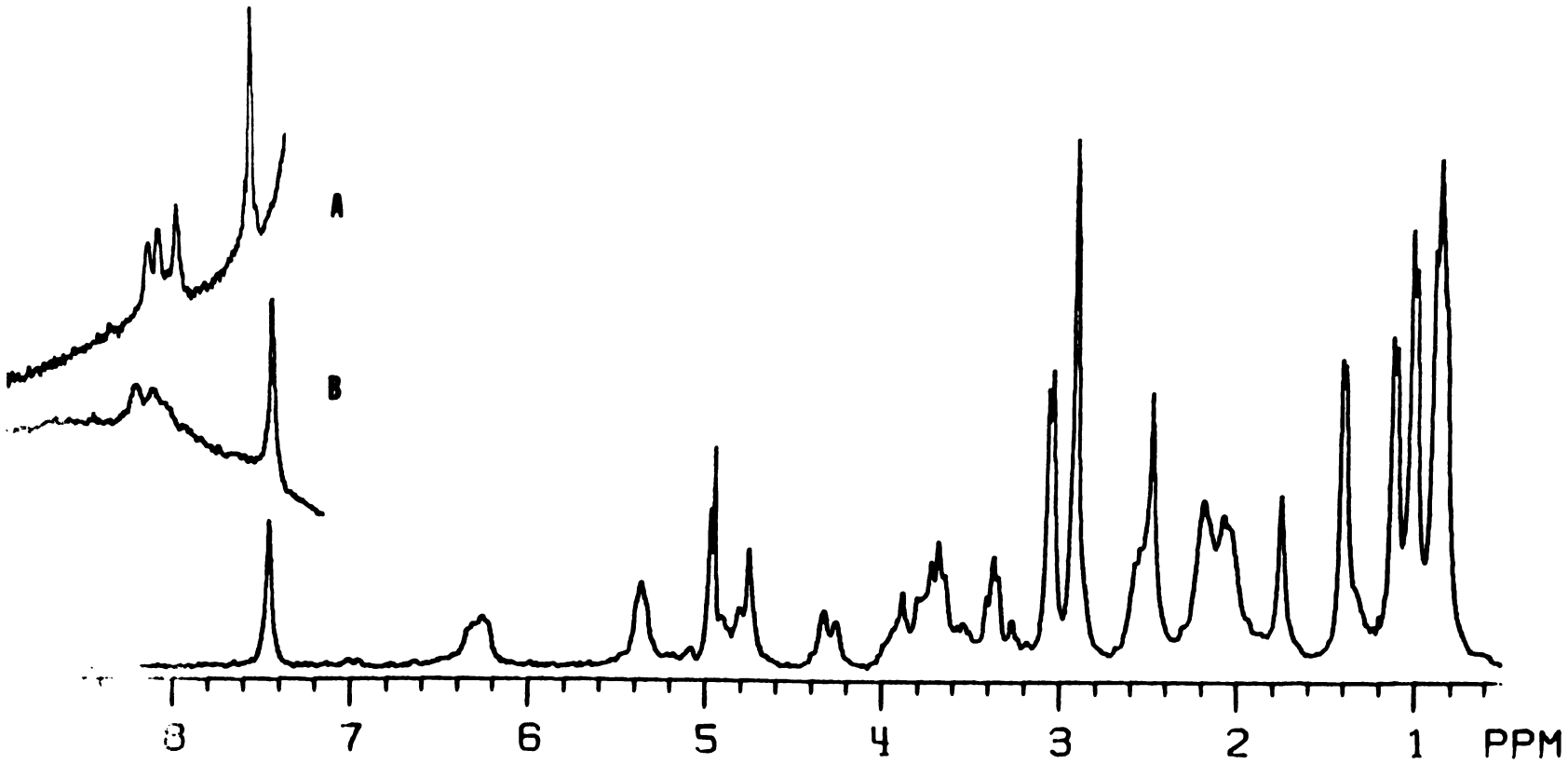

FIGURE 20

Proton NMR spectrum of Actinomycin D (4.0 mM) in BPES buffer (100% D_2O) at 240 MHz., T= 10.0 ^{o}C. Peak assignments are found in Table X. Insert: Downfield portion of ActD proton NMR spectrum of the same sample in 90% H_2O/10% D_2O at; A) 25.0 ^{o}C. and B) 10.0 ^{o}C. Water peak suppressed by selective presaturation. These peaks integrate to four protons and are the Thr and Dva N-H protons in slow exchange with solvent water.

that a conformational difference exists in the two solvents. The chemical shift dependence of several ActD resonances in the concentration range 0.2 to 4.4 mM in buffered D_2O were measured and fit to the known dimerization equilibrium. These shifts were then interpreted as arising from ring current effects, leading to a model of the aqueous dimer structure of the two monomers stacking at the chromophores, the benzenoid ring of one over the quinoid ring of the other and vice versa (Angerman et al., 1972). Transient NOE spectra were done in the course of this work that confirmed the structure of this dimer by NOE contacts (vide infra). However, the signal-to-noise of the ActD spectra in this study (Angerman et al., 1972) was not impressive and it was thought that these assignments should be checked.

Figure 20 shows the spectrum of ActD in D_2O and H_2O(insert). At these concentrations, calculations ($K_d \simeq 2.1 \times 10^{-3}$ M) show populations of roughly 60% dimer and 40% monomer in fast exchange on the NMR timescale. Table X lists the assignments, some of which are different from previously published assignments. These assignments were done by examination of COSY spectra and transient NOE(TOE) experiments.

The COSY spectrum of ActD in BPES(D_2O) is shown in Figure 21. Inspection of the contour plot shows: one AX spin system, which must correspond to the sarcosine H^{α}(sarα) protons; one A_3MX system that must correspond to the threonine residue; one (AA')MM'NN'X spin system that must be the proline residue, and two A_3B_3MX systems that locate the D-valine(Dva) and N-methylvaline(nmv) resonances. Thus, most assignments could be made by this single experiment. The remaining assignments were done by TOE experiments (Wagner & Wuthrich, 1979) that identify protons by their spatial proximity to other resonances already assigned.

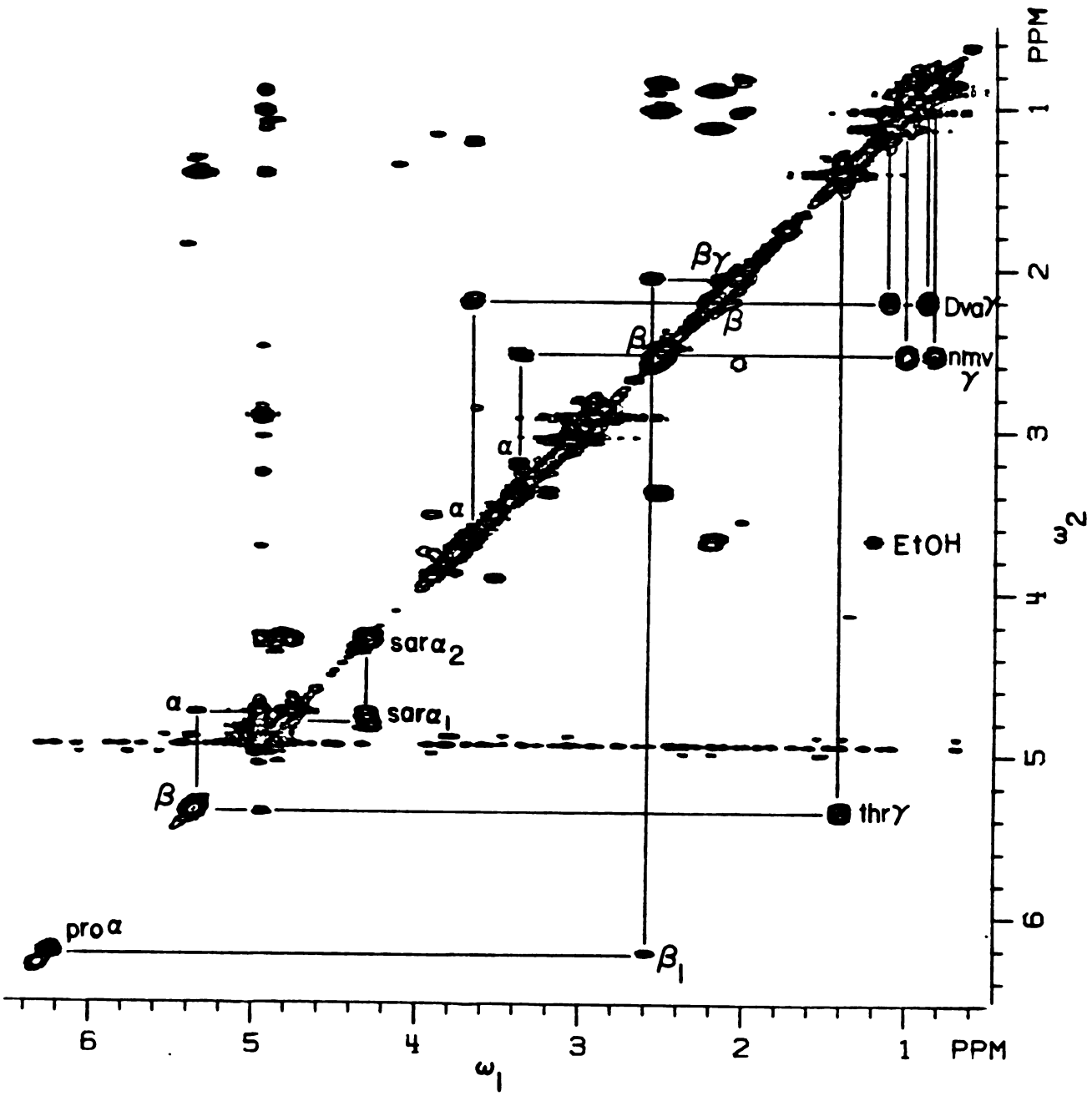

FIGURE 21

500 MHz. COSY spectrum of ActD at 10.0 °C. in BPES(100%D_2O), 512 x 512 points, 10 Hz./DP. Five spin systems are identified: 1) AX (sar), 2) (AA')MM'NN'X (pro), 3) A_3MX (thr), and 4) two A_3B_3MX (valine). The proδ protons are not visible at this contour 'cut'. Trace ethanol in the sample shows a cross peak.

TABLE X

Proton Resonance Assignments for Actinomycin D[a]

Assignment	ppm[b]	Coupling Constant	T_1(sec.)[c]
H7,H8	7.446		1.2
Proα	6.299		.29
Proα*	6.244		.31
Thrβ*	5.348		.56
Thrα_1*	4.959		
Sarα_1*	4.829	^2J= 15.3	.42
Thrα_2*	4.741		.65
Sarα_2	4.282	^2J= 15.3	.31
Proδ*	3.922,3.873,3.789,3.743		.32
Dvaα*	3.672	^4J=9.2	.46
Nmvα	3.360	^4J=7.6	.61
Nmv N-CH_3	3.054, 3.029		.57
Sar N-CH_3*	2.901		.80
Proβ_1	2.552		.47
Nmvβ	2.530		.53
6-CH_3	2.467		.76
Dvaβ*	2.174		.48
Proβ_2,γ	2.061,2.036		.415
4-CH_3	1.739		.82
Thrγ	1.399,1.378		.35
Dvaγ_1	1.113, 1.091		.45
Nmvγ_1	1.005, 0.982		.48
Dvaγ_2	0.879, 0.852		.37
Nmvγ_2	0.852, 0.820		.37

[a] at 4.0 mM in BPES, D_2O, T= 10.0 °C.
[b] referenced to internal TSP
[c] by IRFT, two parameter fit(Hanssum et al.,1978), I=0.83
* assigments different from those of Angerman et al.(1972)

Assignments for the chromophoric methyl groups were confirmed by TOE experiments where the H7,H8 resonance was irradiated and the buildup of the NOE at the 6-methyl group (~3 A) must be faster and stronger than the NOE at the 4-methyl group (~7 A). Assignment of the two valine residues was done in a similar fashion. The large doublet at 3.09 and 3.06 ppm and the singlet at 2.94 ppm have been previously assigned to the *nmv* N-CH_3 protons and the *sar* N-CH_3 protons, respectively (Angerman et al., 1972). An NOE was

observed to one of the valine H^{α} protons upon irradiation of the downfield doublet. Irradiation of the upfield singlet produced NOE effects at the *sara* protons. Irradiation of the *sara* protons produced NOE's at both the doublet and the singlet. This pattern of NOE's confirmed the assignment of the N-CH_3 groups and established the identities of the two valine systems. The assignments not in accord with Angerman et al. (1972) are identified in Table X.

The *thra1* resonance was difficult to observe in the presence of trace amounts of H_2O, but cross peaks could be observed in the COSY and NOESY spectra when the sample was rigorously exchanged with "100%" D_2O. Assignment of resonances to the α or β pentapeptide lactone could not be done due to their superposition from the semi-C_2 symmetry of the molecule. The structure of the aqueous dimer proposed by Angerman et al. (1972) was confirmed by TOE experiments done at 500 MHz in which negative NOE's were generally observed to build up with preirradiation time, but positive NOE's were observed to the chromophore H7, 6-CH_3, and 4-CH_3 groups when the *proα* resonances were irradiated (Figure 22). Inspection of the Angerman model for the dimer revealed that the *proα* protons were within Van der Waals contact of these same three groups, the H7, 6-CH_3 and 4-CH_3 of the other monomer participating in the dimer. Since the dimer is in fast exchange with the monomer at the NMR time scale, this cross relaxation is governed by a rate producing *positive* NOE's instead of the negative NOE's characteristic of intramolecular dipolar cross relaxaton for this size molecule. Figure 23 shows the data from TOE experiments at 500 MHz where the *proα* resonances were preirradiated at various times. It will be of interest to compare the NOE intensities derived from one dimensional presaturation experiments such as this to the dynamic NOE intensities measured by the two dimensional NOESY experiments. This data indicate that the

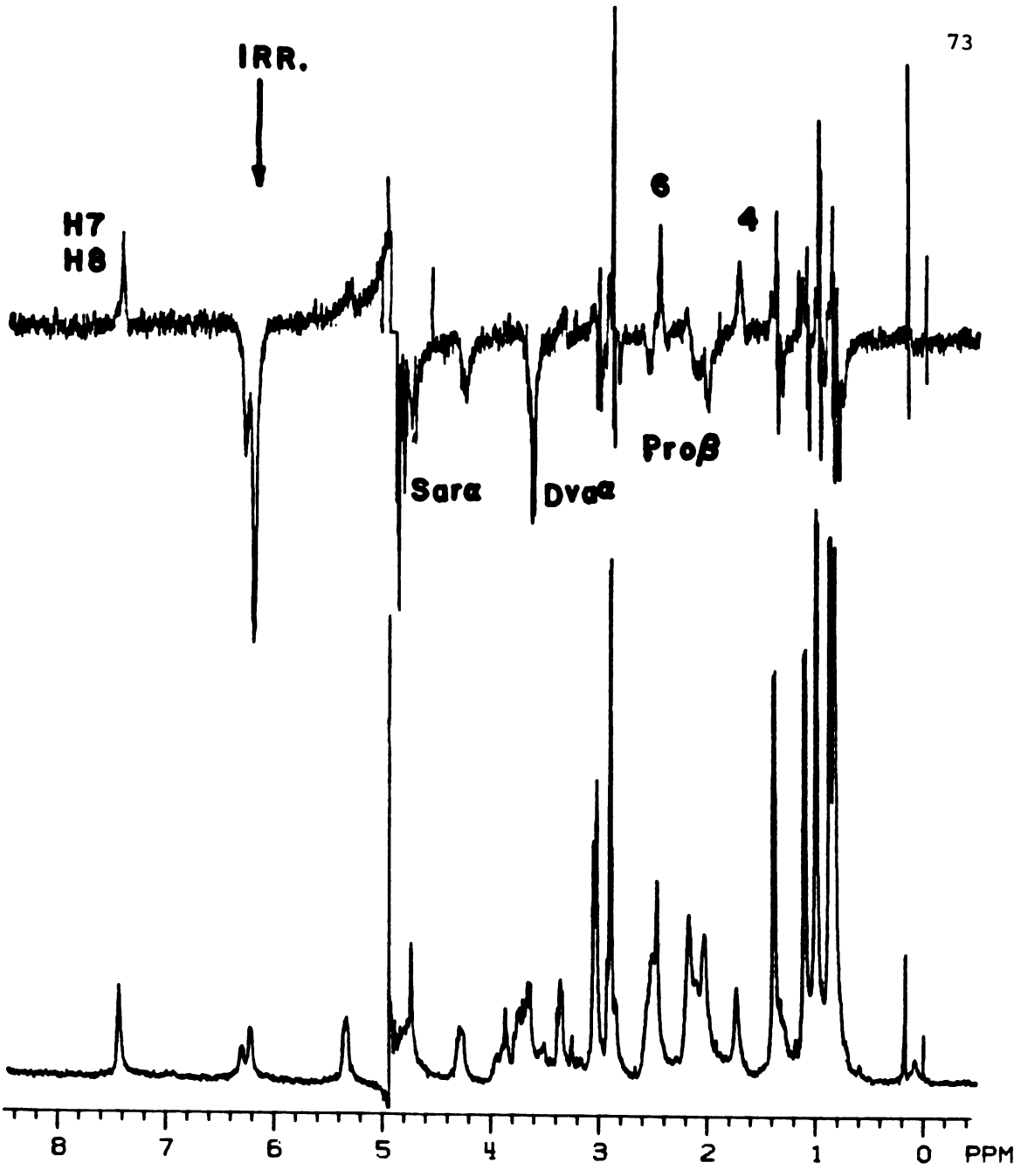

FIGURE 22

Representative TOE difference spectrum of ActD at 500 MHz. with the proα resonances irradiated for 2 seconds prior to acquisition (top) and off-resonance control spectrum for reference (bottom). Negative NOE's are observed to the Dvaα , saraα1,sar α_1, sarα_2, proβ_1, and pro$\beta_{2,\gamma}$ while positive NOE's are observed to the chromophoric H7, H8, 6-CH_3, and 4-CH_3 resonances. 64 acquisitions each.

structure of the aqueous dimer and monomer peptide bonds Dva-pro-sar is *cis-cis* since the *proα* to *Dvaα* and *saraα* protons must be less than 2.5 Angstroms apart to demonstrate such strong NOE effects. If either of the peptide bond configurations had been *trans*, then these proton-proton distances would be greater than 4.0 angstroms. These distances can be determined by the relative intensity of the $saraα_1$ to $saraα_2$ NOE's of 18% at 250 ms, where the distance between these two protons is 1.81 A, to the NOE intensity between the H7 and 6-CH_3 protons of 6%, where the interproton distance is 3.04 A. The buildup of the *proα* to *Dvaα* and $saraα_2$ NOE's does not peak until after preirradiation times longer than one second, indicating that secondary NOE effects due to spin diffusion are seen only for longer observation times.

It was of interest to determine the overall correlation time (τ_c) that governed relaxation for ActD, dATGCAT, and the complex under the experimental conditions that would be employed for the NOESY experiments. It was thought that the correlation time would be roughly around the NOE null point, corresponding to a τ_c of ~0.5 nanoseconds. However, TOE experiments resulted in negative NOE effects for each compound investigated in aqueous solution. Spin-lattice relaxation times(T_1) were measured as well for these molecular species. Analysis of T_1 and NOE data indicated that the correlation time governing relaxation for these molecules was in the range of 2-5 nanoseconds in aqueous solutions at low temperature (0-15 °C.). Thus, spin diffusion was not a problem at mixing times less than about 1 second for ActD and dATGCAT and 0.5 second for the complex.

Spin-lattice relaxation times were measured by the inversion recovery technique and data at 10 τ values were fit to the two parameter equation using the experimentally determined inhomogeneity factor by a non-linear

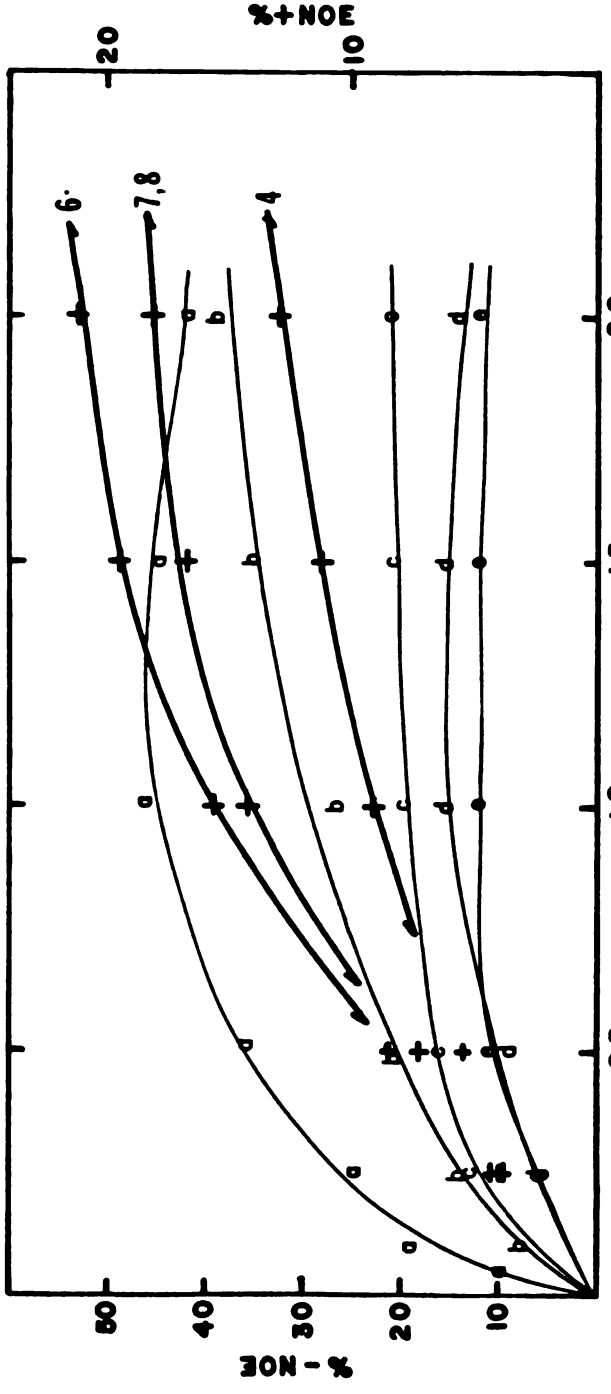

FIGURE 23

TOE data at 500 MHz. for preirradiation of proα resonances at τ= 50, 100, 250, 500, 1000, 1500, and 2000 milliseconds. NOE's measured by integration of difference spectra. Heavy lines through data points (+) are positive NOE's refered to scale on right. Light lines through data points for resonances: a) Dvaα, b) proβ$_2$,γ, c) saraα$_1$, d) saraα$_2$, e) proβ$_1$ are negative NOE's refered to scale on left.

least squares Marquardt-Levenberg algorithm (Hanssum et al., 1978). Data for ActD, 4.0 mM in BPES buffer(100%D_2O) at 10 °C. is found in Table X. Acquisition delay times should be set to greater than 5 T_1 for quantitative peak intensity measurement in the NOE experiments. However, delay times were generally set to 5 seconds due to instrument time limitations. This cycle time was greater than $5T_1$ times except for the adenine H2 protons in the duplex dATGCAT and the terminal adenine H2 protons in the complex, which are sufficiently far from other protons that their relaxation is inefficient and negligible NOE effects can be expected for the same reason.

A NOESY experiment was attempted for ActD in $CDCL_3$ to observe the structure of the molecule in this solvent. Previous experiments had determined that the molecule was near the NOE null point in this solvent at 20 °C. (P. A. Mirau, personal communication). A sample was prepared with these considerations in mind of ActD at a concentration of 40 mM and a NOESY spectrum was run at 30 °C. The spectrum in $CDCl_3$ had been fully assigned by Lackner (1971) and the α and β pentapeptide resonances had also been distinguished by selective deuteration and the narrow linewidths of the ActD resonances in this solvent. Representative slices from this NOESY spectrum are shown in Figure 24. The NOE's are indeed small and positive, since the cross peaks are below the baseline in the NOESY experiment. The pulse sequence used for these NOESY experiments could not filter for zero quantum coherence, so consequently peaks are seen that represent scalar coupling, not NOE effects. These peaks show a characteristic dispersion-like resonance pattern, and the zero quantum contribution in these peaks can be eliminated by integration of the spectrum since they average out to zero (G. Wagner, personal communication). The NOE contacts observed are all within proton-proton distances less than 3 Å in the crystal structure (Jain & Sobell,

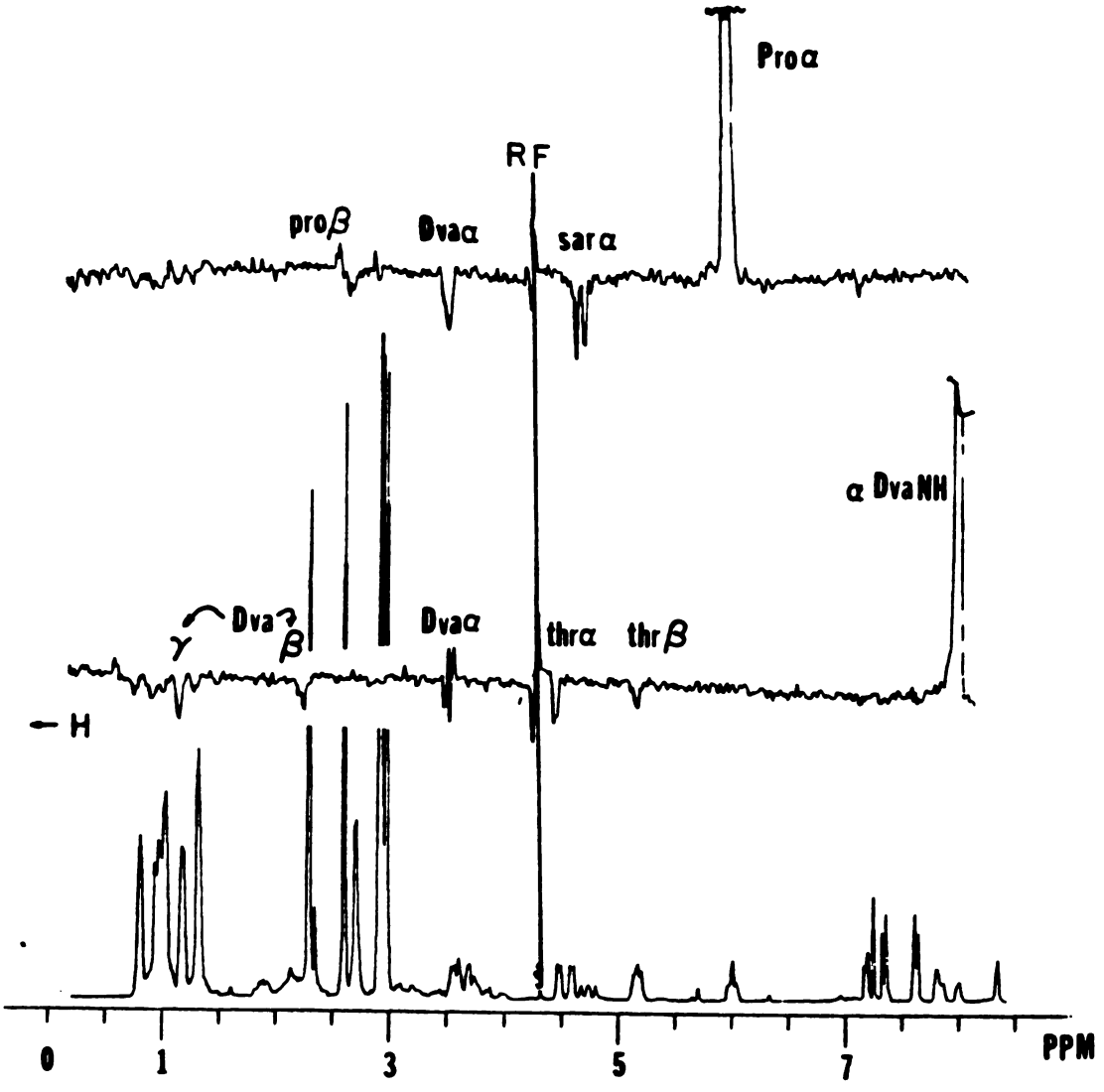

FIGURE 24

Representative 'slices' along ω_2 axis of ActD 240 MHz. NOESY spectrum(τ_m= 200 ms) in $CDCl_3$ (40 mM) at 30 °C. High field is to the left in these plots. (bottom), reference spectrum; (middle) slice along α-Dva N-H resonance on the diagonal, showing small positive NOE cross peaks from this proton to the α-thrβ, α-thrα, α-Dvaβ, and α-Dvaγ protons. In the crystal structure, these and only these protons are less than 2.8 Å from the α-Dva N-H proton. The dispersion character of the cross peak to the α-Dvaα proton is due to zero-quantum effects and shows no net NOE by integration; (top), slice along proα proton on the diagonal, with positive NOE's to the sarα, Dvaα, and proβ protons. Again, the proβ peak shows zero-quantum effects, but does not integrate to zero intensity. In the crystal structure, only these protons are within 2.8 Å of the proα proton.

1972) and scale very well to the relative distances. It was hoped that inter-pentapeptide NOE contacts could be observed that would provide information concerning the position of the pentapeptide lactones with respect to each other, but none were observed and examination of the crystal structure showed that no such distances could be found that were less than 3 A. The results of this experiment indicated that the configuration of the *Dva-pro-sar* peptide bonds of ActD in chloroform were *cis-cis* as found in the crystal structure. It thus appeared that the overall configuration of the ActD pentapeptide lactones in chloroform was similar to that of the crystal structure, corroborating the ^{15}N-NMR results.

NOESY experiments on ActD in BPES(100% D_2O) were done at 240 MHz at mixing times of 100, 250, and 500 ms. The signal-to-noise of these spectra was not as much as desired so a NOESY spectrum at 500 MHz with a mixing time of 250 ms. was done that confirmed the results obtained at 240 MHz and revealed NOE's of smaller intensities that could not be observed in the 240 MHz spectra. This spectrum, which was not plotted as a square matrix, is shown in Figure 25. The lines from intense diagonal peaks that run parallel to the ω_1 axis are termed "t_1 noise" and are instrumental artifacts that were particularly pronounced in this spectrum for an undetermined reason. Table XI contains NOE intensities and distances scaled by the NOE measured between the H7 and 6-CH_3 protons and the NOE between the *sarα*$_1$ and *sarα*$_2$ protons that must be at the fixed distances given in Table XI. Comparison of these distances and the distances taken from the crystal structure shows a good correlation, indicating that the structures are very similar. A comparison of the NOE intensities for the *proα* resonance with the intensities found for the TOE experiment shows that they are comparable for similar observation times. It is thus apparent that the structures of ActD in aqueous

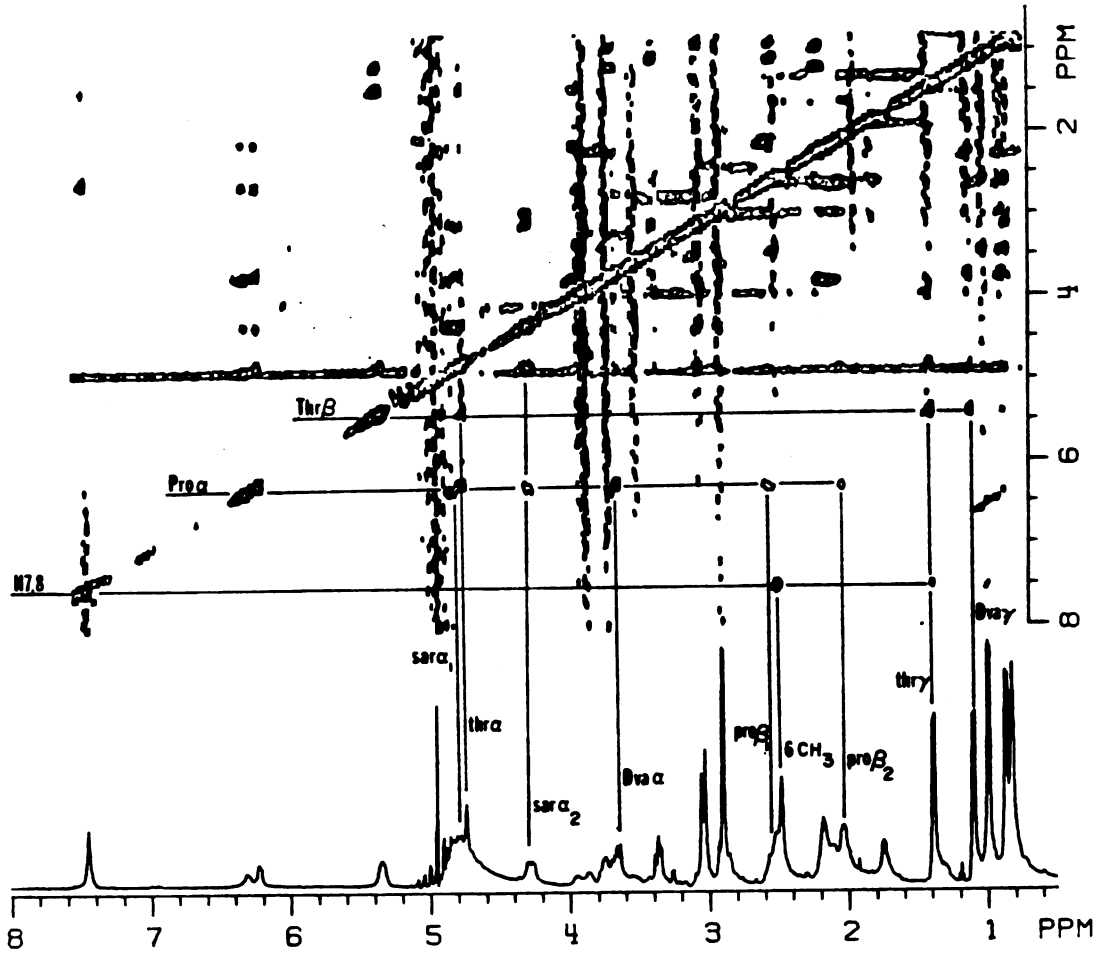

FIGURE 25

500 MHz. NOESY spectrum(τ_m= 250 ms) of ActD in BPES (100% D_2O). The H7,8 protons along the diagonal show cross peaks to the 6-CH_3 and thrγ protons. The proα protons show strong cross peaks to the sarα_1 and Dvaα protons, with weaker cross peaks to the sarα_2, proβ_1, and proβ_2,γ protons. The thrβ proton shows strong cross peaks to the thrα , thrγ, and Dvaγ_1 protons. NOE intensities are consistent with interproton distances in the crystal structure (Jain & Sobell, 1972).

solution, in $CDCl_3$, and in the crystal structure are very similar.

TABLE XI

Comparison of ActD NOE Distances vs. Crystal Distances

proton	cross peak(NOE[a])	Calculated Dist.[b]	Crystal Dist.[c]
4-CH_3	6-CH_3(2%)	2.84	4.65
6-CH_3	H7(6%)	2.35	2.50
H8	thrγ(1.5%)	3.0	3.7
sarα_2	sarα_1(30%)	1.81	1.81
	nmvN-CH_3(5%)	2.44	2.23
	sarN-CH_3(5%)	2.44	2.46
	proα(8%)	2.3	3.5
thrβ	thrα(8%)	2.3	2.52
	thrγ(4%)	2.5	2.3
	Dvaγ_1(2%)	2.85	2.50
sarα_1	sarα_2(24%)	1.88	1.81
	proα(13%)	2.1	1.83
	nmvN-CH_3(3%)	2.7	2.25
	sarN-CH_3(--)	>3.4	3.6
nmvβ	nmvγ_1(9%)	2.2	2.5
	nmvγ_2(6%)	2.4	2.5
Dvaα	proα(28%)	1.81	2.41
	Dvaβ(2%)	2.85	3.09
	Dvaγ_1(3.5%)	2.6	2.9
	Dvaγ_2(3.3%)	2.6	2.9
proα	Dvaα(31%)	1.81	2.41
	proβ_1(9%)	2.2	2.44
	proβ_2.γ(16%)	2.0	3.1

[a] measured by integration of slices, normalized to total intensity of slice.
[b] calculated by equation: $r(1)/r(2)=(\eta(2)/\eta(1))^{1/6}$.
[c] from crystal structure(Jain & Sobell, 1972) with hydrogens attached in standard geometry.

$[dATGCAT]_2$ Assignments and Structure. The sample of dATGCAT was assigned in a similar manner. The extinction coefficient at 20 °C. was determined by weighing 5 mg and dissolving in 5 ml of BPES buffer. The molecular weight was calculated to be 1875 grams per mole of strand for the pentaammonium salt. The extinction coefficient at 260 nm was then calculated to be 44,625 per strand at 20 °C. This is comparable to that for DNA, which is ~7000 per nucleotide. At optical concentrations ($1.6x10^{-5}$ M) in BPES, the T_m of the hexamer is 15 °C., but at NMR concentrations ($4.0x10^{-3}$ M) the T_m is ~45 °C. as measured by the temperature dependence of the base proton chemical shifts. The imino base protons (Figure 28) are observed in BPES(10% D_2O) up to temperatures of 25 °C. and were assigned by observation of different temperatures where the exchange with bulk water began to broaden and shift each resonance due to fraying from the ends. The CD spectrum of dATGCAT was taken and was identical to that of calf thymus DNA (data not shown). It could thus be concluded that the hexamer existed as a double stranded helix at temperatures below ~30 °C. in this buffer at the concentrations employed, and that the structure of that double helix was within the B family.

The spectrum of duplex dATGCAT is shown in Figure 26. It should be noted that there is a dyad C_2 axis of symmetry between the central GC base pairs of this sequence, and therefore resonances at equivalent positions in both strands have identical chemical shifts. The aqueous solution spectrum of duplex dATGCAT has been partially assigned (Patel & Tonelli, 1975), and these assignments were confirmed by the NOESY spectra, except for the thymidine 5-methyl protons. At 10 °C., the terminal thymidine 5-CH_3 (T_t^5, 1.396 ppm) protons are found downfield from the internal thymidine 5-CH_3 (T_i^5, 1.263 ppm) protons. These were correlated by the strong NOE's from their

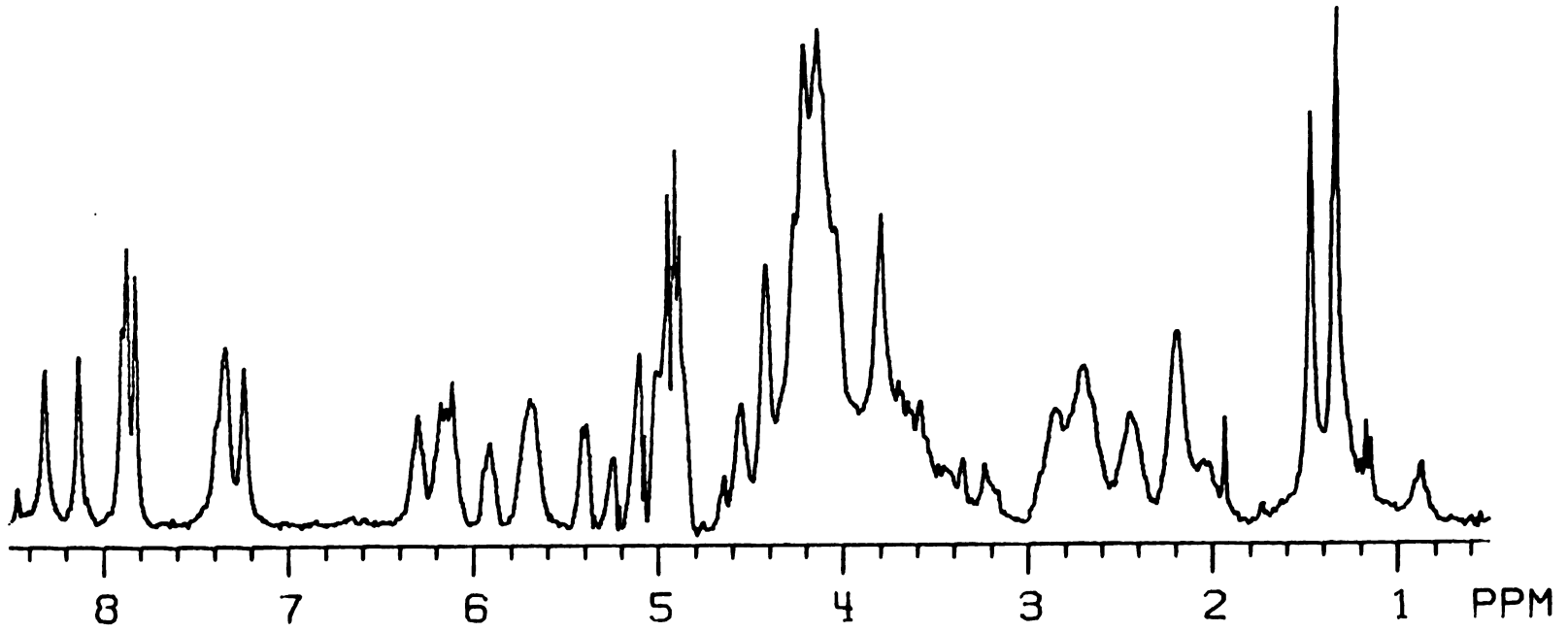

FIGURE 26

240 MHz. proton NMR spectrum of duplex dATGCAT (4.0 mM. strands) in BPES (100% D_2O at 10.0 ^{o}C. Referenced to internal TSP, 64 acquisitions.

corresponding H6 protons. Chemical shifts of the adenine H2 protons change at temperatures above 15 °C. due to fraying, so all NMR experiments were done at 10 °C. to minimize such effects.

The base protons (6.8 to 8.4 ppm) were assigned by several techniques and were found to agree with the assignments of Patel & Tonelli (1975) except for the thymidine 5-CH_3 resonances as explained above. The purine H8 protons were located by their partial exchange with deuterium in the solvent when the solution is held at 70 °C. overnight. The adenine H2 protons were located by their absence of exchange with deuterium and their longer spin-lattice relaxation times compared to the other base protons. The adenine H8 protons are always found downfield from guanine H8 protons. These considerations aided the assignments and were found consistent with the assignments made by examination of the NOESY spectrum. The initial assignments themselves were done solely by inspection of the NOESY spectra in conjunction with chemical shift considerations.

The COSY spectrum of dATGCAT was not helpful due to the very low signal-to-noise, except to locate the cytosine H6 and H5 resonances. These protons gave the only strong cross peak in the COSY spectrum of this compound at 10 °C., whereas the 1'-2',2" and 2',2"-3' cross peaks appeared only at temperatures above 50 °C. where the hexamer is single-stranded (data not shown).

The spectrum of dATGCAT can be expected to show features in common with oligonucleotides of different sequence. Several research groups have shown that for instance: 1)base protons are always found at chemical shifts between 6.8 and 8.5 ppm; 2) anomeric 1' protons are found, along with the cytosine H5, between 5.4 and 6.5 ppm; 3) 3' protons are found between 4.2

and 5.4 ppm, with those of purine residues downfield from those of pyrimidine residues; 4) 4' and 5',5" protons are found together in a broad envelope around 4 ppm and are very difficult to resolve, while the 5',5" protons of the initial residue at the 5' end are shifted upfield from the others if this residue does not have a phosphate attached at its 5' end; 5) the 2' and 2" protons are found between 0.9 to 3.2 ppm, with those of purine residues downfield from those of pyrimidine residues. The purine 2' and 2" resonances show less difference in their chemical shifts compared to the 2' and 2" protons of pyrimidine residues. 6) the thymidine 5-CH_3 protons are found around 1.5 ppm. These generalised considerations about the chemical shifts at which certain protons can be found can, in conjunction with a NOESY spectrum, serve to assign the resonances in a duplex oligonucleotide.

Examination of the NOESY spectrum at 240 MHz of duplex dATGCAT found in Figure 27 shows how this is accomplished. The base proton of the 5' terminal residue (A_t^8) can be identified by two criteria: 1) it is the only base proton that exhibits an NOE to the 5',5" proton region and that NOE is to the 5',5" resonances that are shifted upfield from the others due to the lack of a phosphate residue. The 5',5" protons on other residues are conformationally restricted, and their motion does not bring such a close approach to the base proton at these internal residues. 2) This base proton is the only one that shows an NOE to only one anomeric proton, since there is no residue to the 5' side in the sequence. Identification of the 5' terminal base proton allows one to "walk" along the sequence, assigning all the other protons by NOE contacts and the above chemical shift considerations. The validity of this technique has been confirmed by other groups (Scheek et al., 1983; Feigon et al., 1982; Hare et al., 1983; Broido et al., 1984) and only requires the assumption that the oligonucleotide is in a B form, right handed double

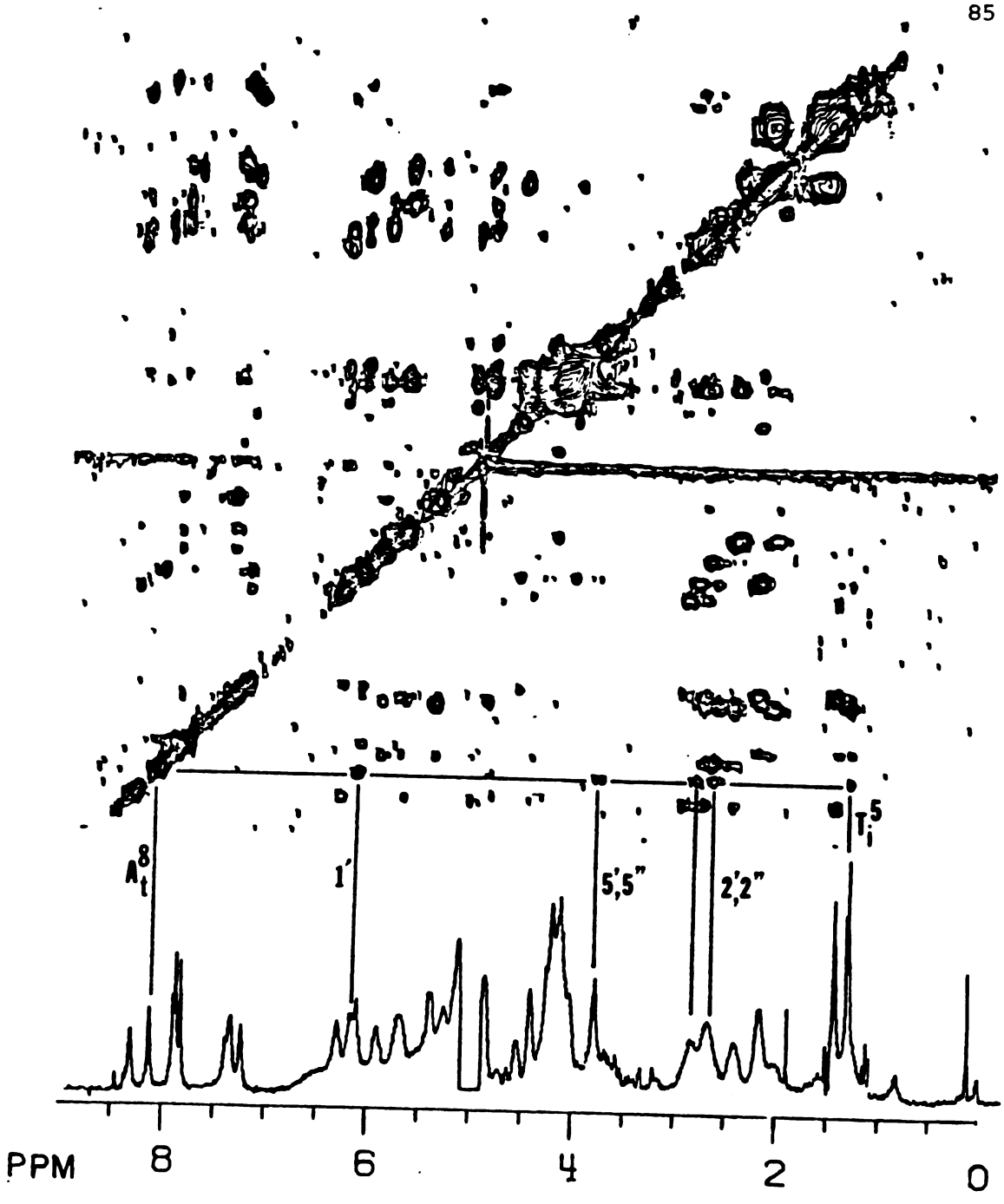

FIGURE 27

240 MHz. NOESY spectrum (τ_m = 200 ms) of duplex dATGCAT in BPES (100% D_2O) at 10 °C. A_t^8 resonance is located by NOE to terminal 5',5" and single NOE cross peak to 1' region; T_i^6 resonance shows NOE to same anomeric proton, and to its own 1'. A fully self-consistent set of assignments can be made in this manner by "walking" from the 5' terminal residue in conjunction with chemical shift considerations general to oligonucleotide spectra.

helix. The CD results indicate this is probably so, and a set of fully self-consistent assignments results from the above procedure. The resulting assignments are shown in Table XII.

Examination of NOE cross peak patterns in Figure 27 shows that the resonance at 8.129 ppm has only one cross peak to the anomeric region and is the only base proton to show a NOE to the terminal 5',5" resonance at 3.800 ppm, identifying this resonance as the terminal adenine H8(A_t^8). The cross peak at 6.170 ppm identifies this resonance as the anomeric proton for this nucleotide residue (A_t1'). The only cross peaks to the 2',2" region at 2.83 and 2.67 ppm identify these resonances as the A_t2',2" protons. The resonance at 8.310 ppm was identified as the A_i^8 by elimination. This proton shows two cross peaks to the anomeric region, one at 6.295 (A_i1') and a weaker one at 5.650 (C1'). Each base proton resonance shows only two NOE's to the anomeric region. The stronger one is initially assigned to be the 1'

TABLE XII

Proton Assignments for dATGCAT in BPES, 10°C.

Residue	H8	H2	H6	H5	H1'	H2',H2"[a]	H3'	H5' H5"	Imino
A_t	8.129	7.825	--	--	6.170	2.82,2.63	4.80	3.795	
T_i	--	--	7.334	1.263	5.695	2.42,2.12	4.85	--	13.77
G	7.895	--	--	--	5.905	2.72,2.64	5.04	--	12.690
C	--	--	7.371	5.394	5.650	2.42,2.04	4.85	--	
A_i	8.310	7.872	--	--	6.295	2.92,2.75	5.04	--	
T_t	--	--	7.236	1.396	6.111	2.20	4.57	--	13.214

[a]assignments for pair, 2" vs. 2' has not been assigned

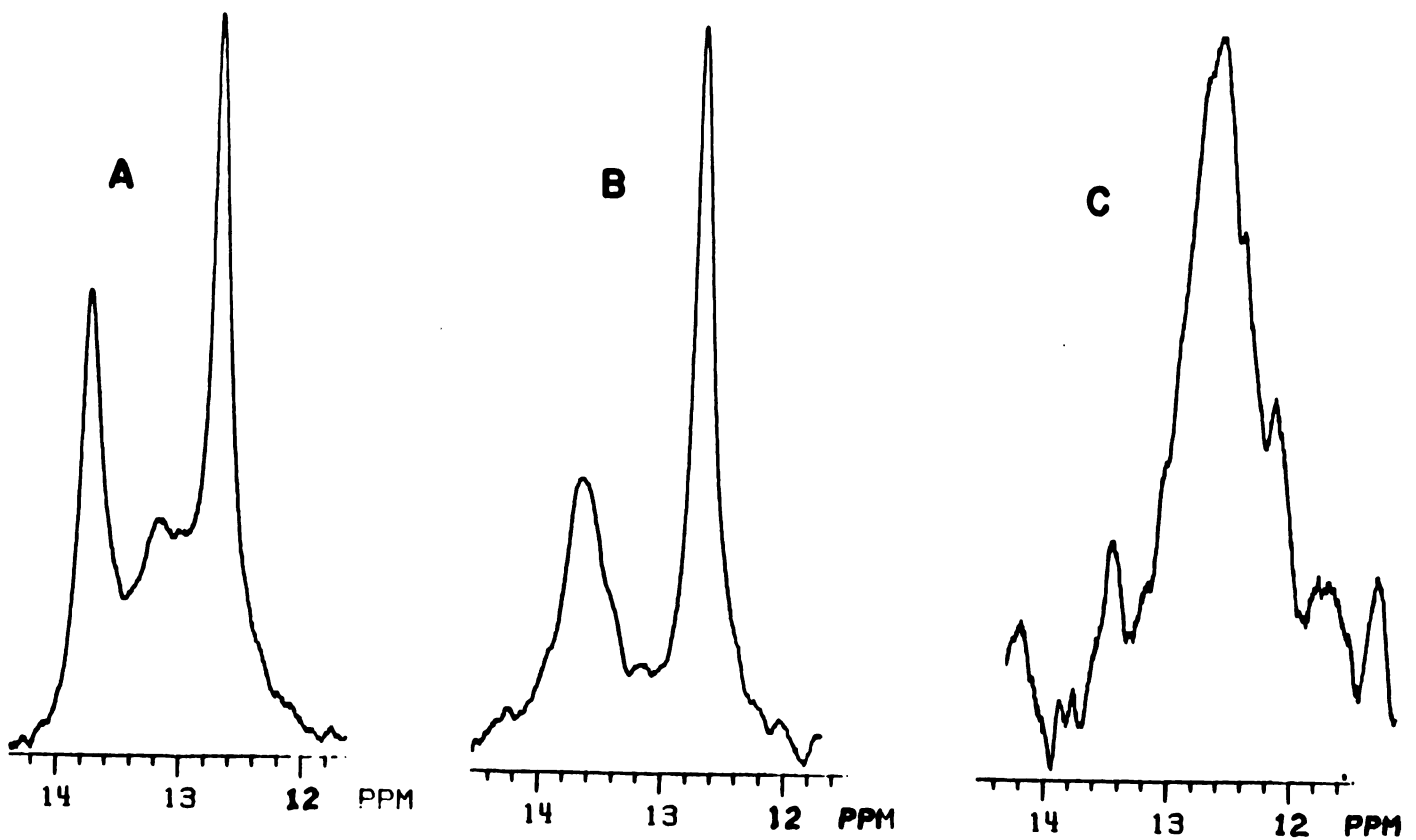

FIGURE 28

Imino proton spectra of duplex dATGCAT (4.0 mM strands) in BPES (90% H_2O, 10% D_2O) at: A) 3.0 $^oC.$, B) 12.0 $^oC.$, and C) 23.0 $^oC.$ The resonance at 13.214 ppm broadens and shifts upfield first, assigning it to the terminal base pair (T_t^3) protons. The resonances at 13.774 and then 12.690 broaden and shift upfield, assigning these protons to the T_i^3 and G^1, respectively. Chemical shifts referenced to internal TSP.

proton on the same residue, while the other is to the 1' proton of the neighboring nucleotide in the 5' direction of the sequence. Base proton to 2',2" contacts show the same pattern. Anomeric (1') protons only show NOE cross peaks to one set of 2',2" protons, while the 2',2" protons show only one set of NOE's to the 3' region. Base proton to base proton contacts are apparent only for A^8 to T^5 protons and G^8 to C^5 protons. Other contacts between neighboring bases can be observed at longer mixing times. Given a minimal amount of peak overlap, a self-consistent set of assignments can be made quickly in this manner. Relative NOE intensities were compared with a model of the B type helix generated for this hexamer using Struther Arnott's coordinates (Arnott & Hukins, 1972). No major inconsistencies were found, implying that the structure is within the B family.

Assignments and Structure of the Actinomycin D/dATGCAT(1:2) Complex. The spectrum of the ActD/dATGCAT(1:2) complex (COMP2) is shown in Figure 29. Resonances of COMP2 are fairly temperature independant in the range 0 to 40 °C., with the anomeric protons showing the most variation of about 0.005 ppm/°C. The spectrum of a sample of ActD/dATGCAT(1:1) (COMP1) was very complex, showing several species in fast exchange on the NMR timescale. At these concentrations, ActD seems to bind to single strands of dATGCAT as well as forming the 1:2 complex, so saturation transfer experiments could not be done to correlate free ActD resonances with bound resonances. A sample of ActD/dATGCAT(1:4) was made up and had a spectrum identical to a sum of the spectra of COMP2 and free dATGCAT. Saturation transfer experiments were done on this sample to assign base proton resonances in the complex.

Saturation transfer was not observed between free and bound dATGCAT resonances until temperatures in excess of 40 °C. were attained. Data was acquired by use of a presaturation pulse of 0.5 seconds at the resonance of interest before acquisition. Off-resonance controls were done and acquired in the interleave mode. The FID's were subtracted and transformed to give difference spectra, some of which are shown in Figure 30. No interference from NOE effects was observed for these experiments. The TOE pulse sequence was used at sample temperatures ranging from 10 °C. to 45 ° C. Negative NOE's were observed to diminish rapidly as the sample temperature was raised from 10 °C. to 35 °C., where the correlation time of the complex reached the NOE null point. No NOE effects could be observed above 35 °C. for this sample. At temperatures over 40 °C., free and bound dATGCAT resonances began to collapse toward one another and saturation transfer could be observed. Resonances of the bound dATGCAT base protons were assigned

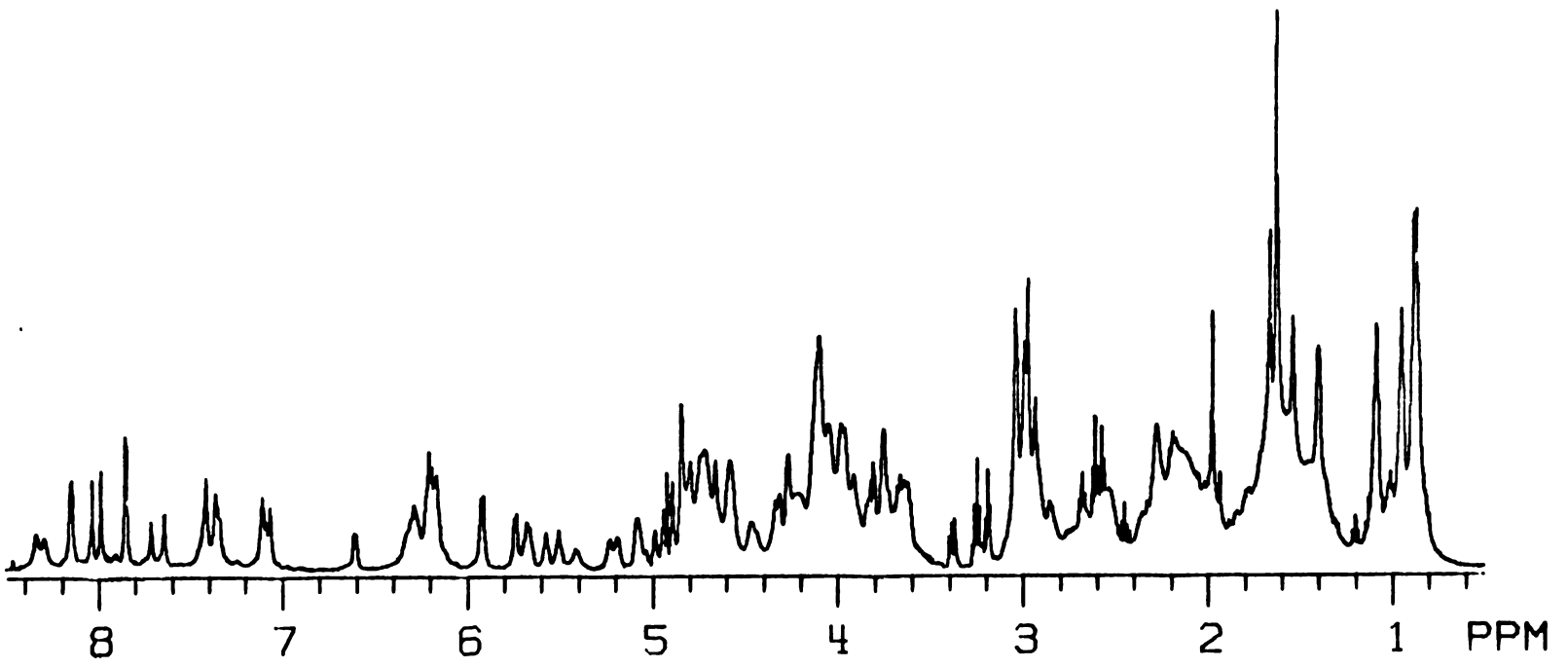

FIGURE 29

Proton NMR spectrum at 500 MHz. of Actinomycin D/dATGCAT(1:2) complex in BPES (100% D_2O). The concentration of ActD is 4.0 mM. and T= 15 ^{o}C. 64 acquisitions, referenced to internal TSP.

FIGURE 30

Selected saturation transfer experiments on COMP2 at 45 °C.: A) downfield spectrum of COMP3; B) reference spectrum of COMP2(35 °C) C) reference spectrum of dATGCAT. Difference spectra: D) T_t^6(dATGCAT) irradiated; E) ? irradiated, effect at A_t^2(dATGCAT); F) ? irradiated, effect at G^8(dATGCAT); and G) ? irradiated, effect at T_i^6(dATGCAT).

in this manner and checked by preirradiation of both bound and free peaks.

A COSY spectrum of COMP2 was then acquired, part of which is shown in Figure 31. Three AX proton pairs were observed in the downfield portion of this COSY spectrum. Two of these could be assigned to C^6 and C^5 pairs in conjunction with the saturation transfer results. The third pair could then be assigned to the ActD chromophore H7 and H8 resonances. Cross peaks were also observed from bound T^6 resonances to T^5 methyl resonances, allowing the correlation of four pairs of thymidine base protons. The portion of the COSY spectrum shown in Figure 31 contains cross peaks correlating anomeric protons and 2',2" protons on the same deoxyribose residue. Cross peaks could be observed from the 2',2" protons to the 3' protons, and from some of these to the 4' and 5',5" protons as well. In this way, most deoxyribose resonances could be grouped into individual nucleotides. Resonances of the bound ActD protons were located within the COSY spectrum by their characteristic spin system patterns in the same way that assignments were made in the free drug. The remaining task of assignments could be finished by examination of the NOESY spectrum.

The NOESY spectrum of COMP2 (τ_m= 250 ms) is reproduced in four sections. The first quadrant (Figure 32) covers the range ω_2 0-5 ppm, ω_1 0-5 ppm; Figure 33 covers ω_2 5-10 ppm, ω_1 0-5 ppm ; Figure 34 covers ω_2 0-5 ppm, ω_1 5-10 ppm; and Figure 35 covers ω_2 5-10 ppm, ω_1 5-10 ppm. Examination of Figure 38 shows that there is only one NOE contact to an anomeric proton for the A_t^8 resonance, as was the case for the free dATGCAT spectrum. This identifies the resonance at 6.118 ppm as the $A_t^{1'}$ proton. The COSY spectrum then is used to identify the 2',2" resoances of this nucleotide. The resonances of the other base protons show NOE contacts to two anomeric

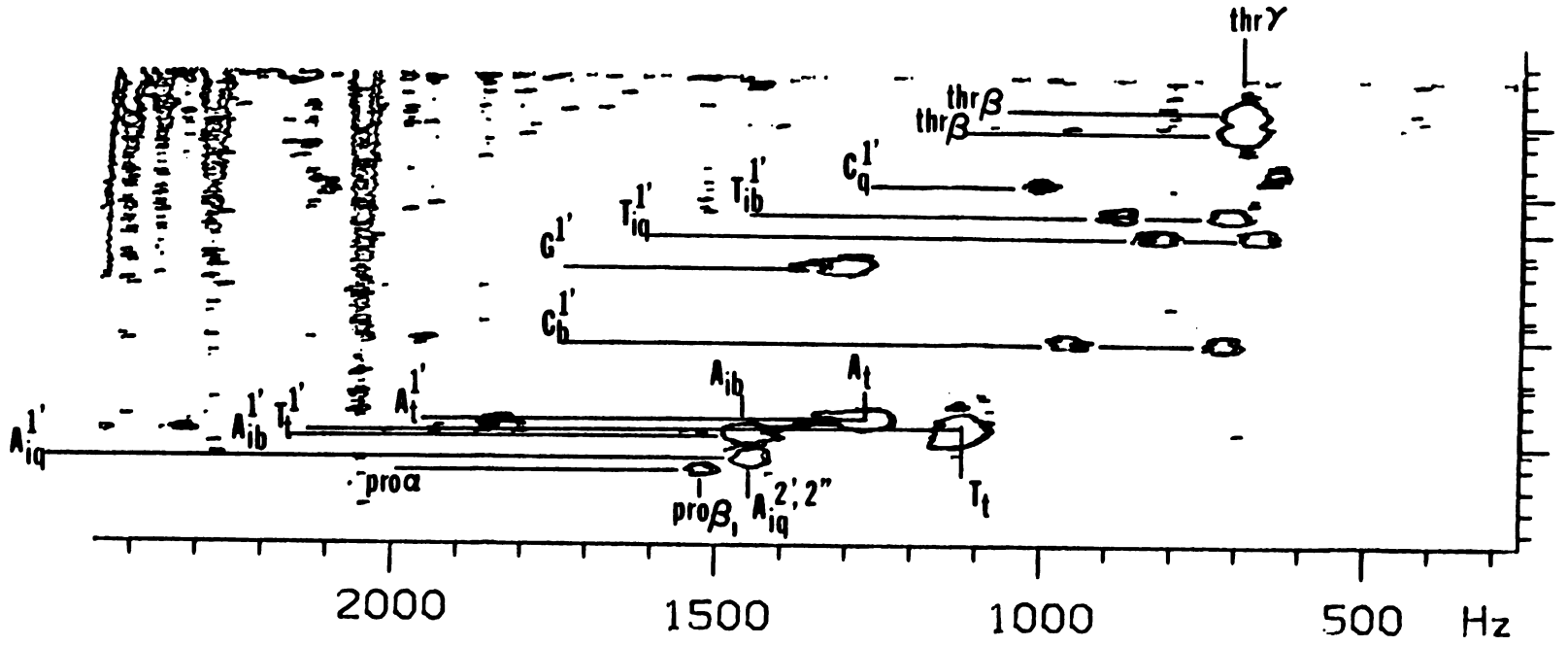

FIGURE 31

Portion of the 500 MHz. COSY spectrum of COMP2 showing the deoxyribose 1' to 2',2" cross peaks due to scalar coupling. The 1' and 2',2" resonances are located by their cross peaks and correlated to individual nucleotide residues.

protons; a stronger one to the 1' proton of the same nucleotide and a weaker NOE to the anomeric proton of the neighboring nucleotide in the 5' direction of the sequence. The base proton to 2',2" NOE contacts show the same pattern and can be used as a check, via the COSY spectrum, on the validity of this procedure. Anomeric protons show NOE contacts only to other deoxyribose protons in the same nucleotide, while the base protons show NOE contacts to base protons of neighboring residues. In this way, all the bound resonances of dATGCAT in the complex can be assigned except for several of the 4' and 5',5" resonances that cannot be definitely assigned due to peak overlap.

Assignments of the bound ActD resonances were mostly made by inspection of the COSY spectrum. The H7 proton was assigned by the strong NOE to a methyl resonance at 2.0 ppm, to which a COSY cross peak had also been observed. This identified the 6-CH_3 protons . The 4-CH_3 resonance was identified by a weak NOE to the 6-CH_3 protons. The H8 resonance was then assigned by elimination. As in the free drug, the semi-C_2 symmetry of the molecule in conjunction with the linewidths did not allow the assignment of resonances to either the α or β-pentapeptide lactone generally. However, the *thr*, *sar*α and *pro*α protons were well separated in the spectrum. These same residues show the greatest asymmetry in the ^{15}N-NMR spectrum of [^{15}N]ActD bound to dATGCAT, corroborating the results of this technique.

Assignment of most protons to a particular residue was possible by use of the following technique. Inspection of the NOESY spectrum (Figure 35) revealed that only one G^8 and one C^6, C^5 resonance had an NOE contact to the chromophore H7 and H8 protons. This assigned these protons to the hexamer strand wrapped around the benzenoid part of the ActD chromophore

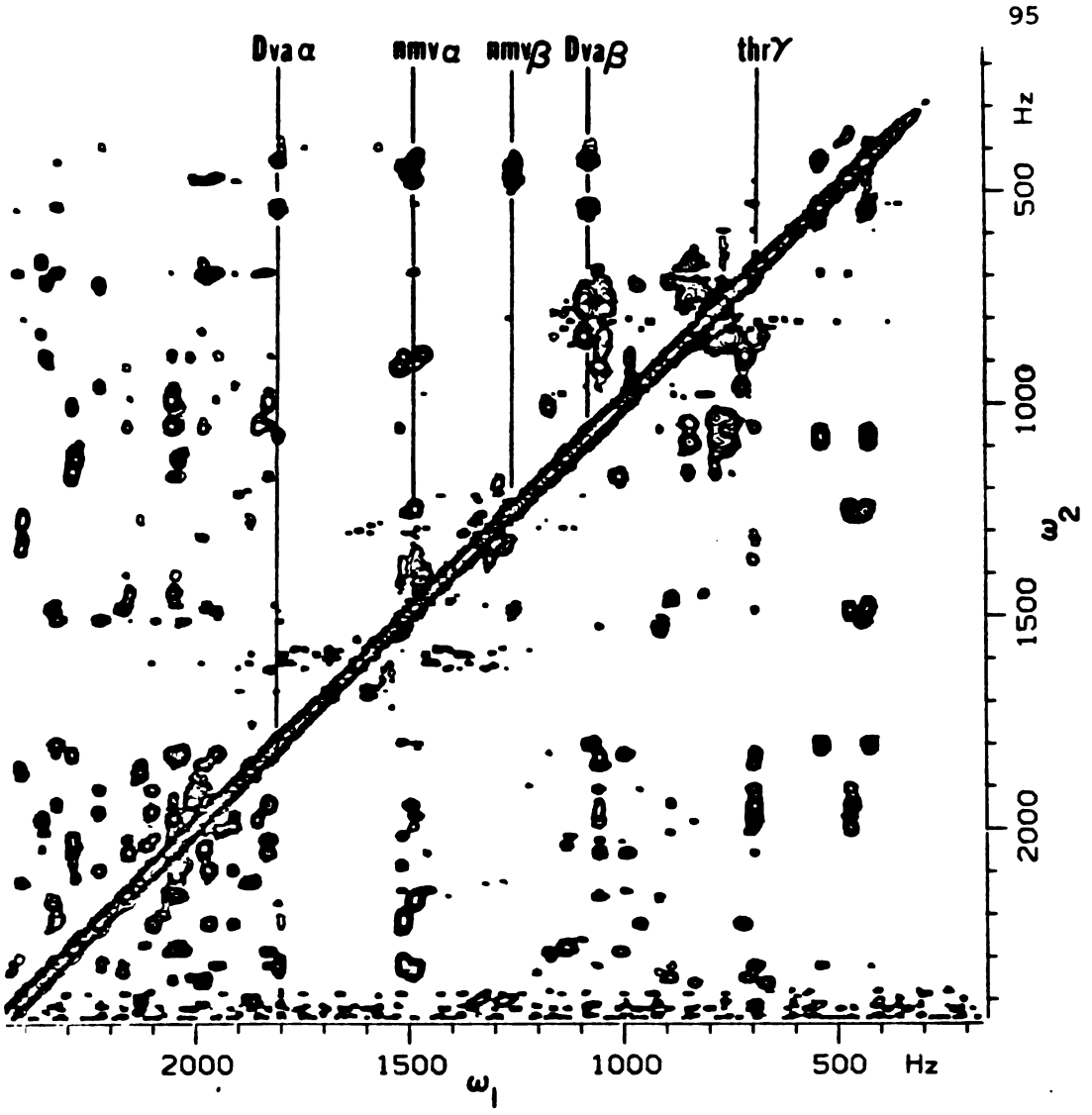

FIGURE 32

Portion of the 500 MHz. NOESY spectrum (τ_m= 200 ms) of COMP2. The normal spectrum from 0-5 ppm runs along the diagonal. Cross peaks from the labeled ActD protons on the diagonal are observed.

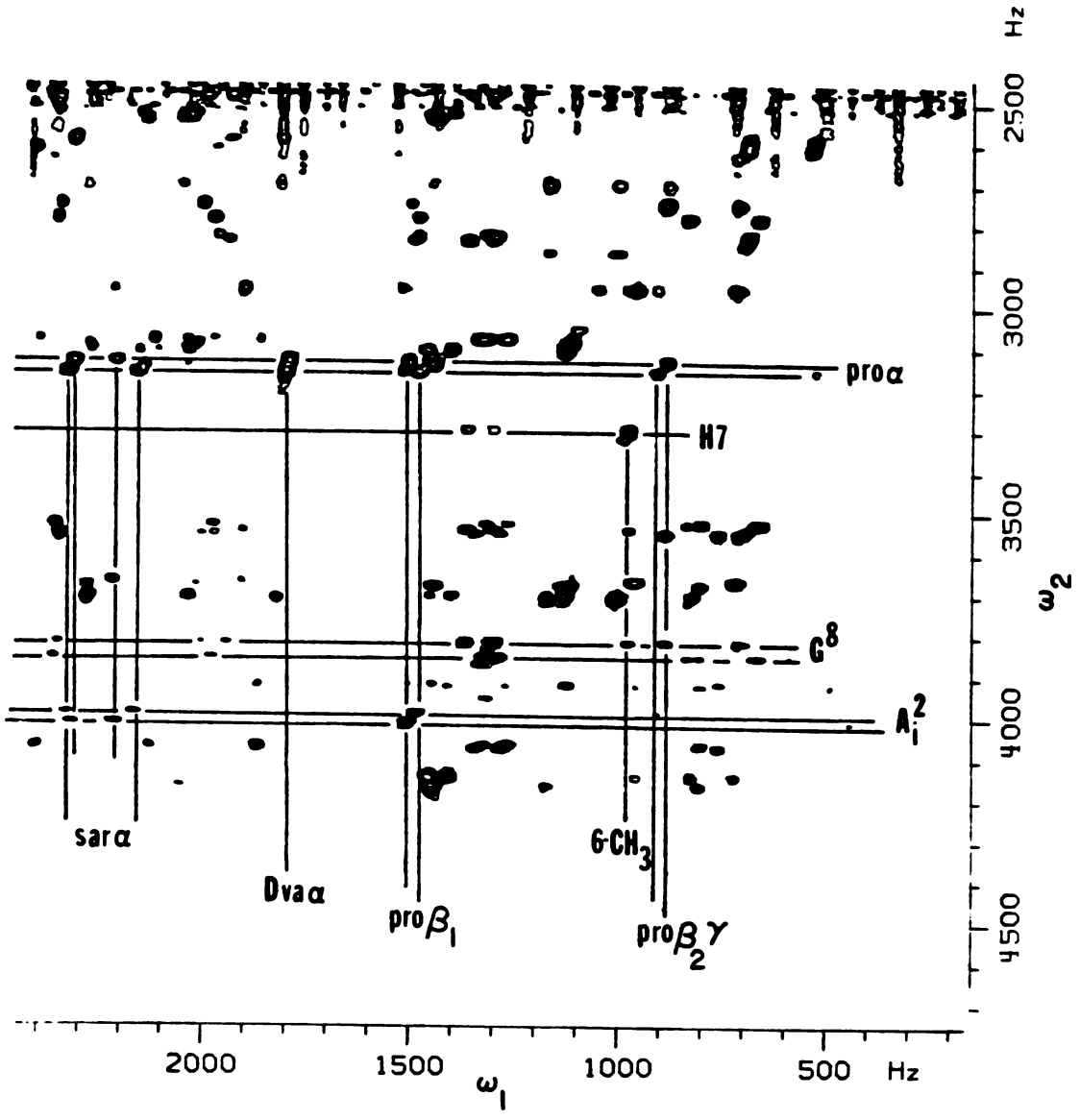

FIGURE 33

Another quadrant of the 500 MHz. NOESY spectrum of COMP2. Cross peaks from several resonances in the downfield portion of the spectrum to various ActD protons are marked. The strong NOE between the proα and Dvaα , sarα protons indicates that the peptide configuration about these residues is the same as that found in the free drug. Contacts from the guanine and cytosine bases to ActD chromophore methyl groups partly demonstrate that the drug chromophore is intercalated between these base pairs.

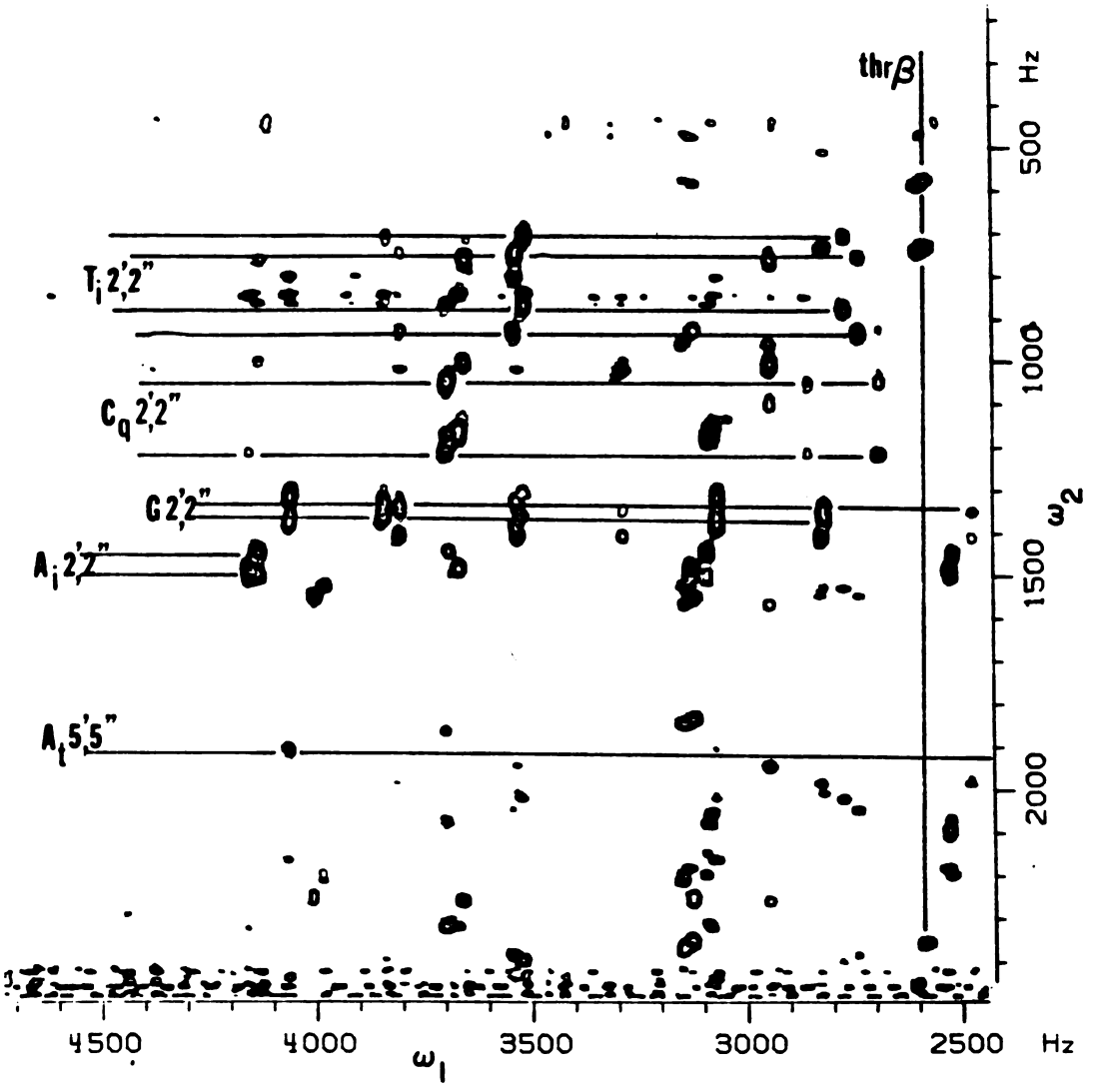

FIGURE 34

Quadrant of the NOESY spectrum that is symmetric to that shown in Figure 33. Several nucleotide 2',2" NOE cross peaks are indicated. The strong NOE from an adenine base proton to the terminal A_t5',5" resonances confirms that this is the A_t^8 proton.

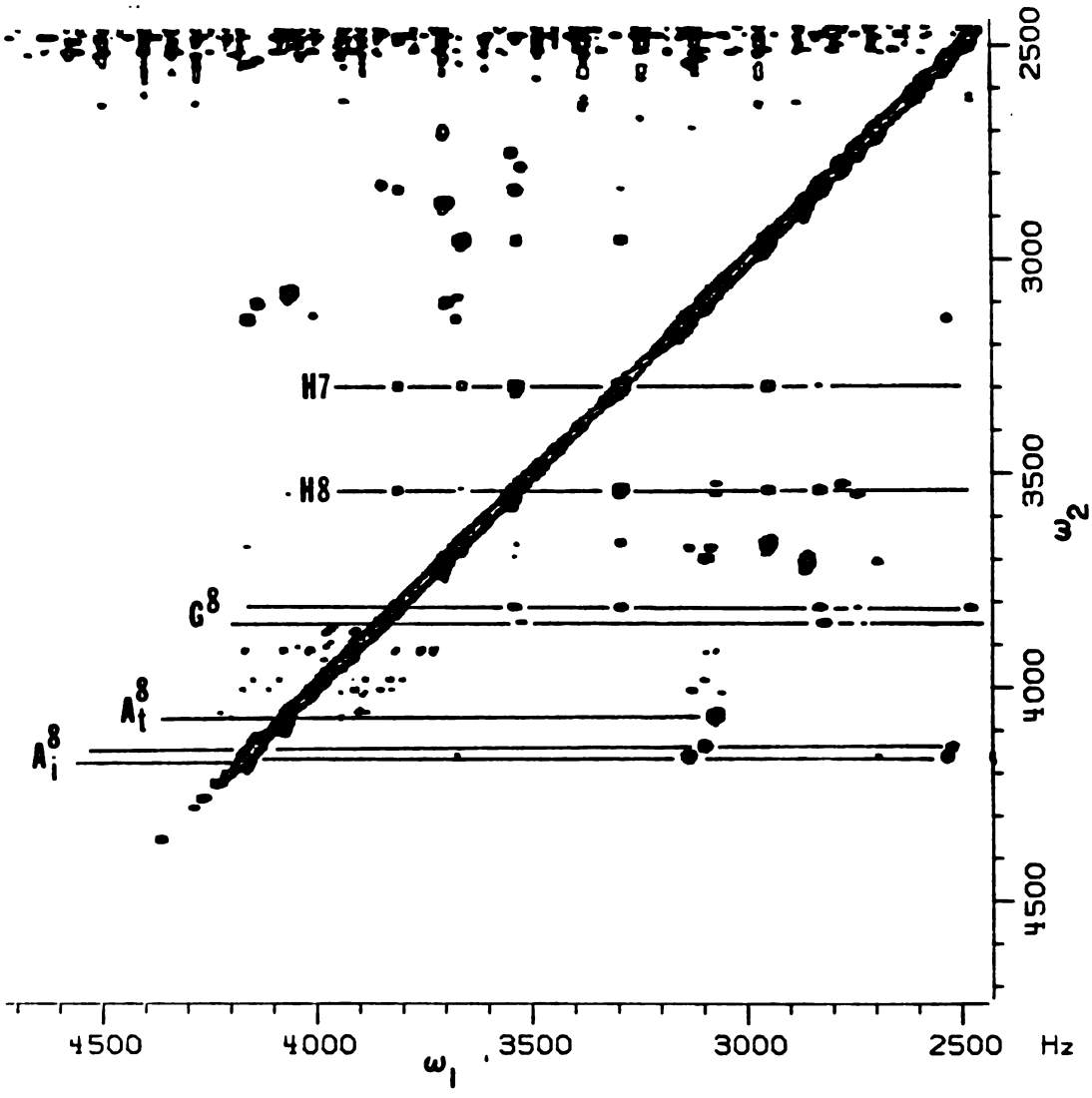

FIGURE 35

Downfield quadrant of the NOESY spectrum, with the normal spectrum (10-5 ppm) along the diagonal. Several base protons are labeled, showing cross peaks between the drug H7 and H8 protons and the base protons of the guanosine and cytosine residues. Base proton to 1' proton cross peaks are observed in this region as well.

(G_b^8, C_b^6, and C_b^5, respectively). The other G^8 and C^6,C^5 resonances must be those of the dATGCAT strand wrapped around the quinoid part of the chromophore and were therefore assigned: G_q^8, C_q^8, and C_q^5 respectively. These assignments could be continued through the base-base proton NOE's until the final residue, (A_t) where the magnetic non-equivalence became too small for resolution of the protons on separate strands. The magnetic non-equivalence of the T_t residues was sufficient for their assignment to either strand.

The *proα* and *saraα* resonances could be assigned to the α and β pentapeptide lactones by NOE contacts and stereochemical considerations, while other resonances of the bound drug were not sufficiently resolved to assign further. Using these procedures, the proton resonances of this complex could be almost completely assigned. Assignments of most importance to the determination of structural features in this complex are listed in Table XIII.

It was of interest to measure the deoxyribose residue scalar coupling constants to gain information concerning the puckering of these rings. The configuration of these residues in oligodeoxyribonucleotides is within the family 2'-endo (S) in crystal structures, while the configuration of ribose residues and deoxyribose residues on the 5' side of intercalated drugs usually lies within the 3'-endo (N) family (Berman & Neidle, 1979). Examination by NMR of oligonucleotides in solution indicates that an equilibrium exists in deoxyribose residues of roughly 30% N and 70% S type conformations that is in fast exchange(James et al., 1983). It is possible to get an estimate of these relative populations by measurement of the 1'-2' + 1'-2" scalar coupling constants and the 2',2"-3' coupling constants(Altona, 1982). Many of these cou-

TABLE XIII

Proton Resonance Assignments of the ActD/dATGCAT(1:2) Complex[a]

ActD Protons

H7	6.611	thrβ	5.234	βproα	6.323	αsarα_1	4.659
H8	7.095	thrγ	1.405	αproα	6.289	αsarα_2	4.454
6-CH_3	1.977	Dvaα	3.625	proβ_1	3.043	βsarα_1	4.680
4-CH_3	1.631	Dvaγ_1	1.093	proβ_2,γ	1.843	βsarα_2	4.359
nmvN-CH_3	3.037	nmvN-CH_3	2.994	nmvα	3.013	nmvβ	2.575

dATGCAT Protons

Residue	H8	H2	H6	H5	1'	2',2''	3'
A_t	8.158	7.854	—	—	6.171	2.703,2.584	4.837
T_{ib}	—	—	7.115	1.543	5.511	1.800,1.441	4.722
T_{iq}	—	—	7.070	1.623	5.579	1.692,1.353	4.743
G_b	7.646	—	—	—	5.685	2.757,2.630	4.982
G_q	7.716	—	—	—	5.664	2.657,2.610	—
C_q	—	—	7.348	5.924	5.924	1.945,1.459	4.485
C_b	—	—	7.423	5.745	5.419	2.387,2.033	4.586
A_{ib}	8.298	7.990	—	—	6.218	2.935,2.833	5.071
A_{iq}	8.342	8.039	—	—	6.292	2.919	5.091
T_{tb}	—	—	7.423	1.667	6.216	2.280	4.586
T_{tq}	—	—	7.369	1.631	6.192	2.273	4.588

[a](4.0 mM) in BPES, 10 °C.

pling constants could not be measured due to superposition of resonances. The values found in Table XIV were obtained by fitting the anomeric proton resonances to a simulation of triplets having 1:2:1 intensity ratios and identical linewidths, using the NTCCAP algorithm supplied by Nicolet on the 1180 data system. It was not possible to obtain the 2',2''-3' coupling constants, but measurement of the 1'-2' + 1'-2'' coupling constants and their comparison shows that there is a shift in the conformation of the guanine deoxyribose ring to more 3' endo character in the complex compared to the free duplex. Other deoxyribose residues in the free and bound dATGCAT show values comparable to those found in other oligomers where the 30% N vs. 70% S equili-

brium exists.

Structure of the ActD/dATGCAT(1:2) Complex. Examination of the COMP2 NOESY spectrum reveals over forty contacts between ActD and dATGCAT. This number of contact points greatly restricts the possible structure of the complex in conjunction with the several hundred NOE contacts between ActD-ActD protons and dATGCAT-dATGCAT protons. The general features of the complex are: 1) The ActD chromophore is intercalated between the central GC base pairs. This is necessary due to the NOE contacts between the chromophore and the guanine and cytosine bases. The

TABLE XIV

Deoxyribose Scalar Coupling Constants[a]		
dATGCAT (10 °C.)		
G1'	13.8	±.3
ActD/dATGCAT(1:2) (15°C.)		
G1'	11.4	±1.2
$T_{iq}1'$	14.3	±0.3
ActD/dATGCAT(1:2) (25°C.)		
T_t1'	13.6	±0.3
$A_{iq}1'$	14.0	±0.3
A_t1'	13.8	±0.3
$A_{ib}1'$	14.0	±0.5
C_b1'	broad, under C_b5	
G_b1'	13.0	±0.5
G_q1'	13.0	±0.5
$T_{iq}1'$	13.6	±0.2
$T_{ib}1'$	13.1	±0.4
C_q1'	broad, under $T_{ib}1'$	

[a]spectra matched by simulated spectra, $J_{1'}$-$J_{2'}$+$J_{1'}$-$J_{2''}$, in Hz.

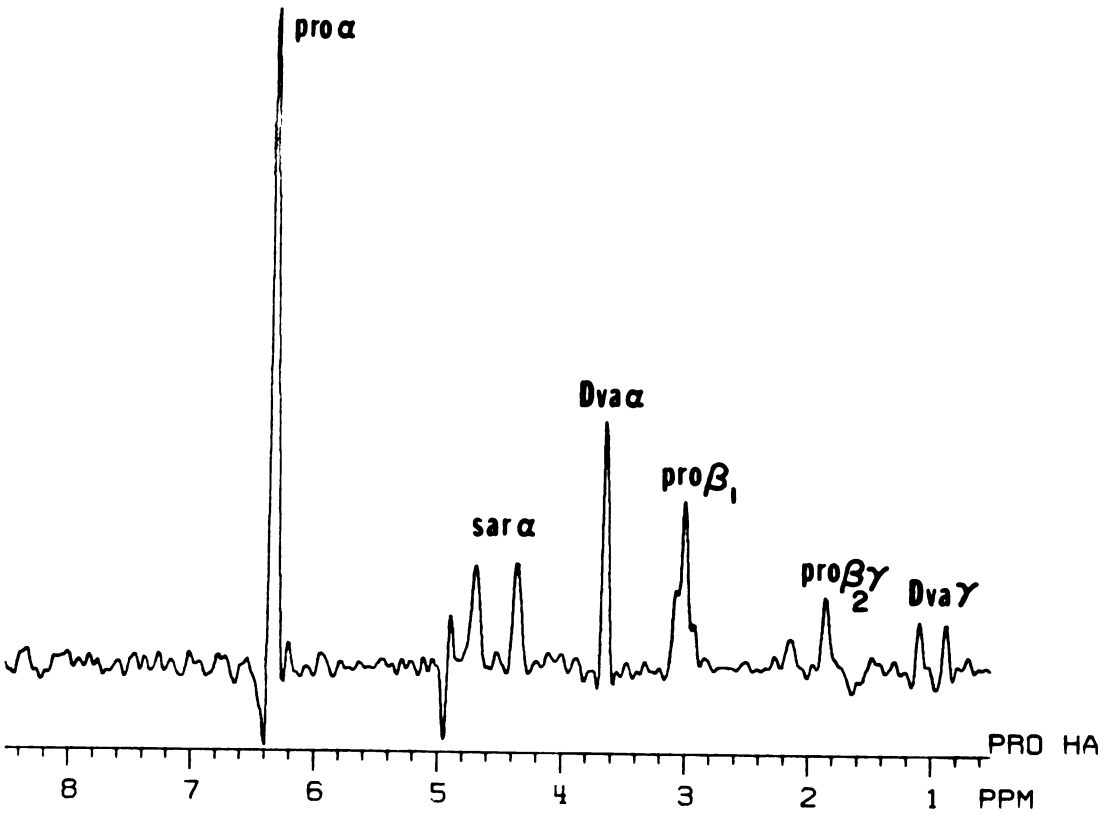

FIGURE 36

Slice along the ω_1 axis containing the β-proα resonance along the diagonal. Strong NOE's to the Dvaα and β-sarα_1, βsarα_2 protons indicate the configuration of the pentapeptides is cis-cis between these three residues, as in the free drug.

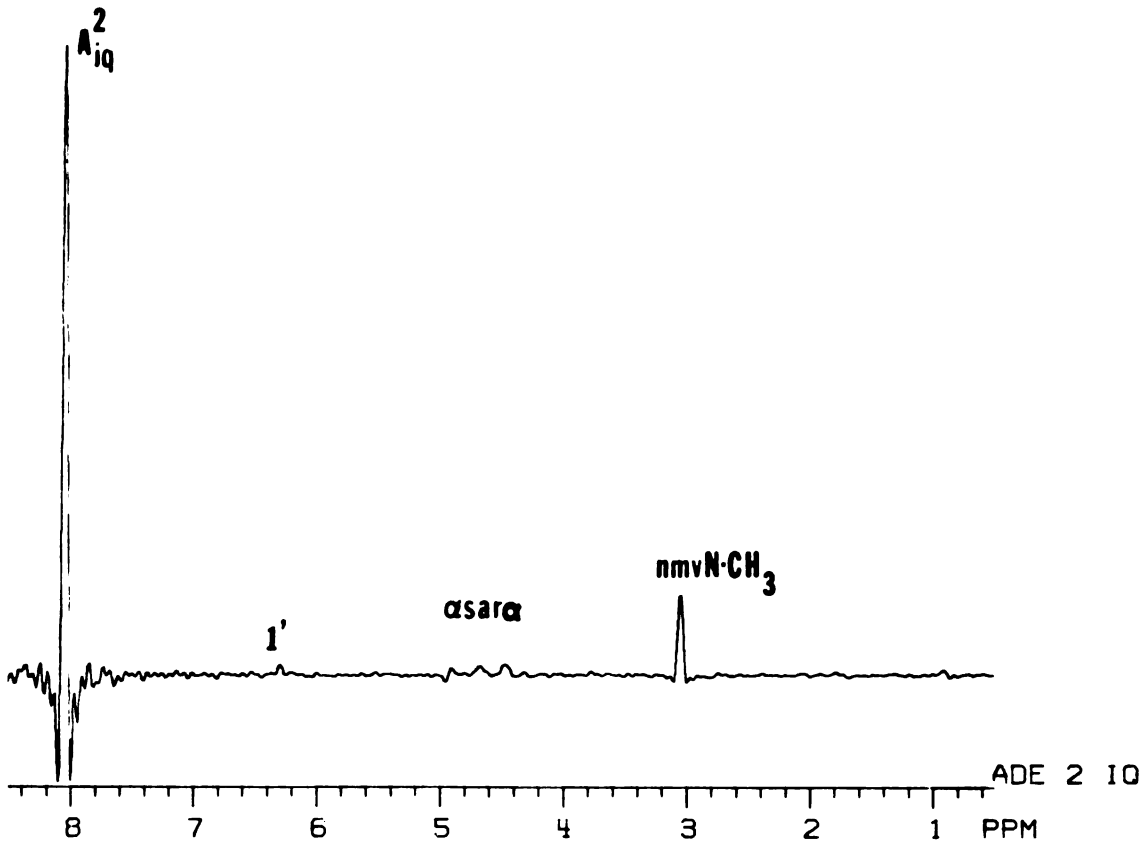

FIGURE 37

Slice along ω_1 containing the A^2_{iq} resonance, showing cross peaks to the αsarα and nmv N-CH_3 protons. These contacts in particular indicate that the drug pentapeptides are nestled in the minor groove of the hexanucleotide and partially confirm the model of Sobell & Jain (1972).

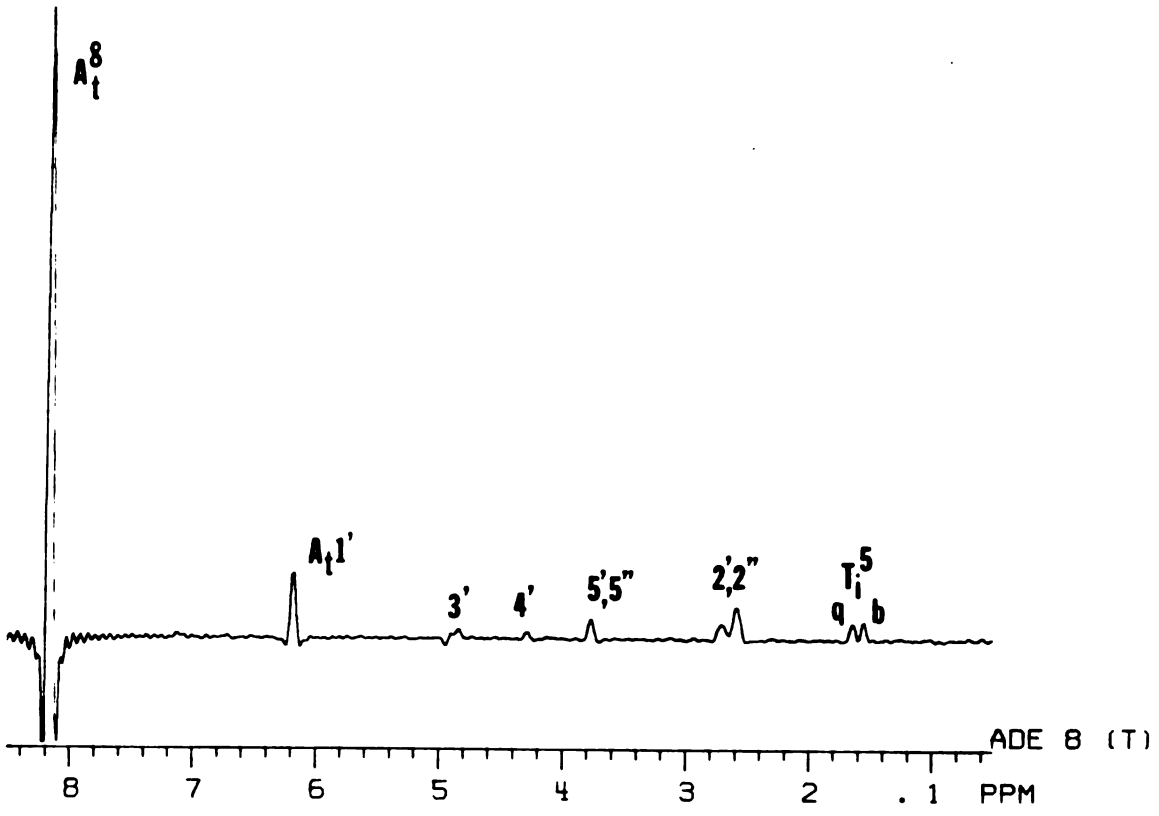

FIGURE 38

Slice along the ω_1 axis containing the A_t^8 diagonal resonances. Only one cross peak is seen to an anomeric proton. Other cross peaks are observed only to protons on the same nucleotide residue, except for base proton contacts with the T_i^5 methyl groups.

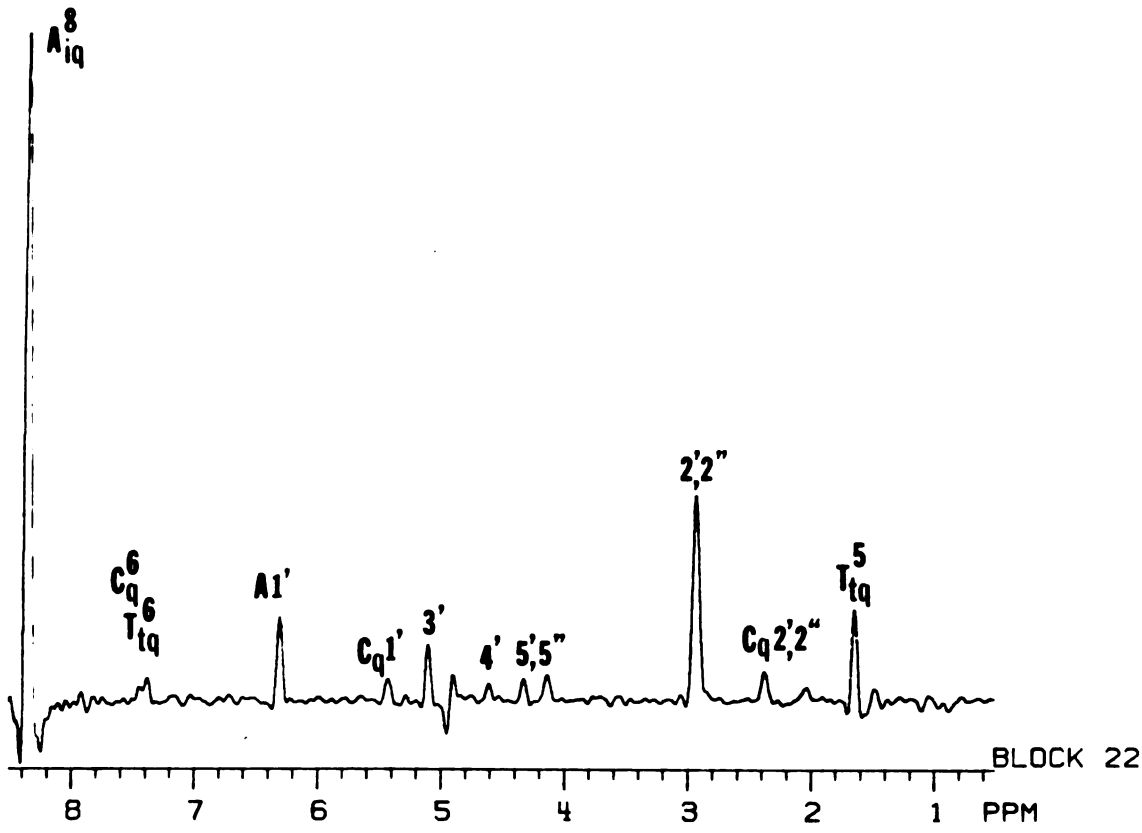

FIGURE 39

Slice along ω_1 containing the A^8_{iq} diagonal resonance. Strong NOE's are observed from such internal nucleotide residue base protons to protons on the deoxyribose portion of the same nucleotide, while weaker ones are seen to 1' and 2',2" protons of the neighboring nucleotide in the 5' direction of the sequence (C_q).

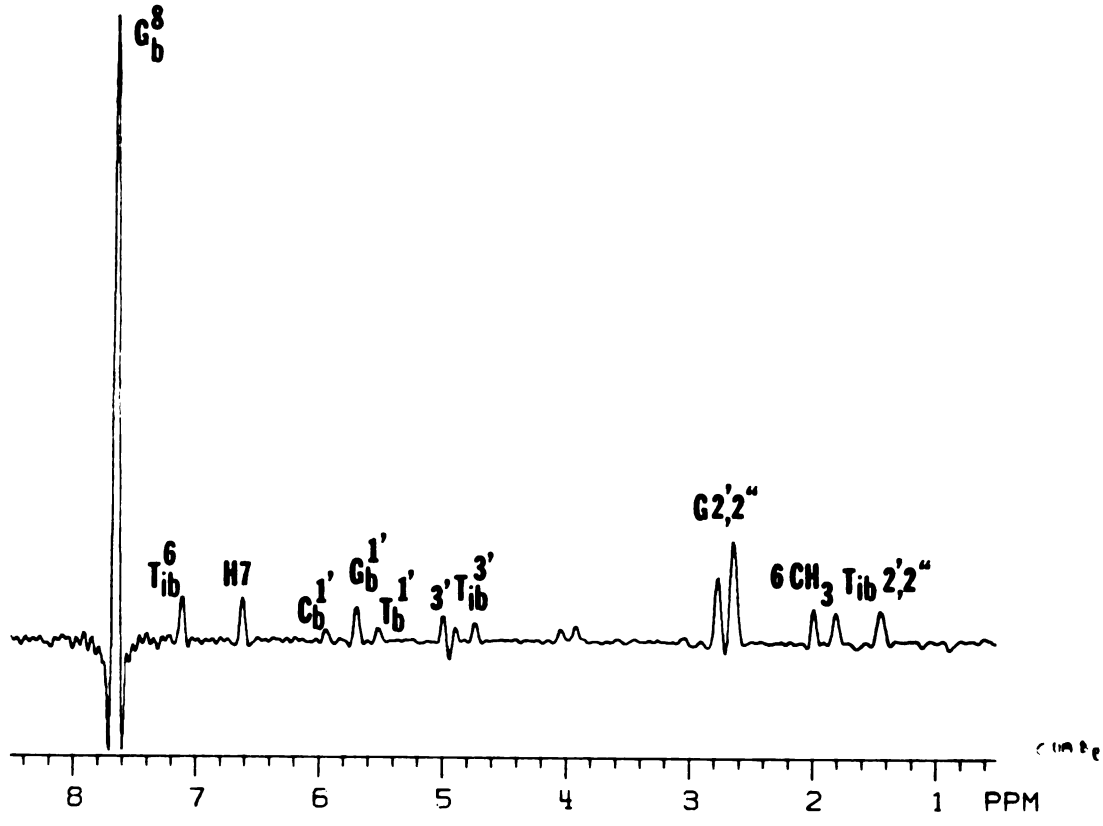

FIGURE 40

Slice along ω_1 containing the G_b^8 diagonal resonance. The typical pattern is seen with, additionally, strong base-base contacts (T_{ib}^6) and contacts with the ActD protons: H7, 6-CH_3, and H8 (weaker) on the benzenoid side of the drug chromophore.

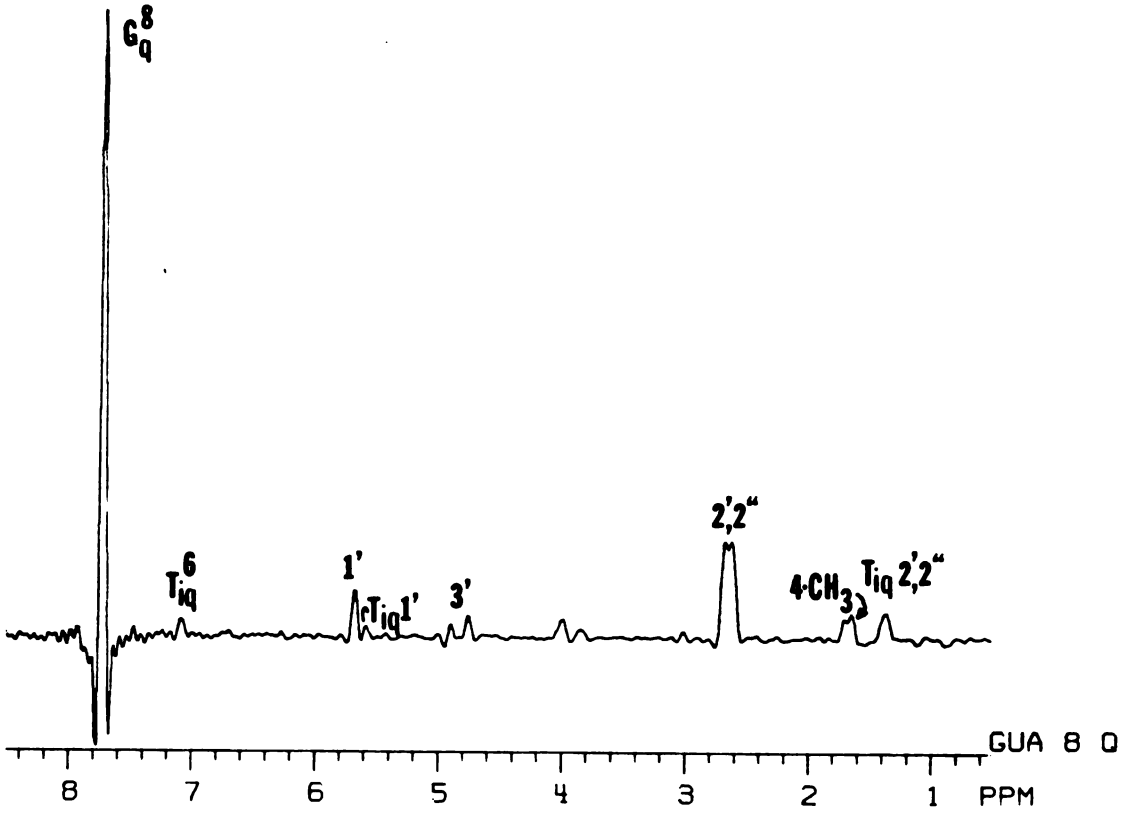

FIGURE 41

Slice along the ω_1 axis containing the G_q^8 diagonal resonance. The typical pattern is seen, with an additional contact to the drug 4-CH_3 protons on the quinoid side of the chromophore.

lack of NOE's observed between the guanines and cytosines in each strand indicates that they are separated compared to the free duplex, where these NOE's are readily observed. 2) The pentapeptide lactones are in the minor groove, since NOE's are observed from the *nmv* N-CH_3 group and the *sara* protons to the internal adenine H2 (A_i^2) protons. 3) The duplex dATGCAT base pairs are intact. This is shown by the observation of NOE contacts between neighboring bases on each strand apart from the intercalation site. The imino proton resonances are observed and NOE's are seen between them (Figure 42). 4) The structure of the drug pentapeptide lactones is very similar to that of the free drug and the crystal structure.

A comparison of NOE contacts and their relative intensities shows that the the structure of this complex is very similar to that proposed by Sobell & Jain, (1972) and that no significant conformational change occurs in either the drug or the oligonucleotide (apart from intercalation of the chromophore). The most important NOE contacts that support this argument are listed in Table XV.

Distances were calculated by scaling with the equation: $r(1)/r(2)=[\eta(2)/\eta(1)]^{1/6}$ and using the NOE intensity between the C^5 and C^6 protons and between the T^6 and T^5 protons as internal reference standards. The model of the complex has the overall dimensions 21 x 21 x 16 Å and the drug is very stiff due to steric constraints, so the overall motion is expected to be fairly isotropic. The distances calculated by a simple scaling relationship will not be as accurate as those determined from relaxation density matrix fitting of the NOE's (Macura & Ernst, 1980; Keepers & James, 1984). Even so, several other mixing times would be required to fit an accurate distance with experimental NOE intensities, and the motion of the molecule

TABLE XV

Comparison of COMP2 NOE Distances vs. Model Distances

proton	cross peak(NOE[a])	Calculated Dist.[b]	Model Dist.[c]
H8	$G_{b5,1'}^{8}$(2.4%)	3.2	4.7
	$C_{b}1'$(4.4%)	3.0	4.0
	$G_{b}1'$(4.6%)	3.0	3.8
	$G_{b}2'$(7.4%)	2.7	1.6
	$G_{b}2''$(6.2%)	2.8	2.7
H7	C_{b6}(3.0%)	3.1	3.8
6-CH_3	G_{b8}(3.5%)	3.0	3.5
4-CH_3	G_{q}(1.9%)	3.4	3.9
A_{iq}	asarα_1(3.0%)	3.1	3.5
	asarα_2(3.4%)	3.0	3.2
	nmvN-CH_3(14.3%)	2.3	2.2
$G_{b,q}1'$	thrγ(13.0%)	2.45	4.0
proβ_2,γ	C_{b5}(2.8%)	3.2	2.7
proβ_1	C_{b}.1'(2.8%)	3.2	2.7
βproα	Dvaα(13.3%)	2.4	2.2
	βsarα_1(10.5%)	2.5	1.6
	βsarα_2(9.0%)	2.6	3.3
	pro$\beta 1_1$(8.5%)	2.6	2.3
	proβ_2,γ(4.9%)	2.9	3.2
thrβ	Dvaγ(13.4%)	2.4	3.3
nmvN-CH_3	$T_{ib}1'$(3.0%)	3.1	4.6
	$T_{iq}1'$(6.5%)	2.8	4.6
	$G_{b,q}1'$(4.6%)	3.0	2.5

[a] measured by integration of slices, normalized to total intensity of slice

[b] calculated by equation: $r(1)/r(2)=(\eta(2)/\eta(1))^{1/6}$.

[c] from energy minimized model(Sobell & Jain, 1972) with hydrogens attached in standard geometry.

must be adequately modeled. A simple scaling relation ignores the NOE dependence on variable motions within the molecule, assuming that identical motions relax each proton. Such a simple treatment also ignores the effects of secondary NOE's in situations where a large number of protons interact. It can be seen that some protons in COMP2 are within NOE contact distance (< 5.0 Å) of up to 15 protons. A simplified treatment will therefore contain

errors by ignoring other factors besides interproton distance that contribute to NOE intensities. Distances derived from simple scaling will contain errors due to these assumptions but will, however, be accurate within ±0.5 Å because of the inverse sixth-power relationship of distance to NOE intensity for distances less than 3.5 Å, and within ±1.0 Å for distances greater than 4 Å, where the NOE cannot be accurately measured anyway. This degree of uncertainty is tolerable since motions within the complex may be expected to modulate proton-proton distances somewhat and if enough proton-proton contacts are known, the overall structure of the molecule will fall out even if the distances are inaccurate to an Angstrom or so. The structure of the complex would be more completely determined in proportion to the number of NOE contacts that can be observed and definitely assigned. Refinement of the distances by relaxation density matrix calculations could improve their precision, but errors in accuracy could persist that are just as great as the uncertainty introduced by the simple scaling method. The motion of the molecule must be accurately modeled by physically reasonable but nevertheless *a priori* assumptions about such motions, while extra parameters must be used to fit a limited set of data. This situation could improve the fit purely by the use of more adjustable parameters, so care must be taken not to overdetermine the analysis of the data. Detailed work using relaxation matrix calculations to derive distances from NOE data should be done on systems that are very rigid, whose motions are simple and extremely restricted, before the method can be applied to this complex.

Table XV contains distances calculated from several NOE contacts and compares them to an energy-minimized model (T. A. Lybrand & P. A. Kollman, personal communication) of the complex proposed by Sobell & Jain (1972). The agreement is good and shows that the complexes have a similar

structure. A *cis-trans* isomerization of the ActD pentapeptide lactones is certainly ruled out by the strong NOE's between the *proα* and *sarα*, *Dvaα* protons which indicate the configuration of these peptide bonds is identical for the free and bound drug. Some of these distances are seen to be greater than one angstrom out of agreement. This could be due to slight differences in the structure of the model and the solution structure probed by the NMR, or to errors arising from the simple method used to calculate these distances from the NOE data. The general features of both models are identical however, since no NOE contacts are observed for distances over 5 Å in the model, and conversely, NOE's are observed for every distance less than 5 Å in the model, while the relative intensities of these NOE's generally scale very well to distances in the model. Several "slices" of the COMP2 NOESY spectrum are shown in Figures 36 to 41 that reveal the signal to noise and the general appearance of the spectra that were integrated to obtain the NOE intensities. The NOE intensities were calculated by adding the slices that covered a particular peak along the diagonal and using the integration algorithm on the Nicolet 1180 data system. The summed spectra (generally three slices, corresponding to three data points per peak) were integrated and normalized to the total sum of intensity over the spectrum. The intensity of cross peaks was then tabulated and distances calculated with reference to the C^5 to C^6 NOE using the simple ratio equation above.

Distance geometry algorithms have been used to generate structures from intramolecular distance information (Kuntz et al., 1979). Several distance geometry runs were done on the pentapeptide lactone alone that indicated its structure was well determined by only three NOE constraints, the *thrβ* to *Dvaγ*$_1$, the *proα* to *sarα*$_1$ and the *proα* to *Dvaα* proton-proton distances of 2.3 to 3.3 Å. Distance geometry will be a valuable technique for the

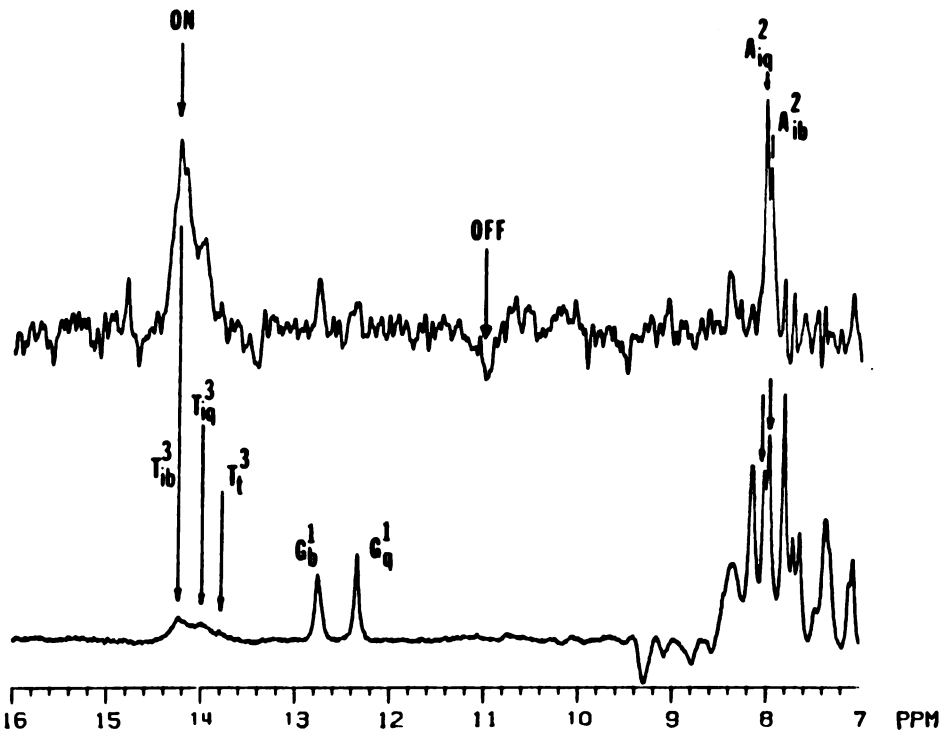

FIGURE 42

500 MHz. proton NMR spectra of COMP2 in BPES (90%H_2O, 10%D_2O) at 0.0 ^oC: (bottom), reference spectrum of intact imino protons in slow exchange with solvent water. (top), NOE difference spectrum with irradiation of the downfield peak at 14.228 ppm that assigns this peak to the T^3_{ib} proton by the strong NOE to the A^2_{iq} proton of the same base pair. Observation of weak NOE to a G^1 proton indicates the helix is intact.

estimation of how well a structure has been determined by the available data.

It was of interest to know whether the duplex dATGCAT base pairs were intact, since a crystal structure of an ActD/dGC(1:2) complex showed an unusual pseudo-intercalated geometry (Takusagawa et al., 1982) where the base pairs next to the intercalation site had "swung out". Results of a one-dimensional NOE experiment on the imino protons are shown in Figure 42. The observation of imino proton resonances indicates that the helix stability is maintained on drug binding. Assignment of the imino protons could be made by the NOE's observed to non-exchangeable A^2 protons. NOE's observed between the internal AT base pair imino protons and the GC base pair mino protons corroborate the intact nature of the helix. The conformation of the duplex is indeed altered slightly due to intercalation of the drug chromophore and an unwinding of the helix, but no major changes in the helix geometry are observed when NOE contacts and intensities are compared to those of the free duplex dATGCAT. The integrity of the double helix implies a classical intercalation structure. Preliminary X-ray diffraction analysis of this same complex strongly indicates classical intercalation (H. Berman, personal communication), and is in agreement with the results of the complex in solution.

Conclusions

The results from the two-dimensional proton NMR study of the ActD/dATGCAT(1:2) complex indicate that no major conformational change of either the drug or double helix, apart from intercalation of the chromophore, occurs upon binding. The observed slow kinetics must be attributed to some other property of the system. Solvation of the transition state and complex may be involved. Thermodynamic measurements of the equilibrium reaction of ActD binding to DNA imply that the association is driven by entropy, not enthalpy. Thermodynamic parameters for the transition state were calculated from Arhennius plots and show large negative entropies of activation for the two slowest processes observed during dissociation. Measurement of the pressure dependence of the association rates and the volume change for association could shed some light on these issues. Since slow associations are observed for mononucleotides as well, the kinetics must be attributed to a property of the drug alone.

An alternative explanation would be that a small percentage of either free or bound ActD, less than 5% of the total population, is in a different conformation and is the cause of the slow kinetics, since the OD change in the slow processes involves about this percentage of the total OD change upon binding. A population this low may not have been detected by the NMR experiments in water. The solubility limit of ActD in aqueous solutions presents an experimental difficulty for the detection of alternative conformations of either free or bound actinomycin D.

Appendix I

Procedure for the production of Actinomycin D given by Professor J. Formica, University of Virginia, Charlotteville, Va. One batch was produced by Drs. J. Formica and C. Delfini and another by Stephen Brown. The materials and their sources given here pertain to the batch made at UCSF.

Preparation of Inoculum

Bacto Casamino acids(DIFCO 0230-01-1)	25 g
Nutrient Broth(BBL 11479)	10 g
tap water	1000 ml

adjust to pH7.1 and distribute 100 ml in ten 250 ml flasks, autoclave at 121 °C. for 20 minutes.

The above media is inoculated with several small spatula fulls of the soil culture containing *Streptomycetes parvulus* (ATCC 12434)

Incubate for 48 hours at 28 °C in a gyrotary incubator.

Preparation of Production Inoculum

Harvest the vegetative culture by centrifugation: Decant the culture into a 250 ml centrifuge bottle and centrifuge for 10 min. at 9,000 rpm in the Sorvall.

Wash the pellet twice with 100 ml of autoclaved 0.9% saline solution. Finally, suspend the pellet in 50 ml of 0.9% saline. Store the pellet in refrigerator, best to inoculate the production medium within two days.

Inoculate the production media with 2 ml of this cell suspension.

Production Media

[^{15}N]L-glutamate(Merck Sharpe,Dohme)	2.5g
K_2HPO_4	1.0 g

Dissolve these two compounds together in about 800 ml of distilled water. Adjust to pH 5.0 with approximately 10 ml of 2N NaOH. Then add the following ingredients in the order indicated:

$ZnSO_4.7H_2O$	0.025 g.
$FeSO_4.7H_2O$	0.025 g.
$CaCl_2.2H_2O$	0.025 g.
$MgSO_4.7H_2O$	0.025 g.
distilled H_2O, qs ad	1000 ml.

adjust to pH 7.2 with 2N NaOH, a fine white percipitate will result
distribute 100 ml among ten 250 ml flasks

autoclave at 121 °C. for 20 min.

It is more convenient to add these salts as concentrated solutions. Prepare solutions at a concentration of 25 mg./ml. The Ferrous Sulfate cannot be treated this way and the solid must be added to the medium. After autoclaving, a white ppt. will be observed which is no cause for alarm.

Fructose Solution

Place 50 grams of fructose(Sigma) in a 250 ml flask, add ~50 ml water and a stirring bar. Heat while stirring and gradually add water to a volumn of 100 ml. Do not boil. When the fructose is fully dissolved, remove the stirring bar and autoclave at 121 °C. for only 15 minutes. The resulting 50% fructose solution will turn a light golden color from caramelization; if the solution is dark, discard and repeat the preparation.

Actinomycin Production

Inoculate the production media with 2 ml of the cell suspension isolated from the vegetative culture. Add 8 ml of the 50% fructose solution.

Incubate the flasks at 28 °C. in the dark in a gyrotary shaker rotated at 230-250 rpm. to efficiently oxygenate the culture. Moniter production by removing 1 ml of culture every 24 hrs., extracting with 1 ml of ethyl acetate and measure the optical absorbance at 440 nm of the ethyl acetate extract. Harvest the culture when the concentration of actinomycin begins to level off. Production will be complete in 6 to 18 days of culture, depending on various factors which are difficult to control.

Extraction of Actinomycin

The supernatant fluid is a deep yellow to orange, with smooth globular colonies of *Streptomycetes Parvulus* in the media, which should otherwise be clear. Separate the mycelium from the growth media by vacuum filtration through a millipore HA filter (.45 μm.). Extract the actinomycins with an equal volume of ethyl acetate. Evaporate the ethyl acetate extract to dryness in a rotavap. Weigh the resulting red solid. Add a minimal amount of acetone (~1ml/50 mg) to the dried residue and transfer to a screw cap vial. Cover the vial with aluminum foil as actinomycin is photosensitive and store at 4 °C. (deep red color).

Procedure for Paper Chromatography

Prepare 10% aqueous solution of Sodium Cresotinate by adding 50 grams of ortho-cresotic acid(Pfaltz & Bauer) with about 10 ml of water to form a paste. Add more water to make the paste more fluid. Add 17.5 grams of Na_2CO_3 slowly to the constantly stirring suspension. The solution will foam a lot as CO_2 evolves and the cresotic acid dissolves, so add the Sodium Carbonate very slowly. After all the Sodium is added, qs to 500 ml. A clear amber solution should result. The pH should be at 10.5. If not all of the cresotic acid is dissolved, check the pH; if less than 10.5, add more Sodium Carbonate until it is. Add a small amount of

charcoal to the solution and continue stirring. Filter the solution, which should be almost colorless, through Whatman #1 paper and store at 4 °C. in a dark bottle.

Descending Paper Chromatography

To prepare the mobile and stationary phase, per 60 mg of actinomycin, mix:

10% Na cresotinate	160 ml
n-butyl acetate	120 ml
n-butyl ether	40 ml

into a separatory funnel and shake vigorously. Allow the phases to well separate. The bottom phase is the aqueous phase.

Cut sheets of Whatman 3MM paper into four 9 x 20 inch sections. Mark an origin by pencil 3 inches from one end. Dip the paper in the aqueous phase of the chromatography mixture, place the wet paper between two sheets of Whatman #1 and hand blot over this sandwich to expell the excess fluid. Apply about .2-.3 ml of the crude actinomycin solution in acetone along the origin of each paper while the sheets are still damp. Spot a little authentic actinomycin D in a neighboring lane. Suspend the paper in the cabinet and place the organic phase in the trough. Check the trough every 6-8 hrs while the chromatogram developes to be sure some mobile phase remains. Develop the chromatogram for about 24 hours in the dark. Remove from the cabinet and air dry overnight in the hood, in the dark.

Processing and Purification

The actinomycin D band should be the major band with an R_f the same as that of the authentic actinomycin standard developed in a neighboring lane. Cut the band out into one inch squares. Place the paper squares into a Waring blender, add 400 ml of water and 400 ml of ethyl acetate. Blend for one minute at high speed.

Filter the pulp through glass wool directly into a 2 liter separatory funnel. After the layers separate, drain off the aqueous layer and return to the blender. Add the drained pulp and 400 ml of fresh ethyl acetate, blend again and filter into the same sep funnel. After the layers separate, remove the aqueous portion and wash the ethyl acetate layer three times with an equal volume of 0.5% Sodium Carbonate, then once with distilled water.

Drain the ethyl acetate layer into a flask and refrigerate overnight. Remove the separated water with a pasteur pipette and dry the ethyl acetate with anhydrous Sodium Sulfate. Rotavap the solution to dryness and dissolve in one ml of benzene.

Purification

Activate a batch of Silicic Acid(Unisil, 100-200 mesh) in the oven at 100 °C. for several hours. Prepare a 1 x 10 cm. Silicic Acid column and wash with benzene. Layer the actinomycin D solution in benzene and elute the column with:

benzene	100%
benzene + 1% methanol	25 ml
benzene + 2% methanol	25 ml
benzene + 3% methanol	25 ml

Collect the eluate until almost colorless. Evaporate to dryness and dissolve in the minimal amount of warm(~40 ° C.) methanol. Slowly add ethanol(95%) until 3 times the volume of methanol has been added. Crystals should begin to form after a 1:1 mixture is attained. Digest at 4 °C. for several days and blow off solvents in a nitrogen stream at room temperature. Crystals made in this way dissolve in aqueous solutions most readily. Weigh and take up a small quantity in $CDCl_3$ for characterization by proton NMR. Generally, the yield is 40-70 mg of labelled [^{15}N]Actinomycin D per 1 gram of starting [^{15}N]- glutamate.

References

Altona, C.(1982). *Recl. Trav. Chim. Pays-Bas* **101**, 413.

Angerman, N. S., Victor, T. A., Bell, C. L., & S. Danyluk (1972). *Biochemistry* **11**, 2402.

Arnott, S., & D. W. L. Hukins (1972). *Biochem. Biophys. Res. Commun.* 47(6), 1504.

Ascoli, F., De Santis, P., Lener, M. & M. Savino (1972). *Biopolymers* **11**, 1173.

Auer, H. E., Pawlowski-Konopnicki, B. E. , Chen, Y.-C., & T. R. Krugh (1978). *Biopolymers* **17**, 1891.

Auer, H. E. & T. N. Thompson (1978). *Proc. Natl. Acad. Sci. U.S.A.* 75, 4729.

Bax, A., Freeman, R., & G. Morris (1981). *J. Magn. Reson.* 42, 164.

Bax, A. (1982). "Two-Dimensional Nuclear Magnetic Resonance in Liquids" Delft Univ. Press, Dordrecht, Holland.

Berman, H. M., & S. Neidle (1979).
in *Stereodyn. Mol. Syst., Proc. Symp.* **1979**(ed. R. H. Sarma)
Pergamon, Elmsford, N. Y., pgs. 367-382.

Bittman, R. & L. Blau (1975). *Biochemistry* **14**, 2138.

Booth, H. , Mauger, A. B. & W. J. Rzeszotarski (1976). *Org. Magn. Reson.* 8, 219.

Braun, W., Bosch, C., Brown, L. R., Go, N., & K. Wuthrich (1981). *Biochim. Biophys. Acta* **667**, 377.

Broido, M. S., Zon, G., & T. L. James (1984).
Biochem. Biophys. Res. Commun. **119**, 663.

Conti, F. & P. De Santis (1970). *Nature* **227**, 1239.

Davanloo, P. & D. M. Crothers (1976). *Biochemistry* **15**, 4433.

De Santis, P., Rizzo, R., & G. Ughetto (1972). *Biopolymers* **11**, 279.

Early, T. A., & D. R. Kearns (1979). *Proc. Natl. Acad. Sci .U.S.A.* 73, 4165.

Feigon, J., Wright, J. M., Leupin, W., Denny, W. A., & D. R. Kearns (1982). *J. Amer. Chem. Soc.* **104**, 5540.

Gellert, M., Smith, C. E., Neville, D., & G. Felsenfeld (1965). *J. Mol. Biol.* 11, 445.

Hanssum, H., Maurer, W., & H. Ruterjans (1978). *J. Magn. Reson.* 31, 231.

Hare, D. R., Wemmer, D. E., Chou, S.-H., Drobny, G. & B. R. Reid (1983). *J. Mol. Biol.* **171**, 319.

Hawkes, G. E., Randall, E. W., & C. H. Bradley (1975). *Nature* **257**, 767.

Hawkes, G. E., Randall, E. W., Hull, W. E., Gattegno, D., F. Conti (1978). *Biochemistry* **17**, 3986.

Hawkes, G. E., Randall, E. W., Hull, W. E., & O. Convert (1980). *Biopolymers* **19**, 1815.

Hollstein, V., Breitmaier, E., & G. Jung (1974). *J. Amer. Chem. Soc.* **96**, 8036.

Hull, W. E., & H. R. Kricheldorf (1980). *Biopolymers* **19**, 1103.

Jain, S. C., & H. M. Sobell (1972). *J. Mol. Biol.* **68**, 1.

James, T. L., Bendel, P., James, J. L., Keepers, J. W., Kollman, P. A., Lapidot, A., Murphy-Boesch, J., & J. E. Taylor (1983). in "Nucleic Acids: The Vectors of Life", (B. Pullman & J. Jortner, eds.), Reidel, New York. pgs. 155-167.

Kalk, A., & H. J. C. Berendson (1976). *J. Magn. Reson.* **24**, 343.

Keepers, J. W. & T. L. James (1984). *J. Magn. Reson.* **57**, 404.

Khaled, Md. Abu, Urry, D. W., Sugano, H., Miyoshi, M. & N. Izumiya (1978). *Biochemistry* **17**, 2490.

Kricheldorf, H. R., Hull, W. E., & V. Formacek (1977). *Biopolymers* **16**, 1609.

Krugh, T. R., & Y. C. Chen (1975). *Biochemistry* **14**, 4912.

Krugh, T. R., Hook III, J. W., Lin, S., & P. M. Chen (1980). in "Molecular Stereodynamics" **I**, (R. H. Sarma, ed.), Adenine Press, Albany, New York, pgs. 423-435.

Kumar, A., Wagner, G., Ernst, R. R., & K. Wuthrich (1981). *J. Amer. Chem. Soc.* **103**, 3054.

Kuntz, I. D., Crippen, G. M., & P. A. Kollman (1979). *Biopolymers* **18**, 939.

Lackner, H. (1971). *Chem. Ber.* **104**, 3653.

Lackner, H. (1975). *Angewandte Chemie, Int. Ed. Eng.* **14(6)**, 375.

Levy, G. C., & R. L. Lichter (1979). "Nitrogen-15 Nuclear Magnetic Resonance Spectroscopy", Wiley, New York.

Live, D., Wyssbrod, H. R., Fishman, A. J., Agosta, W. G., Bradley, C. H., & D. Cowburn (1979). *J. Amer. Chem. Soc.* **101**, 474.

Llinas, M., Horsley, W. J., & M. P. Klein (1976). *J. Amer. Chem. Soc.* **98**, 7554.

Macura, S., & R. R. Ernst (1980). *Mol. Phys.* **41**, 95.

Mauger, A. B. (1980). *The Actinomycins*, in "Topics in Antibiotic Chemistry", (P. Sammes, ed.) **5**, pgs. 229-305.

Meienhofer, J., & E. Atherton (1973). *Advances in Applied Microbiology* **16**, pgs. 203-300.

Mirau, P. A., & R. H. Shafer (1982a). *Biochemistry* **21**, 2626.

Mirau, P. A., & R. H. Shafer (1982b). *Biochemistry* **21**, 2622.

Muller, W. & D. M. Crothers (1968). *J. Mol. Biol.* **35**, 251.

Narang, S. A., Brousseau, R., Hsiung, H. M., & J. Michniewicz (1980). *Methods Enzymol.* **65**, 610.

Patel, D. J. (1974a). *Biochemistry* **13**, 2388.

Patel, D. J. (1974b). *Biochemistry* **13**, 2396.

Patel, D. J., & A. E. Tonelli (1975). *Biochemistry* **14**, 3990.

Patel, D. J., Kozlowski, S. A., Rice, J. A., Broka, C., & K. Itakura (1981). *Proc. Natl. Acad. Sci. U.S.A.* **78**, 7281.

Plateau, P., & M. Gueron (1982). *J. Amer. Chem. Soc.* **104**, 7310.

Reid, D. G., Salisbury, S. A., & D. H. Williams (1983). *Biochemistry* **22**, 1377.

Reinhardt, C. G., & T. R. Krugh (1977). *Biochemistry* **16**, 2890.

Remers, W. A. (1979). "The Chemistry of Antitumor Antibiotics", **I**, Wiley, pgs. 3-62.

Scheek, R. M., Russo, N., Boelens, R., & R. Kaptein (1983). *J. Amer. Chem. Soc.* **105**, 2914.

Shafer, R. H., Burnette, R. R., & P. A. Mirau (1980). *Nucl. Acids Res.* **8**, 1121.

Sobell, H. M., & S. C. Jain (1972). *J. Mol. Biol.* **68**, 21.

Sobell, H. M. (1974). *Canc. Chemotherap. Rep.* **58**, 101.

Sobell, H. M., Tsai, C.-C., Jain, S. C., & S. G. Gilbert (1977). *J. Mol. Biol.* **114**(3), 333.

States, D. J., Haberkorn, R. A., & D. J. Ruben (1982). *J. Magn. Reson.* **48**, 286.

Takusagawa, F., Dabrow, M., Neidle, S., & H. M. Berman (1982). *Nature* **298**, 466.

Ts'o, P. O. (1974). "Basic Principles in Nucleic Acid Chemistry" **I**, Acad. Press, New York, pgs. 537-562.

Victor, T. A., Hruska, F. E., Hickichi, K., Danyluk, S. S., & C. L. Bell (1969). *Nature* **223**, 302.

Von Dreele, P. H., & I. A. Stenhouse (1974). *J. Amer. Chem. Soc.* **96**, 7546.

Wagner, G. & K. Wuthrich (1979). *J. Magn. Reson.* **33**, 675.

Williamson, K. L., Pease, L. G., & J. D. Roberts (1979). *J. Amer. Chem. Soc.* **101**, 714.

Wuthrich, K., Wider, G., Wagner, G., & W. Braun (1982). *J. Mol. Biol.* **155**, 311.